DOE/LC/10442-2545
(DE88001043)

Energy

FOSSIL

Underground Coal Gasification: Development of Theory, Laboratory Experimentation, Interpretation, & Correlation With the Hanna Field Tests

Final Report

R.D. Gunn
W.B. Krantz

March 1987

Work Performed Under Contract No.: DE-AS20-80LC10442

For
U.S. Department of Energy
Office of Fossil Energy
Morgantown Energy Technology Center
Morgantown, West Virginia

By
Department of Chemical Engineering
College of Engineering
University of Wyoming
Laramie, Wyoming

DISCLAIMER

DISCLAIMER

DOE/LC/10442-2545
(DE88001043)
Distribution Category UC-109

Underground Coal Gasification: Development of Theory, Laboratory Experimentation, Interpretation, & Correlation With the Hanna Field Tests

Final Report

R.D. Gunn
W.B. Krantz

Work Performed Under Contract No.: DE-AS20-80LC10442

For
U.S. Department of Energy
Office of Fossil Energy
Morgantown Energy Technology Center
P.O. Box 880
Morgantown, West Virginia 26507-0880

By
Department of Chemical Engineering
College of Engineering
University of Wyoming
Laramie, Wyoming 82071

March 1987

Abstract

The following report is a description of a 7 year effort to develop a theoretical understanding of the underground coal gasification process. The approach used is one of mathematical model development from known chemical and physical principles, simplification of the models to isolate important effects, and thorough validation of models with laboratory experiments and field test data. Chapter I contains only introductory material. Chapter II describes the development of two models for reverse combustion: a combustion model and a linearized model for combustion front instability. Both models are required for realistic field predictions. Chapter III contains a discussion of a successful forward gasification model. Chapter IV discusses the spalling-enhanced-drying model for water influx. Chapter V shows how the spalling-enhanced-drying model is applicable to prediction of cavity growth and subsidence. Chapter VI describes the correct use of energy and material balances for the analysis of UCG field test data. Chapter VII shows how laboratory experiments were used to validate the models for reverse combustion and forward gasification. It is also shown that laboratory combustion tube experiments can be used to simulate gas compositions expected from field tests. Finally, Chapter VII presents results from a comprehensive economic analysis of UCG involving 1296 separate cases.

TABLE OF CONTENTS

LIST OF TABLES

LIST OF FIGURES

EXECUTIVE SUMMARY

Need for a Coherent Theory of Underground Coal Gasification

The following report describes a 7 year successful effort from 1975 to 1982 to develop a theoretical understanding of underground coal gasification. A sound knowledge of the physics and chemistry of the process is essential for developing a commercial UCG (underground coal gasification) process. Empirical development of UCG, not guided by theoretical knowledge, has proved unsuccessful in the Soviet Union where an estimated 2 to 10 billion dollars have been spent on UCG, nor were similar empirical smaller efforts in other countries successful during the 1950's and 1960's.

Complexity of the Underground Coal Gasification Process

Although little expertise is required to inject air into a seam and to ignite and burn the coal underground, the actual process of UCG is a very complicated one involving hundreds of chemical reactions, and many physical processes such as spalling of the overburden rock, permeability enhancement by coal drying, particle plugging of the permeable pathways by condensation of coal tars in cooler portions, by-passing of air through permeable overburden, etc. Successful UCG, therefore, requires an understanding of important chemical and physical effects in order that favorable factors can be optimized and unfavorable effects can be eliminated or at least ameliorated.

The complexity of the UCG process is further intensified because each coal gasification site is different, uniquely determined by local geological processes extending over millions of years. Chemically, UCG is quite similar to the Lurgi process of surface gasification. For the latter process, the chemical reactor which is the Lurgi gasifier is precisely designed for optimum performance; and the coal charged to the gasifier can be blended to achieve constant properties. The situation is very different for UCG. The characteristics of the reactor vessel and the coal have been determined by the vagaries of nature and are different at every site.

Despite this complexity, there is no basis for despair. Gasification design at a seemingly infinite variety of sites can be reduced to a limited set of universally applicable scientific principles. For example, in medicine, it is not necessary to understand all bodily processes in their entirety in order to design a highly successful medical treatment. Similarly, the nature of UCG can be simplified to a limited number of physical processes and chemical reactions which explain well over 90% of the observed behavior of UCG field experiments.

For the foregoing reasons, the DOE UCG program has been characterized by a scientific approach to the process with the use of extensive instrumentation, mathematical modeling and laboratory experimentation to elucidate the important underlying scientific principles of the process. In this vein, the seven year research effort described in

this report has used mathematical modeling with laboratory experimentation and extensive use of field test data to develop a coherent theory of the process.

Chapter I. Introduction

In the following report, Chapter I provides introductory information and a review of the UCG process and need not be discussed further here.

Chapter II. Reverse Combustion Linking

This chapter discusses the development of two separate mathematical models of reverse combustion which is used as a linking procedure in UCG. Both models must be used in order to interpret field test results. Reverse combustion exhibits some very unusual behavior. For example, reverse combustion does not burn coal to completion, but rather leaves a matrix of char behind. Some other unusual aspects of reverse combustion are that an increase in oxygen concentration through the use of high pressure or removal of nitrogen or both leads to lower combustion temperatures. The opposite is true for ordinary combustion processes which is the main principle involved in the use of oxy-acetylene or oxy-hydrogen torches. The reverse combustion front also advances at a much higher rates than ordinary combustion fronts in forward gasification. Reverse combustion does not advance along a broad front as ordinary forward combustion, but burns along a very restricted front leaving a long tube of char behind. Most of the unusual aspects of reverse combustion were first predicted through the use of the two mathematical models and have been verified subsequently by laboratory experiments. From a practical standpoint, it is now possible to calculate reasonably accurately linking velocities and the effects of pressure, injection rate and injection gas composition on linking velocities. The length of the reverse combustion channel is determined by the path of greatest permeability. This path of greatest permeability is generally not known without independent permeability tests for the coal seam in question.

Chapter III. Forward Combustion

This chapter describes a theoretical model for forward gasification which was developed in 1975 and 1976 at a time when there was almost no understanding of the UCG process. The model was designed to answer such questions as: Why does the gas heating value decline as a UCG field test progresses? What effect does air injection rate and injection pressure have on the performance of UCG? What major variables affect the gas heating value? Can the effect of varying the injected gas composition (air, oxygen, steam-oxygen) be predicted so that an expensive field test need not be conducted for each possibility? Is water-influx into the reaction zone favorable because of the steam-carbon reaction or unfavorable due to quenching of the combustion process? The theoretical gasification model has provided answers to these questions which have been described in a number of technical publications and have

been summarized in Chapter III. For example, the model has clearly shown that heat loss from the combustion zone is the most important factor affecting gas heating value -- an important factor not known prior to development of the model. Heat loss in turn is caused by water influx and by heat lost to spalled overburden.

The mathematical gasification model was verified by comparing model predictions with field test results. The agreement between predicted and calculated results was excellent especially because no curve-fitting parameters were used for this work, that is, only physical or chemical properties taken from the technical literature or measured in the laboratory were used.

The coal gasification model has provided the theoretical knowledge needed for designing laboratory combustion tube tests which reproduce field tests results in the laboratory relative to gas composition, heating value and flow rate. Comparisons between field data, laboratory data and predicted values showed good agreement.

Chapter IV. Water Influx

Water influx is a major variable affecting unfavorably the heating value of produced gas. The harmful effects of water influx arises from the large amount of heat required for vaporization which robs much of the process heat needed to drive the highly endothermic steam-char reaction, a major source of combustible gas.

$$C + H_2O \rightarrow CO + H_2$$

Aside from water already in the coal, water orginates from two major sources. The first major source of water-influx is via permeation from highly permeable coal beds which are common throughout the West. One example of this type of deposit occurs at the Hoe Creek site where Lawrence Livermore National Laboratory conducted three UCG field tests. Rock overburden is a second major source of water. Shales and siltstones, even though they may be impermeable, contain as much as 40% by volume water. As coal burns away during UCG, the overburden is exposed to intense heating. This causes extensive spalling of the rock as it dries and is exposed to thermal stresses and steam pressure. Eventually, the cavity left after the coal has burned away is filled with dried rock debris.

The process just described has been developed into a predictive model, the spalling-enhanced-drying model for water influx. This model has been successful in predicting water influx for the Hanna and Hoe Creek UCG field tests.

Chapter V. Cavity Growth and Subsidence

An understanding of rock spalling during UCG is important because it exerts a major influence on both water influx and subsidence. The more rigorous solution to this problem is through the methods or rock

mechanics. However, progress with this approach has been very slow because of the complexity of the calculations and because of the need for thermal stress parameters which are very difficult to measure.

For this reason, the authors have developed a simpler statistical approach. It probably will never be possible to describe accurately the time and location that a particular rock fragment will spall from the overburden under the influence of gravity and thermal stress. Nor will it be possible to predict the shape, cross-section area and thickness of that rock fragment. These factors are determined by minute variations in the physical properties of the rock and by small variations in the heating rate and heating intensity. This information cannot be determined economically in sufficient detail for practical calculations.

The spalling model developed in this chapter is based on the assumption that the cross-section area of spalled rock fragments varies randomly, but is always small compared to the total cavity area. The thickness of these rock fragments is also assumed to be distributed randomly about a well-defined mean. In this way, it is possible to predict the rate of spalling of overburden with a single parameter, the mean spalling length. This parameter can be measured in the laboratory by subjecting rock cores to thermal stress and by measuring the average thickness of the resulting rock fragments. Or the needed parameter can be back-calculated from field test results. This spalling model is used as a major component of the spalling-enhance-drying model for water influx. The spalling model has been successful in calculating the shape of the spalled roof overlying the area of burned out coal, and it has been successfully incorporated in the water-influx model described in Chapter IV. The model can also incorporate with a minimum of complexity the effect of several overburden strata with different physical characteristics.

Chapter VI. Material and Energy Balances

Although material and energy balances are not predictive models, they are an extremely important tool for analyzing UCG data. Carbon and hydrogen balances are used to calculate the amount of coal consumed during a UCG test and the amount of water-influx. Some investigators have also tried to use an oxygen balance to calculate the amount of coal char which is left behind. Unfortunately, the simultaneous solution of the carbon, hydrogen and oxygen balances leads to algebraically unstable equations which enormously enhance small errors in the input data. For example, an error of one percent in the measured mole fraction of carbon monoxide in the product gas can lead to errors of 100% or more in the predicted amount of char. With the oxygen balance, it was predicted that at the end of the Hanna II field test, about 60-70% of the coal affected was left behind as char. Later, the field test site was extensively cored, and almost no char was found. A moderate amount of coal was recovered from the bottom of the seam in wells where the combustion front had consumed the overlying coal. Analyses of these cores, however, has shown that almost all of this coal had not been thermally altered except for a few inches immediately adjacent to the burned out area.

Energy balances have shown that the Hanna field tests were very efficient thermally. Cold gas efficiencies varied from 75-90%, which is better than all of the commercial processes currently available. The reason for this high efficiency is that the earth is an excellent insulator, and very little heat is lost in the process.

Chapter VII. Experimental Studies

This chapter describes the laboratory experiments used to verify the mathematical models for forward gasification, for reverse combustion and for two dimensional cavity growth. In all cases, good agreement exists between laboratory data, model predictions and field test data.

Chapter VIII. Economics

Many economic studies of UCG are available; however, this economic analysis was undertaken in order to overcome some of the shortcomings of many of the previous analyses. These shortcomings were:

1. Unnecessary and sometimes contradictory assumptions about the process.

2. Predicted gas selling price varied by more than a factor of four leading some to believe that enormous uncertainties existed in the process.

3. Failure to reduce process design to the minimum number of independent variables.

4. Failure to utilize the economic study to define future needs, that is, what uncertainties in the process affect the process economics most seriously.

Some 1296 separate economic analyses were completed accounting for variations in seam depth, seam thickness, well spacing, dry gas heating value, sweep efficiency and gas leakage. Two of the more important conclusions were the following. Previous economic studies varied widely because of differences in seam depth and seam thickness. On a common basis, such studies varied no more than 25% in the required cost of gas produced. Well spacing particularly in thin, deep seams and gas heating values have a very significant effect on gas cost. Therefore, at least two major research goals should be methods to maximize wellspacing and methods to maintain a high gas heating value.

CHAPTER I - INTRODUCTION

There is a pressing need to develop energy alternatives to oil and natural gas. For example, the U.S. obtains 75 percent of its energy from oil and natural gas and only 17 percent from coal, its most abundant fuel. Unfortunately, only 0.4 trillion tonnes or approximately 7 percent of the 5.8 trillion tonnes of U.S. coal reserves can be mined economically (U.S. D.O.E., 1979). The remainder of the coal reserves cannot be mined because of the depth of the deposit, unsafe mining conditions, or a variety of other reasons. Much of this enormous, currently uneconomic resource is potentially recoverable by the underground coal gasification (UCG) process.

This report will not discuss the history of UCG process development, the many possible uses for the product gas, or the many advantages of UCG technology relative to conventional mining and other synfuels technologies. The interested reader is referred to a recent paper by Krantz and Gunn (1980) for more information on these aspects of UCG.

The UCG Process

The UCG process is a technology for converting coal into a useful gas by partial combustion underground in the presence of water and a limited amount of air or oxygen. A sketch of the UCG process is shown in Figure I-1. Injection (well 1) and production (well 2) well bores are drilled into the virgin coal seam (I-1-A). The permeability of the coal seam must be enhanced to ensure reasonable gasification rates and to avoid condensation of tars and other volatile matter from the product gas as it passes through cooler portions of the coal seam. This permeability enhancement step is referred to as "linking" and can be accomplished by reverse combustion, directional drilling, electrolinking, and hydraulic, pneumatic or explosive fracturing. Only reverse combustion linking will be discussed here since it has been used successfully in several UCG field tests. Air is injected to permit ignition of the coal at the base of the production well (I-1-B). High pressure air (at approximately 23 kPa per meter of depth) then is injected at low flow rates (typically 3 to 6 m^3/min) into well 1 in order to draw the combustion front towards the injection well (I-1-C). The coal is not consumed in this relatively low temperature process, but only carbonized along one or more narrow (approximately 1 m in diameter) linkage paths. Linking is completed when the reverse combustion front reaches the bottom of the injection well (I-1-D). It is then possible to inject air (or oxygen) into well 1 at high volumetric flow rates and low pressures to effect gasification of the coal by forward combustion (I-1-E). The combustion cavity initially expands somewhat spherically in the direction of the linkage path(s) under ideal conditions until it reaches the overburden after which, under ideal conditions, it proceeds to gasify the coal over the full thickness of the seam until breakthrough occurs (I-1-F). Gasification of subbituminous coal typically proceeds at a rate of 0.3 to 0.6 m/day consuming all the coal in a sweep 12 to 15 m wide for a well spacing of approximately 18 m.

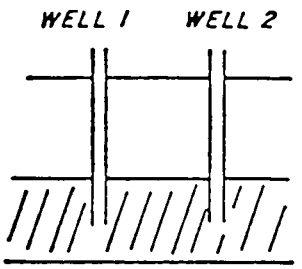

(A) VIRGIN COAL

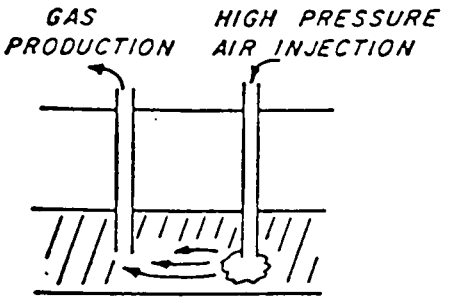

(B) IGNITION OF COAL

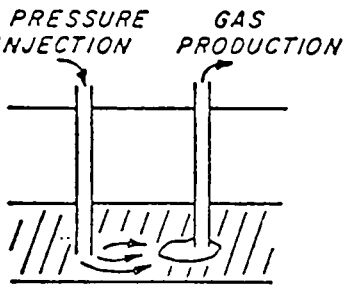

(C) COMBUSTION LINKING FRONT PROCEEDS TO SOURCE OF AIR

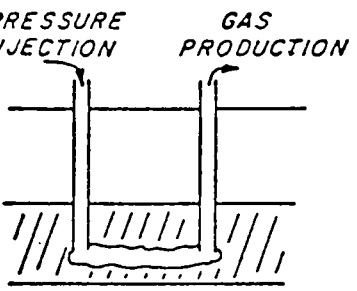

(D) LINKAGE COMPLETE WHEN COMBUSTION ZONE REACHES INJECTION WELL (SYSTEM READY FOR GASIFICATION)

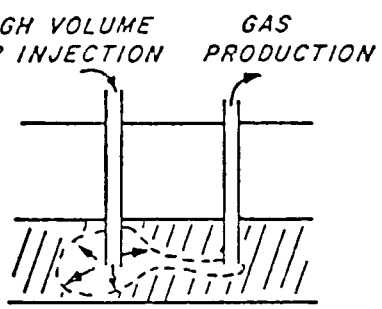

(E) COMBUSTION FRONT PROCEEDS IN THE SAME DIRECTION AS INJECTED AIR

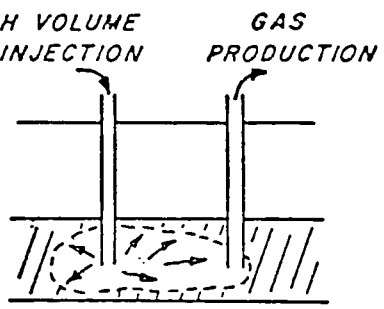

(F) COMBUSTION FRONT EVENTUALLY REACHES PRODUCTION WELL

Figure I-1. Sequence of Events in UCG Process Employing Reverse Combustion Linking

The UCG process is divided into gasification, devolatilization/pyrolysis, and drying zones. The combustion processes occurring in the gasification zone provide the energy to drive the endothermic gasification reactions. The principal oxidation reactions occurring during forward gasification are the following:

$$C + O_2 \rightarrow CO_2 \qquad +394 \text{ kJ/mol} \qquad (1)$$

$$C + \tfrac{1}{2}O_2 \rightarrow CO \qquad +111 \text{ kJ/mol} \qquad (2)$$

$$CO + \tfrac{1}{2}O_2 \rightarrow CO_2 \qquad +283 \text{ kJ/mol} \qquad (3)$$

These oxidation reactions consume the available oxygen over a zone thickness of 0.3 m or less. Reaction (2) yielding a combustible gas is favored at temperatures above 1000 K. The endothermic gasification reactions include the steam-char reaction and the carbon dioxide reduction reaction:

$$C + H_2O \rightarrow CO + H_2 \qquad -131 \text{ kJ/mol (steam-char reaction)} \qquad (4)$$

$$CO_2 + C \rightarrow 2CO \qquad -172 \text{ kJ/mol} \qquad (5)$$

The fact that water influx into the combustion cavity both promotes the steam-char reaction given by (4) and competes for process heat for vaporization implies that there is an optimum ratio of water influx to air or oxygen injection rate which maximizes the product gas heating value.

Downstream from the reaction zone, the hot product gases heat the coal and cause pyrolysis and drying to occur. The coal is carbonized to form a char in the pyrolysis or devolatilization zone which extends through the region having temperatures of 1200 K to 625 K. The hot product gases and steam can participate in additional reaction in this region:

$$CO + H_2O \rightarrow CO_2 + H_2 \qquad +41.0 \text{ kJ/mol (Water-gas shift reaction)} \qquad (6)$$

$$2CO \rightarrow CO_2 + C \qquad +172 \text{ kJ/mol (Boudouard reaction)} \qquad (7)$$

$$C + 2H_2 \rightarrow CH_4 \qquad +74.9 \text{ kJ/mol} \qquad (8)$$

The water-gas shift reaction given by (6) and Boudouard reaction given by (7) are undesirable since they lower the product gas heating value.

Scope and Organization of this Report

Although UCG technology offers the promise of being able to recover deep, low rank, relatively thin coal seams in a manner which minimizes the environmental impact of recovering such coal deposits, it has been considered to be a high risk technology. The fact that UCG occurs deep underground, thus precluding direct observation, implies that the process must be very well understood in order to achieve good control and optimization. In order to address this need, Professor Robert D. Gunn initiated a research program in UCG in 1975. The following year,

an interuniversity research team was formed under the joint direction of Professor Robert D. Gunn of the University of Wyoming and Professor William B. Krantz of the University of Colorado. This research team, with financial support from the U.S. Department of Energy - Laramie Energy Technology Center and the Electric Power Research Institute, sought to address a wide spectrum of problems associated with UCG technology. This report is a summary of the research results obtained by the Wyoming-Colorado UCG research group during the period extending from 1975 through 1982, during which time this research was supported by DOE Contract nos. DE-AS20-80LC10442 and DE-AS20-82LC10887. This report is not intended to be a review of all the technical literature pertaining to UCG; rather it will focus exclusively on the results of the Wyoming-Colorado UCG research group. In the period 1975 to 1980, about half the research funds were provided by the Electric Power Research Institute (EPRI). No attempt is made here to separate out that portion of research funded by EPRI because all work has been conducted as a single cohesive project.

The scope of the problem areas in UCG technology which are addressed in this report covers nearly all facets of this process. A brief rationale for focusing on these problem areas is appropriate. Since UCG requires some permeability enhancement step prior to actual gasification, Chapter II addresses the subject of reverse combustion linking, the most widely used linking technique employed thus far in the UCG field test program in the U.S. Chapter III then focuses on process modeling of the forward combustion gasification step. The brief summary of the UCG process chemistry given above underscores the importance of water influx in the UCG process. For this reason, Chapter IV is devoted to the water influx modeling efforts of the Wyoming-Colorado UCG research group. The UCG cavity grows laterally because of gasification of the coal and vertically because of spalling of the overburden rock. Whereas the lateral growth determines the resource recovery, the vertical growth influences the water influx, heat losses and surface subsidence. This important topic of cavity growth is discussed in Chapter V. Material and energy balances are among the most powerful tools available to us in interpreting UCG field test data; these are described in Chapter VI. Since large-scale field tests are both costly and time-consuming, carefully designed laboratory-scale experiments provide an attractive alternative for elucidating the physics and chemistry of the UCG process. The laboratory combustion tube studies conducted by this research group are reviewed in Chapter VII. If and when UCG is to be employed commercially depends ultimately on the economics of the process for producing marketable products. The results of the recent economic analysis of this research group are given in Chapter VIII.

Each chapter in this report begins with an introduction which defines the UCG problem area to be addressed. This is followed by a detailed summary of the approach used to address the problem and the principal results of the research. Each chapter ends with a section which focuses on the practical implications of the research results with respect to controlling and optimizing the performance of UCG.

CHAPTER II - REVERSE COMBUSTION LINKING

Role of Reverse Combustion in UCG

Virgin coal seams cannot be gasified underground efficiently by a forward combustion process in which the flame front propagates in the same direction as the gas flow. There are two principal reasons for this. First, the low natural permeability of the virgin coal seam precludes the use of large enough air- or oxygen-injection rates to achieve efficient gasification. Secondly, the tars devolatilized from the coal downstream from the combustion front condense out in the cooler regions of the coal seam, thus partially plugging the formation and further reducing the permeability. For these reasons, a preparatory or linking step is required in UCG to provide one or more channels of high permeability through which the hot tar-laden product gases can pass quickly. This linking can in theory be accomplished by reverse combustion, directional drilling, hydraulic or pneumatic fracturing, or electrolinking. Reverse combustion is the most extensively tested of these linking techniques as it has been used in the majority of the U.S. field tests. Furthermore, if a reverse combustion link can be effected low in the coal seam by a fairly direct path, it represents the most economical method of linking. However, the UCG field test program conducted by the Laramie Energy Technology Center revealed that reverse combustion linking exhibited some apparently anomalous behavior. In particular, the 13 instrumentation wells in the Hanna II Phase II field test indicated that the reverse combustion link consisted of two channels having diameters between 0.76 to 1.1 m (2.5 to 3.5 ft). Furthermore, the Hanna field test program demonstrated that the time required to link by reverse combustion over a fixed well spacing was independent of the rate at which air was injected. The product gas composition during reverse combustion linking also was found to be independent of the air-injection rate. The focus of the initial modeling efforts of the Wyoming-Colorado UCG group was to discern the physics of reverse combustion linking and to develop predictive models for the flame speed and associated linking time, number and size of the channels, and combustion temperature as functions of the gas-injection rate and oxygen content, back pressure, and coal properties.

Modeling Studies of Reverse Combustion Linking

The first predictive model for reverse combustion linking was that of Kotowski and Gunn (1976). This model assumes that the reverse combustion is sustained by the combustion of a portion of the volatile matter driven from the coal by thermal conduction in advance of the combustion front. This devolatilization is assumed to be an equilibrium rather than a rate process such that the amount of volatile matter released is determined solely by the local temperature. The combustion of the volatile matter is assumed to follow Arrhenius type reaction kinetics with a pre-exponential factor assumed to be first order in both the local oxygen concentration and the volatile matter concentration which is treated as a pseudocomponent of the form $C_lH_mO_n$, where l, m and n are specific to the particular coal. The four differential equations

included in this model consist of the thermal energy equation incorporating heat conduction, convection, and generation; the overall mass balance in the gas phase; and species balances on the oxygen and gaseous fuel considered as a pseudocomponent. The reaction zone is very thin, typically 3 cm or less; consequently the pressure variation within the reaction zone is very small. For this reason, the flow which is described by Darcy's law is assumed to be completely decoupled from the thermal, mass, and species balances. These four differential equations are strongly coupled through the temperature-dependent combustion kinetics and physical properties which in this model include the density, enthalpy and heat capacity of the gas phase, and the density, heat capacity, thermal conductivity and devolatilization equilibrium relationship of the solid phase. Kotowski and Gunn invoked the quasi-steady-state approximation for which the relevant equations become independent of time in a coordinate system convected at the flame speed. This approximation allows considerable simplification since it converts the system of partial differential equations into a set of ordinary differential equations in a convected coordinate system. In order to solve this system of equations, Kotowski and Gunn consider two regions, the preheat zone and the devolatilization-combustion zone. An analytical solution is obtained for the temperature profile in the first region which provides a boundary condition for the numerical scheme used to solve the equations in the second region.

Kotowski and Gunn present their model predictions only for the lower pressure conditions characteristic of reverse combustion linking in the relatively shallow Hanna field tests. Britten et al. (1982) have applied the model of Kotowski and Gunn to prediction of reverse combustion behavior at the higher pressures characteristic of linking at great depths. Britten et al. also used their model to study the effect of oxygen concentration on reverse combustion behavior. Figures II-1 and II-2 show the predicted maximum flame temperature and combustion front velocity, respectively, as a function of injected gas flux at back pressures from 300 to 4000 kPa (3 to 40 bar) for oxygen mole fractions from 0.105 to 1.0. Both the maximum flame temperature and flame speed are seen to increase with increasing injected gas flux and increasing oxygen mole fraction. The flame temperature, however, is seen to decrease with increasing pressure, whereas the combustion front velocity is seen to increase.

Both Kotowski and Gunn's model as well as its extension to higher pressures by Britten et al. ignore the effects of vaporization of any water present or injected into the coal seam. The coal seams used in the Wyoming UCG field test program are natural water-bearing zones. Excessive water influx during forward combustion gasification was a problem for many of the Wyoming UCG field tests. The effects of water influx on reverse combustion, however, are less well documented. Lovell (1982) recently has generalized Kotowski and Gunn's model to include the effects of water influx on the propagation of reverse combustion fronts in coal seams. Lovell's analysis shows that the reverse combustion front velocity decreases whereas the maximum flame temperature increases with increasing water influx for a fixed air-injection flux. Under most practical UCG operating conditions, any water injected will be evaporated before it reaches the combustion front. A distinct steam front never

exists in reverse combustion since the vapor pressure of the water at the prevailing local temperature can never equal the total pressure. However, Lovell's analysis shows that the unusual condition of "super wet combustion" is theoretically possible. Under super wet combustion conditions, liquid water passes through the combustion front. In order for this to occur, the maximum flame temperature must be less than the boiling point of water at the prevailing pressure at the combustion front. Hence, super wet combustion can occur only for relatively deep coal seams at low injected air fluxes. The combustion front velocity decreases and the maximum flame temperature increases with increasing water influx rates for super wet combustion conditions as well.

The model of Kotowski and Gunn (1976), its extension to higher pressures by Britten et al. (1982) and Lovell's (1982) analysis of the effects of water influx, shed considerable light on the nature of the reverse combustion process. The following picture emerges. Under normal operating conditions, the reverse combustion process is oxygen-limited. Hence, for a fixed air- or oxygen-injection flux, the rate of combustion of volatile matter and, correspondingly, the rate of heat generation are predetermined for a particular set of coal properties. The flame temperature is determined by the balance between heat generation and heat loss; the latter comprises heat conduction into the uncarbonized coal and heat convection downstream by the product gases. The flame speed, on the other hand, is determined solely by how rapidly heat is conducted upstream into the uncarbonized coal. The effect of any change in process parameters, physical properties, or kinetic parameters thus can be understood then solely in terms of how this change affects the heat generation relative to the heat loss as conduction or convection.

In the development of new technologies such as UCG, the diagnostic capabilities of mathematical models assume great importance. They become an invaluable guide in the development of a physical understanding of the process under investigation. They show which parameters and operating variables affect the process and how these variables interact with each other. If a field test fails, models can indicate what site-specific factors contributed to the failure, what steps, if any, can be taken to solve the problem and what selection procedures are needed to avoid similar failures in future tests. If a field test succeeds, the models may identify those factors contributing to the success of the project and suggest selection procedures to ensure future successes. Models are especially useful for the interpretation of unexpected or anomalous behavior. For example, Figure II-1 shows that at an air flux of 2.5 kmol/hr-m^2, the peak combustion temperature is approximately 100 K lower at 40 bar than at 10 bar pressure. This might appear to be an incorrect prediction; however, this phenomenon has been observed experimentally as well. Intuitively, one would expect that a higher total pressure and, therefore, a higher oxygen concentration would lead to faster reaction rates and higher temperatures, which is the opposite of what is predicted in Figure II-1. However, a closer examination of the mathematical model for reverse combustion provides a physical explanation for this unexpected result. As explained earlier, the rate of heat conduction into the unheated coal ahead of the combustion zone determines the velocity of the combustion front. A high

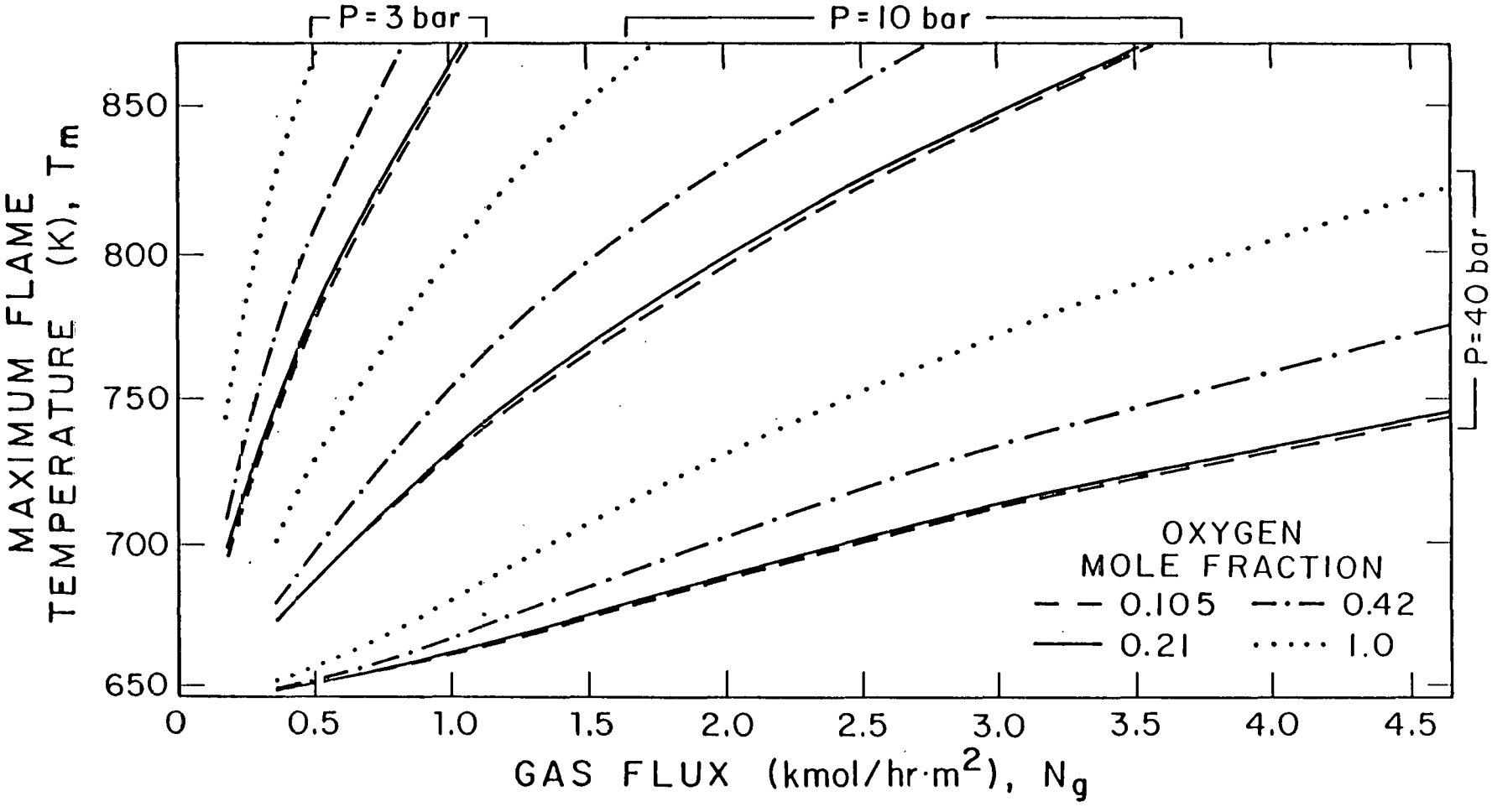

Figure II-1. Maximum Combustion Temperature as a Function of the Injected Gas Flux for Various Back Pressures and Oxygen Mole Fractions

pressure does lead to faster reaction rates for the oxygen and correspondingly steeper temperature gradients. These steeper temperature gradients increase the rate of heat conduction and, therefore, increase the combustion velocities as shown in Figure II-2. An increased combustion front velocity, however, implies the development of a longer carbonized channel within a fixed period of time. For this same fixed period of time, the amount of oxygen supplied is the same for both pressures; hence, the amount of heat generated in both cases is the same. The longer channel, however, contains a larger volume of coal char which had to be heated to the peak temperature. Conservation of energy then requires that this peak combustion temperature must be lower at the higher pressure in order to heat the longer channel with the same amount of energy as that generated at the lower pressure. In summary, higher pressures lead to faster combustion rates, increased combustion velocities and, consequently, lower combustion temperatures.

One difficulty in using the reverse combustion model of Kotowski and Gunn is that the air or oxidant flux is a required input parameter. In an actual UCG operation, only the total air- or oxidant-injection rate (not flux) is known. In order to convert this injection rate into an injection flux, both the number and diameter of the reverse combustion channels must be known. The Hanna field test program revealed that reverse combustion linking proceeds via one or more relatively narrow channels rather than as a broad curved front. It was necessary to develop an appropriate model in order to explain the nature of the reverse combustion channeling process and to predict the number and size of the resulting channels.

Krantz and Gunn (1977) show that reverse combustion in a porous medium such as coal will propagate via one or more channels rather than as a smooth, broad, nearly planar flame front because of the inherent instability of the reverse combustion process. The instability of a process refers to its tendency to change in response to small perturbations or disturbances. In reverse combustion, instability refers to the propensity of a planar one-dimensional combustion front to transform to a system of combustion channels in response to minute perturbations in the operating variables or system properties. These perturbations arise from random pulsations in the flow rate, small-scale heterogeneities in the permeability, thermal conductivity or reactivity of the coal, or from the effect of small cracks and fissures in the coal seam. The linear stability analysis of Krantz and Gunn predicts that a planar reverse combustion front is always unstable; that is, reverse combustion in porous media will not propagate as a planar front but will degenerate into reverse combustion channels. The reason for this is easy to see by referring to Figure II-3, which shows an overhead view of a reverse combustion front separating the uncarbonized coal in region I from the carbonized coal in region II. A perturbation in the planar reverse combustion front causes an intrusion of the high permeability carbonized region into the low permeability uncarbonized region. Hence, a point such as "A" in Figure II-3 experiences an increase in air or oxidant flux at the expense of air or oxidant flux at "B". This local relative increase in oxygen supply leads to faster burning and to further intrusion of the high permeability region into the low permeability region. Progressively more of the air or oxygen flow is intercepted by the flame

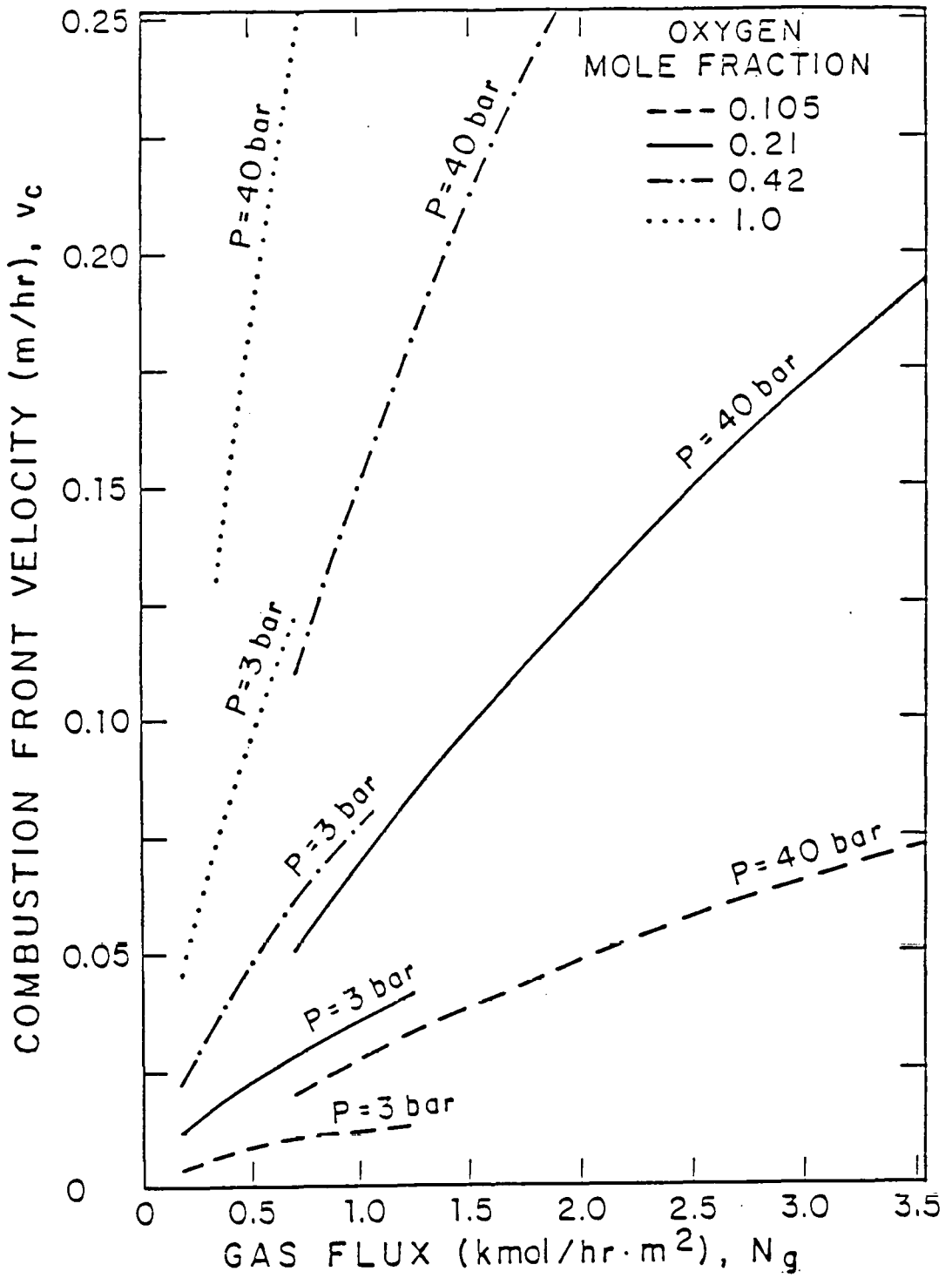

Figure II-2. Combustion Front Velocity as a Function of the Injected Gas Flux for Various Back Pressures and Oxygen Mole Fractions

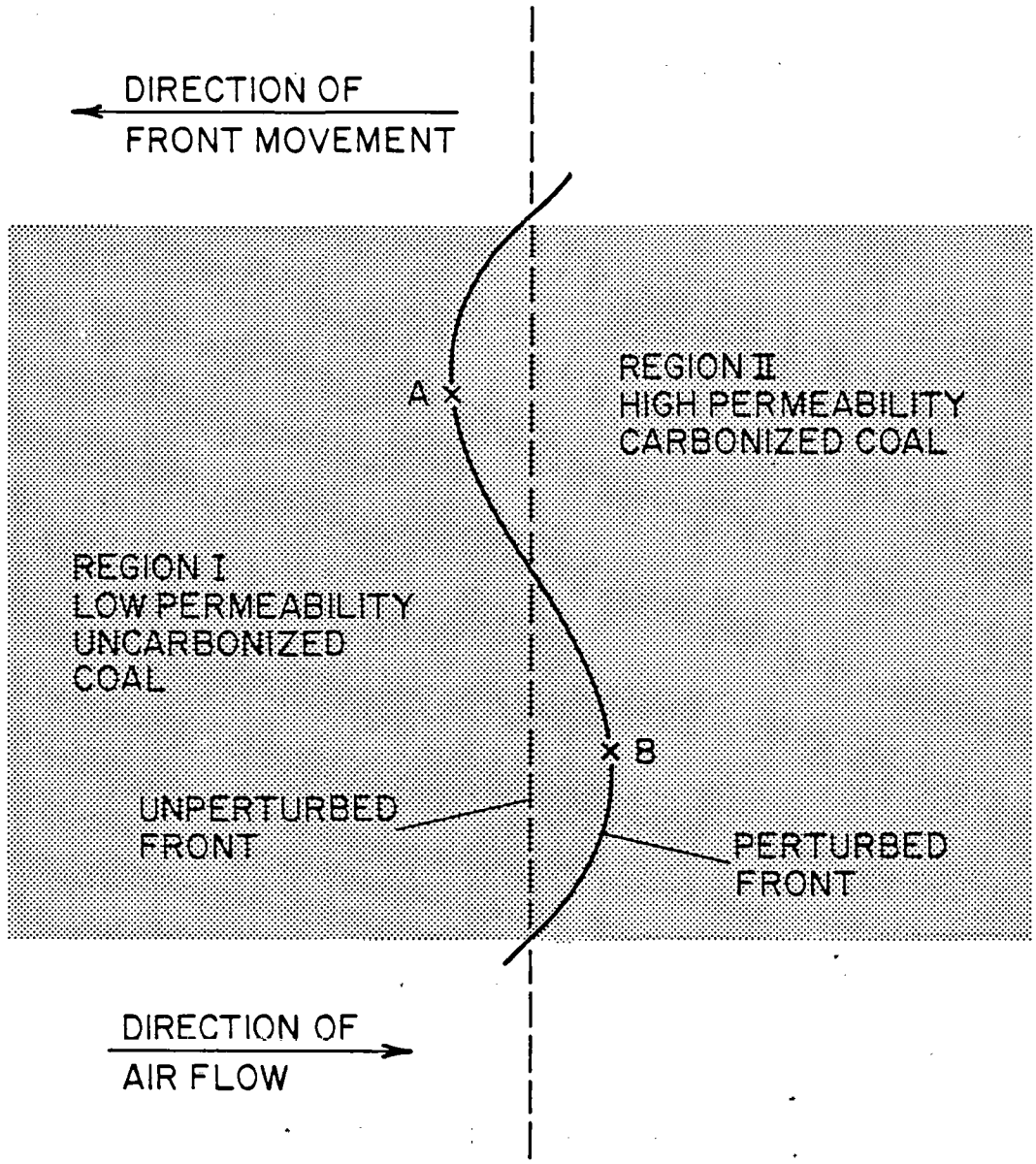

Figure II-3. Overhead View of the Unstable Reverse Combustion Front

surface near point "A" as it advances further into the uncarbonized region relative to point "B". Ultimately, a relatively small diameter combustion channel is formed which intercepts most of the air or oxygen flowing towards the production well. In theory, it is possible for several reverse combustion channels to be generated simultaneously by this mechanism.

Any small amplitude perturbation imposed on the reverse combustion process can be represented by a Fourier integral of sinusoidal wave forms or normal modes having a continuous spectrum of wave lengths. Linear stability theory not only determines if a process is unstable but also determines which modes or wave lengths will propagate or be amplified and which will decay. Among the unstable modes, there is one wave length which propagates most rapidly. This most highly amplified wave length is assumed to determine the diameter of the reverse combustion channels.

The initial reverse combustion stability analysis of Krantz and Gunn (1977) was restricted to conditions such that the ratio of permeability in the carbonized region to that in the uncarbonized region was infinite. In later papers, Gunn and Krantz (1977, 1980) generalized their reverse combustion stability model to encompass a broader range of conditions. The generalized results of this stability analysis are summarized in Figure II-4 which plots the dimensionless wave number or reciprocal channel diameter α versus a dimensionless flow rate $D/(1 - N_4)$ where

$$\alpha = \sqrt{8}\,\pi n_s/\lambda$$

$$D = Bm_I/(T_F - T_0)$$

$$N_R = C_{pg}(T_0 - T_F)/F_{O_2}\Delta H_R$$

in which

$$n_s = k_h(T_0 - T_F)/(F_{O_2}\Delta H_R m_I)$$

k_h = thermal conductivity of the coal

T_0 = ambient temperature in the coal seam

T_F = maximum flame temperature

F_{O_2} = mass fraction of oxygen in injected gas

ΔH_R = heat of combustion per unit mass of oxygen consumed

m_I = mass flux of the injected gas

λ = diameter of reverse combustion channel

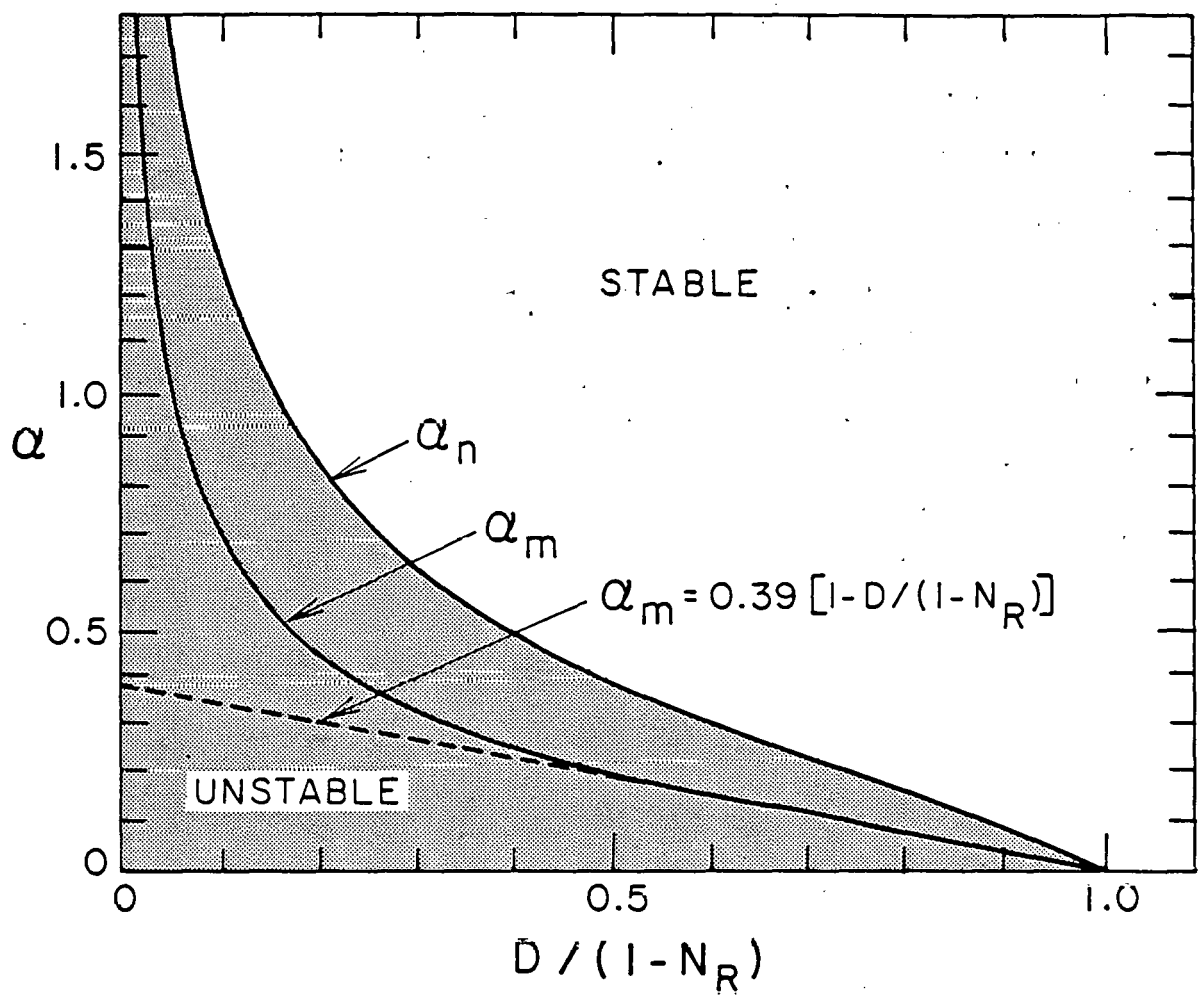

Figure II-4. Neutrally Stable and Most Highly Amplified Combustion Channel Wave Number as a Function of Dimensionless Gas Injection Velocity

B = slope of the maximum flame temperature versus gas-injection flux plot

C_{pg} = heat capacity at constant pressure of injected gas

Any dimensionless wave number which falls within the shaded region below the curve labeled α_n corresponds to a channel diameter which can propagate in reverse combustion. For a fixed dimensionless flow rate on the abscissa in Figure II-4, there is a unique channel diameter which propagates most rapidly; the locus of these most highly amplified wave numbers is denoted by the curve labeled α_m in Figure II-4.

The advantage of Figure II-4 is that it is a generalized plot in terms of dimensionless variables. As such, the results in Figure II-4 are general and apply to reverse combustion channeling in all types of media, not just coal. Whereas a generalized plot is convenient for representing the predictions for a broad class of material properties and operating conditions, it does not provide the clearest picture of the unusual characteristics of the reverse combustion process. For this reason, Krantz and Gunn (1981) applied the generalized predictions in Figure II-4 to the specific case of reverse combustion in the Hanna No. 1 coal seam in which all the Hanna, Wyoming, UCG field tests were conducted. These specific predictions for the Hanna field tests are shown in Figure II-5. The locus of the channel diameter versus air-injection rate can be viewed as a dimensional form of the α_m curve in Figure II-4 where α_m and the abscissa in Figure II-4 have been dimensionalized using the physical properties of the Hanna No. 1 coal seam. However, the plot in Figure II-5 differs from that in Figure II-4 in one substantial respect. The abscissa in Figure II-4 is a dimensionless injection flux, whereas the abscissa in Figure II-5 is a dimensional injection flow rate.

Figure II-5 was prepared by assuming that the total air-injection rate was specified and that two reverse combustion channels were active; these conditions determine a unique channel diameter and air flux within the two channels. The channel diameter is seen to increase markedly with air-injection rate in Figure II-5. For this reason, Figure II-5 shows that the air flux in the channels increases only slightly with the total air-injection rate; recall here that the air flux is the air-injection rate divided by the cross-sectional area of the channel. Consequently, Figure II-5 shows that the combustion front velocity, which is a unique function of the air flux for a fixed set of coal properties, is nearly constant over a wide range of air-injection rates.

Figure II-5 then provides an explanation for the unusual behavior observed for reverse combustion linking in the Hanna UCG field tests. The range of injection air rates for the Hanna II Phases II and III, and Hanna III field tests are shown above the abscissa in Figure II-5. One observes that the air flux and combustion front velocity remained relatively constant over the entire range of air-injection rates during these field tests. These predictions then explain why both the time (approximately 10 days) required to link the 18.3 m (60 ft) distance between wells and the product gas composition remained nearly constant during these field tests despite wide variations in the air-injection

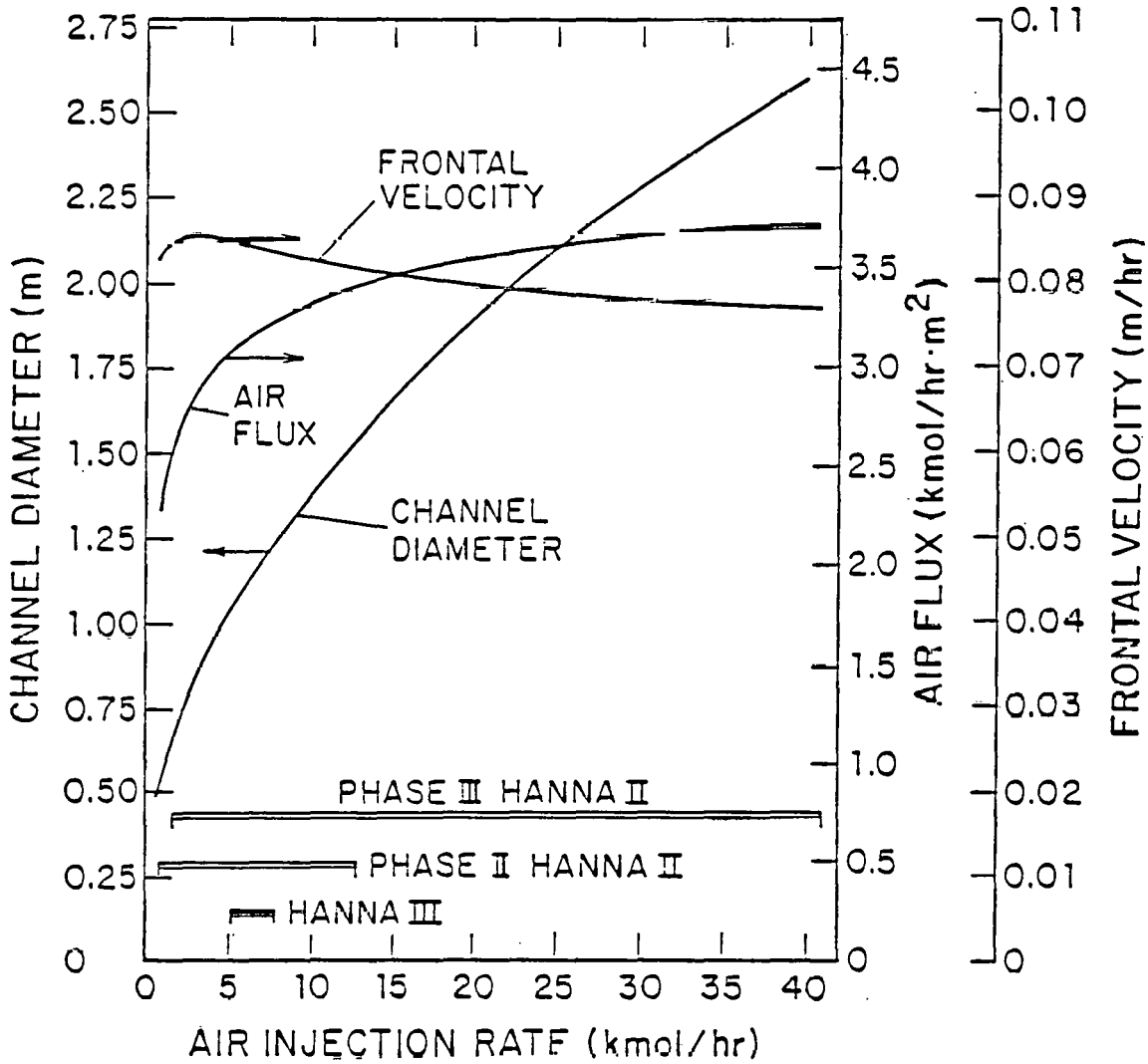

Figure II-5. Reverse Combustion Channel Diameter, Air Flux, and Frontal Velocity as a Function of Total Volumetric Air Injection Rate

rate. That is, the combustion front velocity and correspondingly the linking time as well as the product gas composition are determined solely by the air-injection flux which remained nearly constant during these Hanna field tests because the reverse combustion channel area increased approximately proportional to the air-injection rate. The reverse combustion stability model results summarized in Figure II-5 have been shown by Gunn and Krantz (1980) to predict channel diameters and linking times in good agreement with the Hanna UCG field tests. These results of Gunn and Krantz for the Hanna II Phases II and III, and Hanna III UCG field tests are summarized in Table II-1. Two reverse combustion channels were assumed to be operative for all these Hanna tests in determining the predicted channel diameter and linking time from the measured air-injection rate. The predicted linking time represents the minimum possible linking time since it was determined by assuming that the two links propagate nearly along the 18.3 m line-of-centers distance between the injection and production well bores. Since the two reverse combustion links will undoubtedly follow slightly curved paths, it is not surprising that the predicted linking times are slightly smaller than the measured values.

Several assumptions made in Krantz and Gunn's reverse combustion stability analysis have been considered in more depth in subsequent studies. The analytical solution of Krantz and Gunn evaluated all physical properties including the gas density at the maximum flame temperature. This approximation in particular appears to ignore the large thermal expansion of the injected gas. However, Puri (1979) has utilized an integral transformation on the compressible form of Darcy's equation to show that the stability analysis which includes thermal compressibility effects can be reduced to exactly the same equations as resulted in the analysis of Krantz and Gunn. Hence, the results of Krantz and Gunn are unchanged by the thermal compressibility effects which they omitted.

The original predictions for reverse combustion channeling resulting from the stability analysis of Krantz and Gunn were restricted to the relatively low back pressures characteristic of the Hanna UCG field tests. This limitation arose because the parameter "B" appearing in the abscissa of Figure II-4 had to be determined from the one-dimensional reverse combustion model of Kotowski and Gunn (1976); the fact that the results of the latter model were available only for a pressure of 300 kPa (3 bar) restricted the stability theory results to this same pressure. Britten et al.'s (1982) extension of Kotowski and Gunn's one-dimensional analysis permitted determination of "B" at higher pressures and at oxygen mole fractions other than that for air injection. These revised values for "B" then permitted extension of the reverse combustion stability analysis to linking at higher production well back pressures and variable oxygen mole fractions. The results of Britten et al. are summarized in Figures II-6 and II-7. Figure II-6, which plots the predicted reverse combustion channel diameter as a function of air flux for pressures of 300, 1000, 2000 and 4000 kPa (3, 10, 20 and 40 bar), shows that the channel diameter decreases markedly with increasing pressure. Figure II-7, which plots the channel diameter as a function of injected gas flux at pressures of 300 kPa (3 bar) and 4000 kPa (40 bar), shows that the channel diameter decreases with increasing oxygen

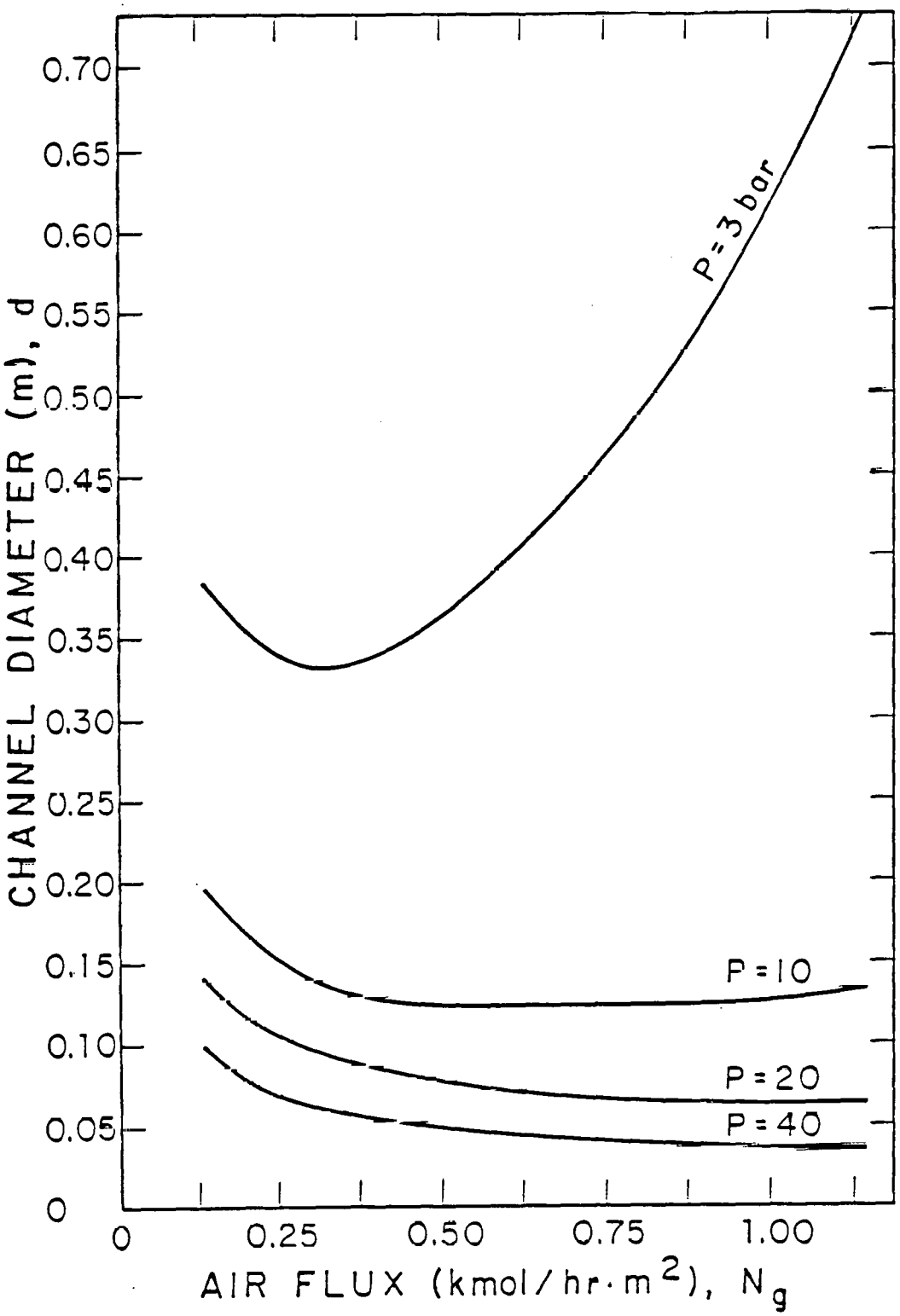

Figure II-6. Predicted Link Diameter as a Function of the Injected Air Flux for Various Back Pressures

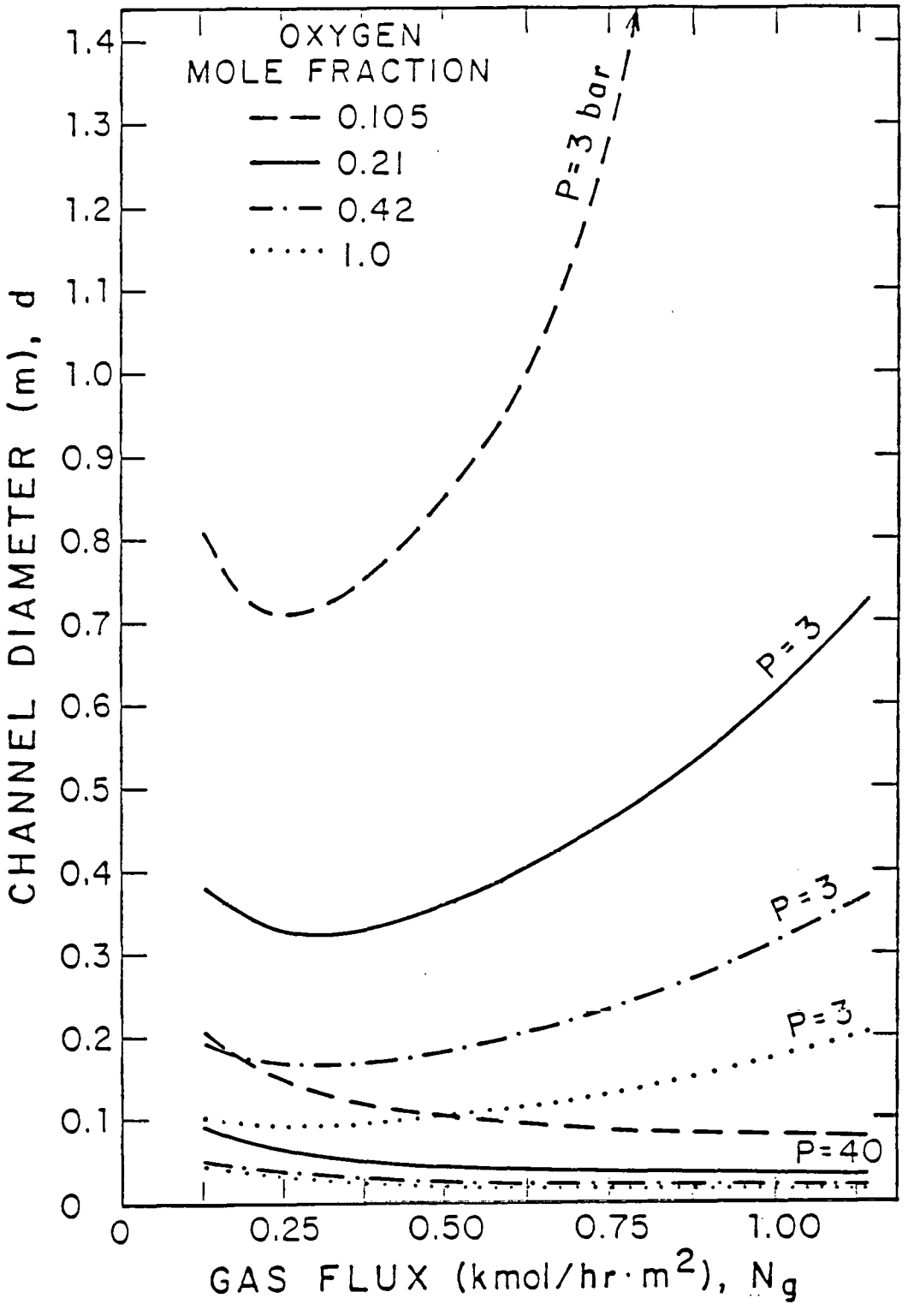

Figure II-7. Predicted Link Diameters as a Function of the Injected Gas Flux for Various Oxygen Concentrations at Back Pressures of 3 and 40 Bar

mole fraction. The effect of increasing oxygen mole fraction is seen to be more pronounced at the lower pressure.

The stability analyses discussed thus far have been restricted to a planar reverse combustion front in the absence of lateral boundaries. Whereas these planar stability analyses can predict the reverse combustion channel diameter, they necessarily imply that an infinite number of channels are generated. In order to predict the number of channels formed, one must consider the initial stages of reverse combustion during which the flame front is expanding approximately radially about the production well. Puri (1979) considered the linear stability of a cylindrically expanding reverse combustion front. A rather tenuous assumption in his analysis was removed in a subsequent analysis by Bumb (1982) who in addition considered the linear stability of a spherically expanding reverse combustion front. Bumb's analyses indicate that there is a minimum air- or oxidant-injection flow rate above which reverse combustion channels will not form initially about the production well bore, but will form only after the reverse combustion front has expanded somewhat about the well bore. At air- or other oxidant-injection rates below the minimum rate for stabilizing the process, the number of channels formed increases as the injection rate is decreased. The effect of either an increase in production well back pressure or oxygen mole fraction is to increase the minimum injection flow rate required for stabilization and to increase the number of channels formed at any lower injection rate. For the conditions appropriate to the initial stages of reverse combustion linking during the Hanna field tests, Bumb's analyses indicate that two to three channels were formed. Although it is not always possible to confirm how many reverse combustion channels are present during a UCG field test, two channels have been inferred for the Hanna II Phase II, Hanna IV-A, Hanna IV-B, and during the initial stages of the Hoe Creek II UCG field tests. Furthermore, Gunn and Krantz (1980) assumed that two channels were present also in the Hanna II Phase III and Hanna III field tests and obtained good agreement for model predictions of the linking time, as shown in Table II-1, thus suggesting that two channels were present during these tests as well.

The reverse combustion stability analyses complete the picture of the nature of reverse combustion linking in coal. The analysis of Krantz and Gunn (1977) indicates that reverse combustion forms channels because of the unfavorable mobility ratio associated with the carbonization process accompanying reverse combustion in coal. That is, the advancing reverse combustion front separating the low permeability uncarbonized coal from the high permeability carbonized coal is unstable to small perturbations due to random variations in flow rate or back pressure, or due to small-scale inhomogeneities in the coal. A local intrusion of the carbonized region into the uncarbonized region will draw additional air or oxygen to itself and thereby can develop progressively into a channel. The number of such channels formed is determined during the initial stages of reverse combustion when the flame front is expanding approximately radially about the production well bore. For any well bore radius, there is a minimum air- or oxidant-injection rate above which channels will not form initially about the well bore, but will form subsequently after the flame front has expanded radially

Table II-1

Stability Theory Model Predictions for Reverse Combustion Linking in the Hanna, Wyoming, UCG Field Tests

UCG Field Test	Measured Average Air-Injection Rate (kmol/hr)	Predicted Average Reverse Combustion Channel Diameter (m)	Predicted Minimum Linking Time (days)	Measured Linking Time (days)
Hanna II Phase II	3.29	0.81	9.1	9.7
Hanna II Phase III	4.2	1.48	9.4	10.2
Hanna III	6.23	1.13	9.1	10.5

somewhat. This is an accommodation effect since, for a fixed well bore radius, there is a minimum injection rate above which unstable modes have a wave length which is too large to permit placing an integral number of wave lengths around the circumference of the radially expanding combustion front. Ultimately the radially expanding reverse combustion front must form two or more channels since the air or oxidant flux decreases as the radius or circumference of the flame front increases. If the air- or oxidant-injection rate initially is above the minimum value required for suppressing channel formation, then two reverse combustion channels will be formed when the flame front expands sufficiently to permit instabilities to grow. This may well explain why two reverse combustion channels have been observed or inferred in most UCG field test operations. Figure II-8a shows two such channels being formed at the reverse combustion front which is expanding radially about the production well bore. As these reverse combustion channels continue to propagate, they begin to bend towards the source of oxygen coming from the injection well as shown in Figure II-8b. Their channel diameter appears to adjust to changes in the air- or oxidant-injection rate such that it is always equal to the wave length of the most unstable mode predicted by the linear stability model. The manner in which changes in the process variables or physical properties affect this channel diameter can be understood solely in terms of how they affect the ratio of heat conduction into the uncarbonized region relative to the heat convection downstream. This follows from the fact that the channel diameter is determined by that mode or wave length which maximizes this ratio for a specified rate of air- or oxidant-injection. Hence, since increasing either the pressure or oxygen mole fraction for a fixed gas-injection rate increases the rate of combustion of volatile matter, it decreases the thickness of the combustion zone and hence steepens the temperature gradient at the combustion front. Hence, either an increase in pressure or oxygen mole fraction will decrease the diameter of the reverse combustion channels. Increasing the pressure or oxygen mole fraction while holding the total flow rate of oxygen constant should also result in an increase in the number of reverse combustion channels which are initially formed. That is, if the diameter of the most unstable mode decreases, then a larger integral number of wave lengths can be generated in the reverse combustion front expanding about the production well bore. On the basis of these considerations, one might infer that increasing the liquid water-injection rate will result in larger channel diameters. This follows from the fact that increasing the water-injection rate for a fixed oxidant-injection rate decreases both the oxygen mole fraction upon vaporization of this water as well as decreases the temperature gradient since energy is required to heat and vaporize this water.

Implications of the Reverse Combustion Modeling Studies

The modeling studies which have been discussed here not only provide an understanding of the reverse combustion linking process, but also suggest operating procedures whereby the linking process can be optimized and coal recovery increased. The questions which any modeling study of reverse combustion linking must address include how can linking be achieved more rapidly; how can plugging of small diameter links be

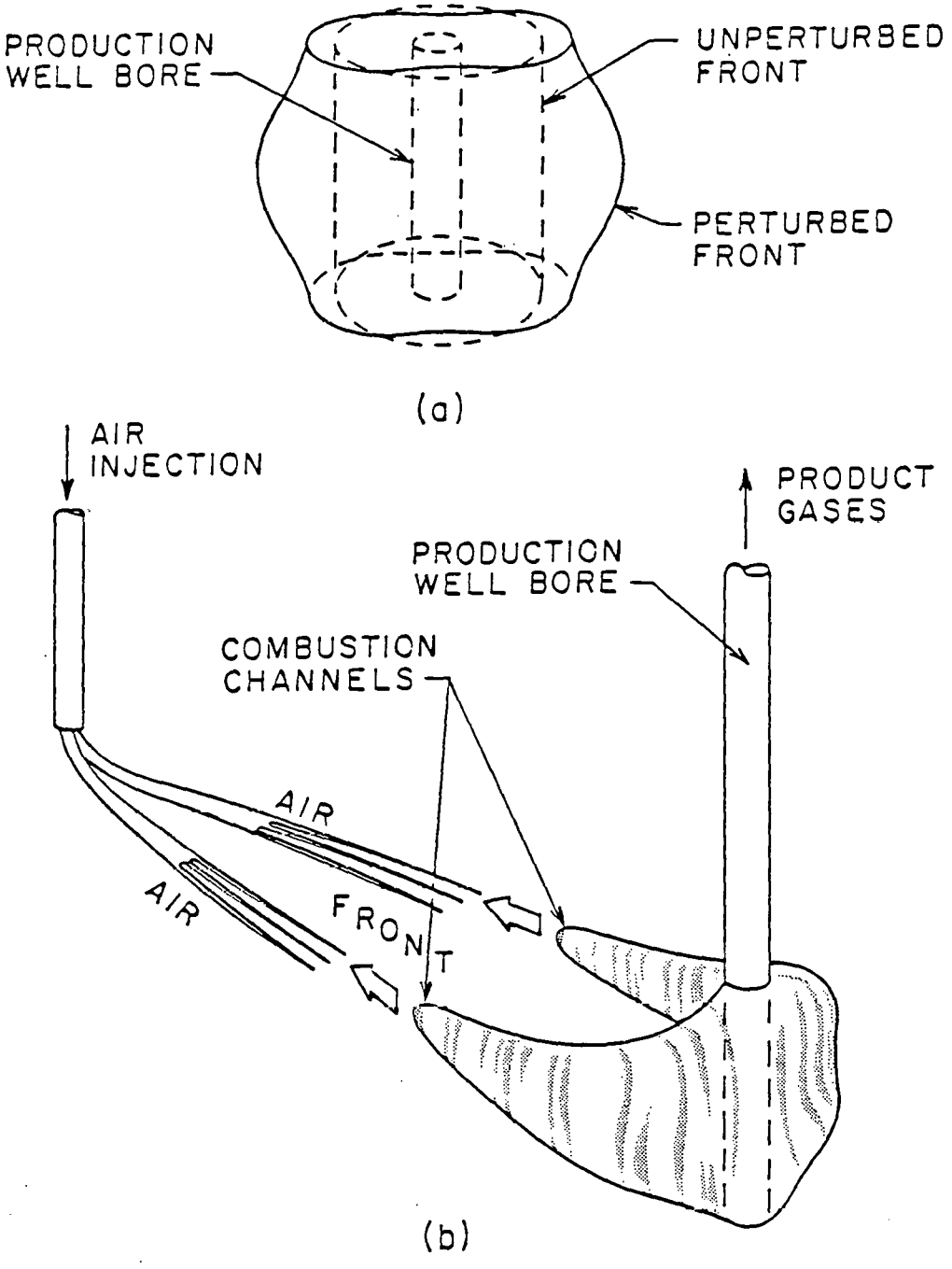

Figure II-8. (a) Initial Stages of Radially Expanding Reverse Combustion Front Showing Development of Two Diametrically Opposed, Three-Dimensional Reverse Combustion Channels; (b) Subsequent Migration of These Channels Towards Air Injection Well

avoided; how can the reliability of linking be improved; and how can linking be effected so as to increase the resource recovery achieved in the subsequent gasification step in UCG. Each of these application areas of the modeling studies will be addressed briefly.

The modeling studies indicate that, at least in the Hanna UCG field tests, the cross-sectional area of the reverse combustion channels which formed was nearly directly proportional to the total air-injection rate per channel. For this reason, the air flux in each channel remained nearly constant. Therefore, the flame speed and hence the linking time, as well as the product gas composition, remained nearly constant during reverse combustion linking in all the Hanna field tests despite wide variations in the total air-injection rate. This nearly direct proportionality between channel area and total air-injection rate per channel for the Hanna tests was a somewhat fortuitous consequence of the physical properties of the Hanna No. 1 coal seam and the relatively low pressure used for these field tests. At higher pressures or for linking in other coal seams, a dependence of both the linking time as well as product gas composition on total oxidant-injection rate is indeed possible. At higher pressures, the modeling studies suggest that the channel diameter and hence its area remain nearly constant as the total oxidant-injection rate is increased. This would imply that at higher pressures, linking times can be decreased by increasing the oxidant-injection rate. Theory also suggests that an increase in either the production well back pressure or the oxygen mole fraction will decrease the channel diameter and thereby decrease the time required for linking.

Decreasing the linking time by decreasing the channel diameter and thereby the flame speed is only practicable under conditions such that the link diameter remains sufficiently large to assure effective communication between the wells. The modeling studies indicate that reverse combustion may become ineffective as a primary means of linking at the high production well back pressures characteristic of the very deep UCG operations being considered. This follows from the fact that the channel diameter progressively decreases with increasing pressure. Excessively small diameter links undoubtedly have a tendency to plug more easily due to condensation of tars and volatile matter; furthermore, they are more likely to follow deviated linking paths since they will be more strongly influenced by small-scale cracks and fissures in the coal. For very deep UCG operations, particularly in swelling bituminous coals, it may be necessary to effect initial linking by directional drilling, fracturing or electrolinking. However, reverse combustion may still be needed to enlarge the diameter of the primary link. The modeling studies suggest some steps which can be taken to ensure that the channel diameter effected by either primary or secondary reverse combustion linking will be as large as possible. Clearly, theory suggests maintaining a production well back pressure which is as low as is compatible with the formation conditions. Reducing the oxygen mole fraction in the injected oxidant flow or injecting liquid water as well will tend to enlarge the reverse combustion link diameter.

The principal criticism of reverse combustion as a means of linking in UCG is that it is unreliable. Yet, the UCG field test program in the U.S. has demonstrated that when a reverse combustion link can be a-

chieved low in the coal seam by a fairly direct path, the subsequent forward combustion gasification will be successful. Again the theory developed here suggests some means to increase the reliability of reverse combustion linking. These studies indicate that the number of links is determined during the initial stages of reverse combustion when the flame front is expanding approximately radially about the production well bore. It is likely that many of the problems associated with reverse combustion linking originate in the inability to initiate two or more well-defined links. Poor well-bore completions or casing techniques in many cases may result in a relatively impermeable zone immediately around the well bore, thus making the initiation of channels difficult. Radially directed cracks resulting from drilling the production well bore may also cause small diameter links to propagate via many indirect paths towards the injection well. The theory suggests that initiation of reverse combustion channels can be delayed by maintaining oxidant-injection rates above the minimum injection rate required for stabilizing the process to channel generation. This would permit the reverse combustion front to expand to a larger diameter by an approximately radially expanding combustion process. After the combustion front has expanded radially somewhat, the oxidant-injection rate then can be decreased below the minimum injection rate required for stabilization at that diameter in order to initiate a few links of relatively large diameter. These larger diameter links are less likely to be influenced by small-scale cracks and fissures. Another means suggested to improve the reliability of reverse combustion linking is to predrill the desired number of links into the coal surrounding the production well bore at least for a meter or two. The cornering water jet drill is a promising tool for initiating these links. Theory suggests that subsequent reverse combustion will follow the paths dictated by these predrilled links. Preliminary electrolinking may also provide a possible technique for predetermining the number and direction of the reverse combustion links.

The techniques employed to improve the reliability of reverse combustion linking are closely coupled to techniques that can be used to increase the resource recovery achieved in UCG. The UCG field tests in the U.S. suggest that the forward combustion gasification in UCG tends to sweep down a path dictated by the linking technique used. The field tests suggest that if the included angle between the two reverse combustion links can be increased, then more coal will be gasified for the same well bore spacing. Indeed, the increased resource recovery potentially possible with multiple curved link paths is one advantage of reverse combustion linking over techniques, such as directional drilling, which link by a single straight link path. The modeling studies of the initial stages of reverse combustion linking indicate that although two links are most probable under the conditions of the Hanna field tests, more links are possible. Clearly, downhole drilling techniques provide the possibility of controlling both the number and direction of the reverse combustion links. Laboratory scale studies are needed at this time in order to determine just how effective predrilling might be in improving both the reliability and resource recovery associated with reverse combustion linking.

CHAPTER III - FORWARD COMBUSTION

After linking is completed so that air can be injected at sufficiently high rates to achieve efficient gasification, forward gasification or synonymously, forward combustion, is initiated. This is the major gas producing step in underground coal gasification. Typically, 97 to more than 99% of the total gas produced will be produced during this stage.

Reverse combustion was used as the linking method for all of the Hanna field tests. Once the reverse combustion front reaches the gas injection well, the source of oxygen, it reverts automatically to forward combustion and begins burning back toward the production well. For reasons explained later, this is an incomplete combustion process which produces a fuel gas rather than purely combustion products. Important chemical reactions and other aspects of the process have been discussed already in Chapter 1.

The Necessity of a Forward Combustion Model

The first research carried out in this project was the development of a one dimensional model for forward gasification. By 1975, the need for such a model was overwhelming. The data from the Hanna I and Hanna II Phase I field tests were very puzzling and superficially impossible to interpret. Originally, these tests were expected to utilize only a small amount of coal; and the gas heating value was expected to be very low. These expectations were based on the nearly universally unfavorable results from a number of tests conducted in the United States and in Europe during the 1950's. When the results from the first two Hanna tests proved to be very favorable, it was believed by many that either serious measurement errors had occurred or that the Hanna site was unique and that the favorable results could not be reproduced anywhere else. In 1975, there was virtually no understanding of the process and no knowledge of what physical or chemical parameters influenced the data. No one knew why field tests failed or performed successfully, why the gas quality was good or bad or how a good gasification site should be selected. In almost all tests including the Hanna tests, the gas heating value gradually declined over time from high initial values; and the reasons for this behavior was unknown. Consequently, it was not known if this behavior could be eliminated or alleviated. The major goal, therefore, in model development was to determine what physical or chemical characteristics controlled the behavior of underground coal gasification.

As shown later in this chapter, the successful development of a forward gasification model provided a major breakthrough in understanding of the process. Model calculations have clearly shown that the Hanna field site was a favorable one but by no means unique. Without the technical analyses based on models developed in this work, the Hanna field test data would be confusing and not very informative especially relative to underground coal gasification at other potential sites. In underground coal gasification, model analyses are especially important.

Because of the remoteness of the gasification zone and because of high cost, field tests are always limited. Needed data are often largely unobtainable, direct observation is virtually impossible, simulation is an inexact science and successful data interpretation without models is nearly impossible. These difficulties have led to a tendency in the Soviet Union and elsewhere to develop UCG technology based only on empirical field observations gained from many field tests. Aside from the extremely high cost, this approach has led to many unexpected failures and to a lack of reproducibility in field test data.

Type of Process Modeled

Model development prior to 1975 had been very limited. None successfully reproduced field test behavior, and almost all effort had been devoted to modeling the burning at the walls of an open channel. The forward gasification model undertaken in this project was based on the concept of gasification in a packed bed, which was a radical departure from previous efforts. However, a large body of experimental data indicated that in the permeable, shrinking, subbituminous coals of the Hanna basin, UCG was in fact a permeation or packed bed process. It is well known in the chemical engineering profession that in packed bed processes such as distillation, liquid-liquid extraction, adsorption and chemical reaction the efficiency of these operations is very high. When channeling develops in these processes, however, there results a serious decrease in efficiency. Additional differences between packed bed and open channel gasification are listed below.

	Property Affected	Characteristics of Open Channel Gasification	Characteristics of Packed Bed Gasification
1.	Gas heating value	Relatively low, and sensitive to air flow rate.	High, insensitive to air flow rate
2.	Production gas temperature	High, due to partial oxygen by-pass and subsequent burning of the product gas in or near the production well.	Relatively low
3.	Thermal efficiency	Low, due to partial oxygen by-pass.	High
4.	Resource recovery	Low, due to increased oxygen by-pass as channel grows wider.	Excellent
5.	Particulate production	High, with a predominance of larger particles.	Low, a predominance of fine particles

6. Similarity to Lurgi gasification, a proven packed bed process.	Dissimilar		Very similar

In all six categories above, the Hanna II Phase I field test essentially reproduced the characteristics of a packed bed process. This mimicking of packed bed gasification explains the high gas heating value, the excellent resource recovery and the other favorable performance characteristics of the Hanna field tests. Earlier field tests performed in Western Europe and the United States were carried out predominantly in swelling, nonpermeable, bituminous coals. Almost certainly, extensive channeling occurred in these processes; and correspondingly poor results were obtained.

An examination of Figures III-1 and III-2 helps to clarify the reasons for the differences between packed bed and channel gasification. Figure III-1 shows the forward combustion of a packed bed. Air or oxygen flowing toward the right first contacts devolatilized coal which burns essentially to completion. This process produces carbon dioxide and a large amount of heat which is needed to drive the endothermic gasification reactions. As the oxygen is depleted, carbon dioxide and steam begin reacting with the coal char to produce carbon monoxide and hydrogen according to the reactions:

$$C + CO_2 \rightarrow 2\ CO$$

$$C + H_2O \rightarrow CO + H_2$$

As carbon monoxide and hydrogen are produced, the temperature of the flowing gases drops rapidly as their heat content is absorbed by these highly endothermic reactions. With the decrease in temperature, there is an exponential decrease in the reaction rate until the temperature profile with respect to distance is nearly flat. This produces the first plateau in the temperature profile shown in Figure III-1. The hot gases flowing further along the packed bed vaporize the water in the coal, heat the solid to reaction temperature, and devolatilize the coal. This devolatilization process further enriches the fuel content of the flowing gases by adding substantial amounts of tar vapors, methane, hydrogen, carbon monoxide and smaller amounts of heavier paraffins and olefins. The temperatures in this region are generally below 800 K (1000°F) and chemical reactions are less important; however, some hydro- and thermal-cracking of tars will occur to produce methane and other gases and some methanation will occur according to the reaction

$$CO + 3\ H_2 \rightarrow CH_4 + H_2O$$

Because the reaction temperatures are relatively low and reaction rates are slow, the catalytic nature of the coal ash and char are probably very important in determining how much methane is formed.

Figure III-2 shows the substantially different channel gasification. Air or oxygen flows down the central channel and is convected by

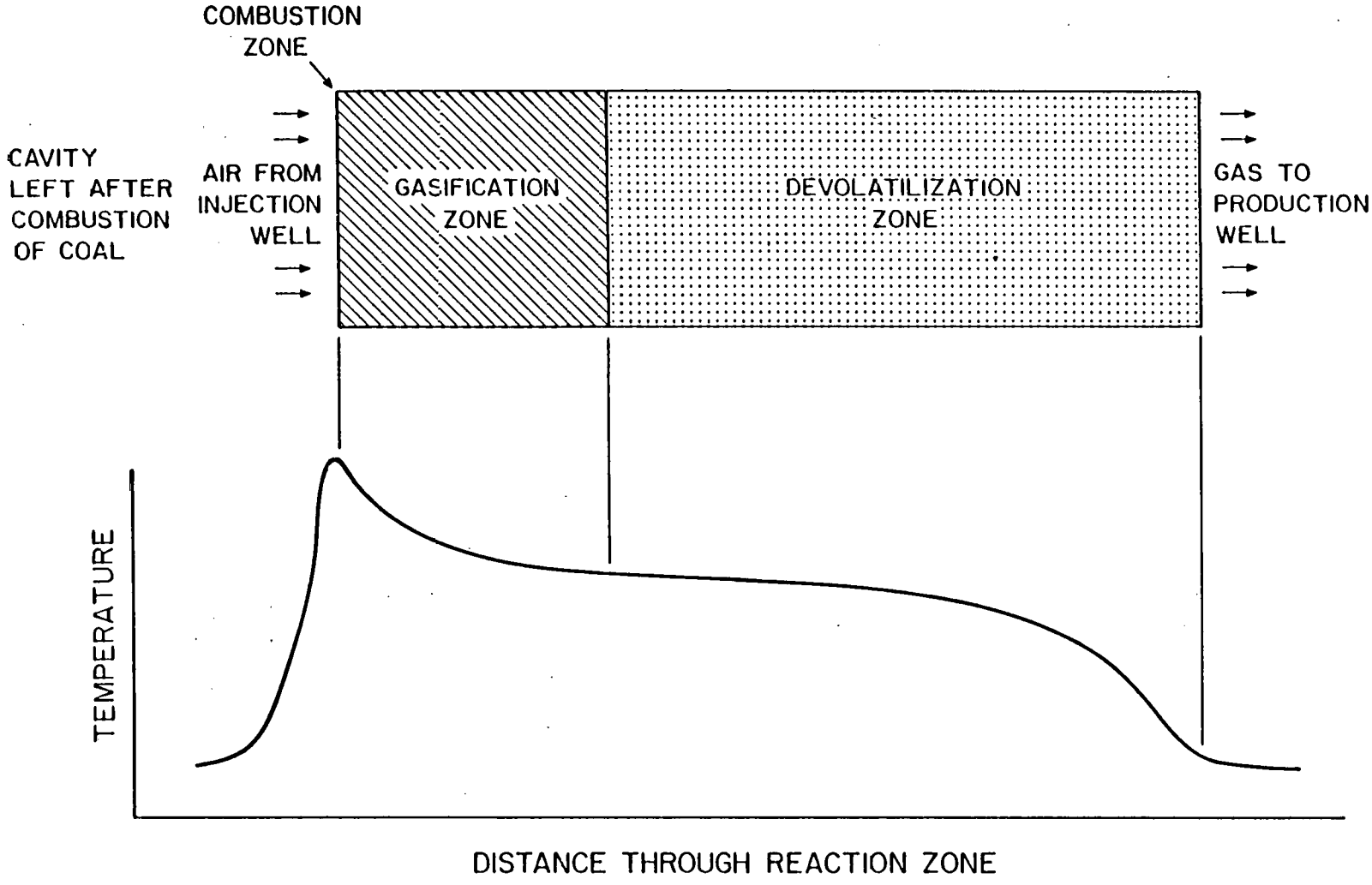

Figure III-1. Schematic Diagram of the Gasification of a Packed Bed

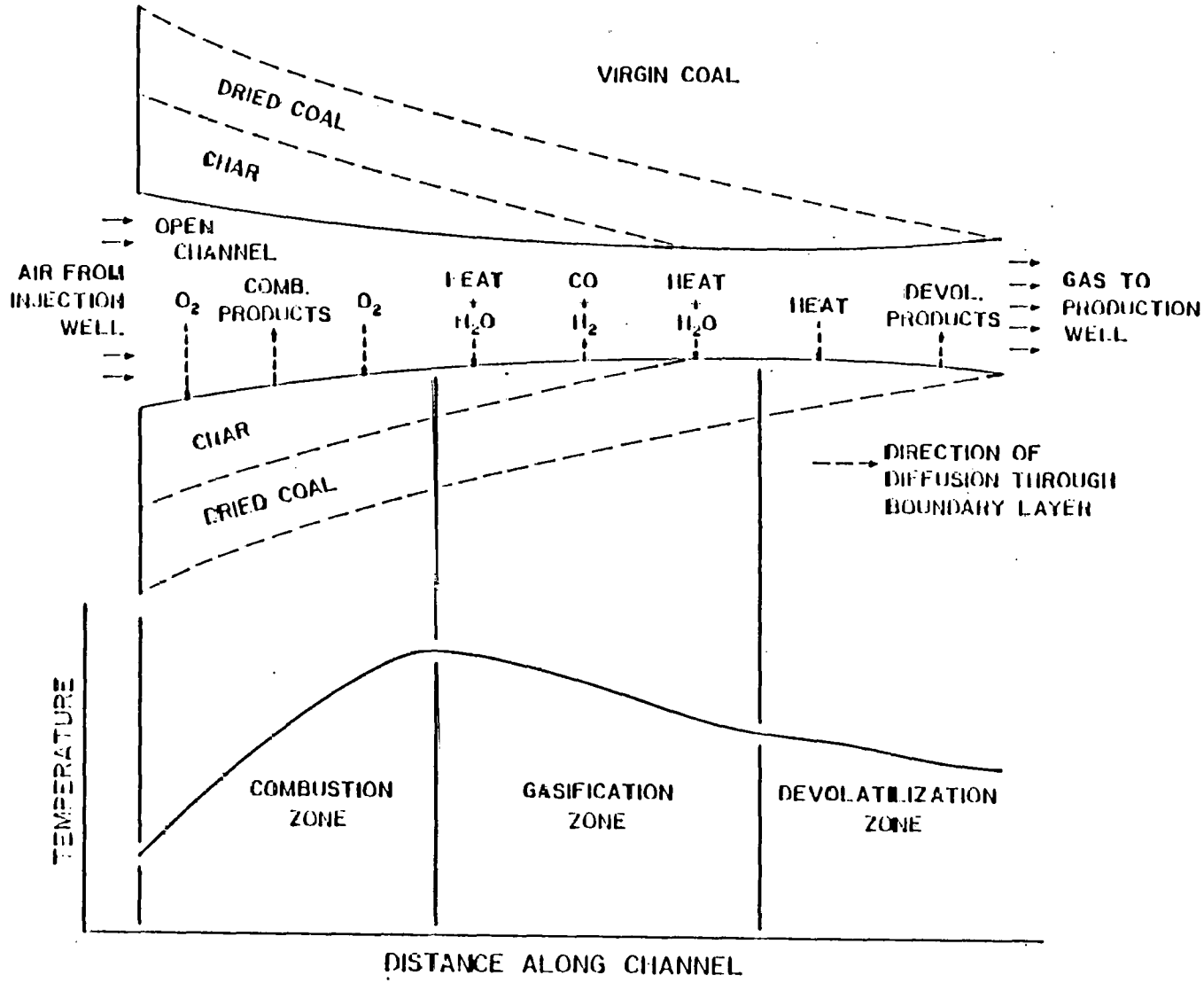

Figure III-2. Schematic Diagram of Coal Gasification in an Open Channel

turbulent flow to the boundary layer along the channel wall. The oxygen diffuses through the boundary layer to the solid surface and reacts. The hot combustion gases diffuse back through the boundary layer to the channel. Further down the channel the oxygen is depleted, and the heat generated begins to drive the usual gasification reactions. Heat and water vapor diffuse through the boundary layer to the solid interface; devolatilization products and products from the water gas reaction diffuse outward into the bulk gas phase. Any oxygen remaining in the mainstream will react with the combustible components and degrade the gas heating value. Much particulate matter spalling from the solid face is carried in the gas stream to the surface whereas in the permeation process (Figure III-1) the particulate matter tends to be filtered out by the packed bed and remains underground.

In packed bed gasification, the combustion front moves slowly down the bed parallel to the flow of gases as shown in Figure III-1. Hot combustion gases always have intimate contact with the unburned coal ahead of the combustion zone until the fire breaks through to the production well. In channel gasification, the combustion zone moves outward at nearly right-angles to the flow of air and combustion gases. As the walls of the channel move farther apart, problems of oxygen by-pass become increasingly severe. In addition, the process is sensitive to the air/oxygen flow rate because the characteristics of turbulent mixing in the channel and the thickness and characteristics of the boundary layer are sensitive to gas velocities as well (Schlichting, 1948).

Obviously, the differences between channel and packed bed gasification are considerable. One of the best ways to determine if UCG is proceeding via packed bed or channel gasification is to test field data with values predicted by a packed bed model. Close agreement then indicates that UCG is proceeding by the process modeled.

Model Description

The mathematical model developed for forward gasification consists of 10 time dependent, tightly coupled partial differential equations. These are an energy equation and nine continuity equations (mass balances) for inert gases (nitrogen and argon), oxygen, carbon monoxide, carbon dioxide, hydrogen, water vapor, methane, ethane and devolatilization products from the coal which are lumped together as a single pseudocomponent. An algebraic or macroscopic material balance on the solid is used to determine combustion front velocities. More detail and derivations of the model have been presented by Gunn and Whitman (1976), Gunn et al. (1978) and by Whitman (1978).

The model is essentially that of a packed bed chemical reactor with several modifications for coal. To reduce the model to a reasonable level of complexity, a number of simplifying assumptions are necessary. The more important of these are discussed here.

The pressure drop across the reaction zone is small and, therefore, the momentum equation can be decoupled from the model and ignored. In

permeable coals, the gases flow through the cleats. These cleats are closely spaced, and it is assumed that gas temperature and the temperature of the adjacent solid are the same. To a good approximation, then, the energy balance for the solid and for the gaseous phase can be lumped together in a single relationship.

The solution to a set of 10 coupled partial differential equations presents a formidable task; however, it has been observed in combustion tube experiments and in field tests that the UCG process tends to operate at nearly steady state conditions for periods of hours and even days.

Combustion tube experiments have clarified the reasons for nearly steady state conditions. Drying of the coal, devolatilization and chemical reactions are all controlled by temperature. During UCG a thermal wave is formed which gradually travels through the coal bed toward the gas production well. The shape of the thermal wave tends to change very little. Since the shape of the wave remains unchanged, the processes occurring at each temperature level in the moving wave remain unchanged in time, and an apparent steady-state or psuedo-steady-state condition prevails. Under these conditions in a one-dimensional system, it is possible to transform the mathematical model to a moving coordinate system which converts partial differential to ordinary differential equations, a major simplification of the problem. This transformation is:

$$\eta = x - vt \qquad \text{III-1}$$

where, x = fixed spatial coordinate

t = time

v = velocity of thermal wave or combustion front

η = coordinate system moving with frontal velocity v

With this transformation, the resulting ordinary differential equations can each be integrated once analytically. The final mathematical model, consists of ten algebraical mass balance equations and a first order differential energy equation. Because of the tightly coupled, nonlinear nature of the equations, it is necessary to solve the entire system simultaneously by trial and error finite difference integration; nevertheless, this represents a major simplification compared to a solution of the original partial differential equations.

Modeling of a process such as UCG presents other potential problems. The physical properties of coal tend to vary widely over short distances even in a single coal seam. For example, in the Hanna No. 1 seam, the coal heating value varies as much as 3500 to 28,000 kj/kg (1500 to 12000 Btu/lb) over a 15 cm interval. Thus, it becomes possible to predict UCG behavior at a specific location only if the coal properties are known at that specific location. For large field tests such detailed information is not known. Fortunately, coal properties averaged across the entire seam are much less variable. For example, the

heating value of ash free Hanna No. 1 coal averaged across the entire seam thickness has been shown to vary by less than 3% between locations a kilometer apart. For these reasons, it probably will never be possible to predict UCG behavior at a single location, but it is possible to predict average UCG behavior for the coal seam as a whole. Gas heating value at the production well is one example of the type of average behavior that can be predicted, because this is the average heating value of all of the gas coming from myriad different flow paths within the coal seam.

Guiding Principles in Model Development

It is emphasized here that in the early stages of research the major objective of the modeling effort is not the quantitative prediction of field performance. In the specific case of UCG, the initial major objective must be to determine the governing physical and chemical phenomena controlling the process; to determine what parameters are important in site selection; to determine how controllable variables such as gas injection rate, pressure and injection gas composition affect the process; to determine the physical cause of specific problems and to provide potential solutions to those problems. A well-conceived, theoretical model can provide information of this sort. First, however, the model must be proved valid; and this can be accomplished only by testing with experimental data for the process being modeled.

The importance of the testing procedure cannot be overemphasized, and the field of quantum theory provides a graphic example of this. Rayleigh and Jeans developed an unusually elegant thermodynamic model for black body radiation; yet, when compared with experimental data, the theoretical model predictions were so bad that the Rayleigh-Jeans theory has been nicknamed the "ultraviolet catastrophe". Knowledge of the model has persisted for more than 80 years only because of the rigor and elegance of its derivation. To physicists of the early 20th century, the black body radiation model of Planck violated common sense and was intuitively unsatisfactory. Yet, Planck's theory eventually launched the entire field of quantum mechanics and now has been accepted by scientists everywhere. It was Planck's theory, improbable as it seemed, which correctly predicted the experimental data.

The following question expresses a second consideration in model development. Can a model which correctly predicts experimental results nevertheless be incorrect? As explained below, the probability of this happening is infinitesimal. Out of thousands of theories that have been advanced, the authors know of only one case in the whole field of the physical sciences when this has occurred. The BET adsorption isotherm has proved useful in fitting nonhomogeneous adsorption data for which the theory used in the derivation is incorrect. The BET theory has proved inaccurate in fitting homogeneous adsorption data for which the derivation is correct. Brunauer, Emmet and Teller, authors of the BET isotherm, recognized the shortcomings of the theory from the outset. The BET theory worked partly because of cancelling physical effects and partly because a relatively simple curve was being fitted with the aid of two empirically adjusted constants, that is, the BET model is primar-

ily a curve-fitting equation.

The number of curve-fitting parameters represents a third consideration in modeling. It is indeed possible to fit an incorrect theory to experimental data provided that enough adjustable parameters are available. Therefore, the development of a good theoretical model requires that curve-fitted constants be held to an absolute minimum and that the model be tested over as wide a range as possible. The forward gasification model discussed in this chapter contains no curve-fitted parameters. The only input data which is used are variables controlled by the operator such as air injection rate or pressure or are chemical and physical parameters for the coal seam. These parameters have all been measured experimentally for the Hanna No. 1 coal seam or have been taken from correlations in the literature for coals similar to those found in the Hanna Basin. The model has been tested on a daily basis for four Hanna field tests conducted over a wide range of conditions. The model reproduced experimental data quite well except for the initial 24 hours of the test and for the last few days of a test.

Model limitations represent the final consideration discussed here. All models have some limitations. Major limitations for the forward gasification model are that it is restricted to a steady-state, packed-bed, forward gasification process. The Hanna I field test data were not used because the complexity of the well system used resulted in simultaneous forward and reverse combustion. The initial start-up period is not correctly predicted because nonsteady conditions prevail. During the final days of a test, it is believed that channeling of the combustion front toward the gas production well begins to occur, and the packed bed assumption begins to break-down. Most of the Hanna IV field test was spent in the reverse combustion mode. The reverse combustion link rose to the top of the seam which led to channeling during the forward gasification phase and a consequent rapid deterioration in gas quality. Because of the channeling during forward gasification, the packed bed model is not applicable.

Field Analyses

The development of the forward gasification model as well as much of the field analyses were supported by the Electric Power Research Institute. Consequently, a summary of the field test analyses has been included in a report to EPRI (Gunn, 1984). Some of this information is reproduced here for the sake of completeness and continuity in this report.

Gunn and Whitman (1976) reported a comparison of forward gasification prediction with experimental data from the Hanna II Phase I field test. The comparison was made on a daily basis for the entire test. Agreement was good, however, this test was less thoroughly instrumented than subsequent tests; and data from the Hanna II Phase I test is less accurate. Only Table III-1 is reproduced here from the report cited.

Gunn, Whitman and Fischer (1978) reported the comparison of calculated and experimental data for the Hanna II Phase II field test.

Table III-1

Comparison of experimental and calculated data for June 10, 1975 (Hanna II Phase I field test). Ref. Gunn and Whitman, 1976.

Type of Data	Field Test Results	Calculated Data
Gas Compositions (mole %)		
Hydrogen	18.57	18.60
Methane	4.10	4.92
Nitrogen & argon	47.81	47.13
Carbon monoxide	16.35	15.83
Carbon dioxide	12.33	13.29
Hydrogen sulfide	0.04	0.07
Ethanes and heavier	0.80	0.14
Gas Production Rate M^3/day	73,100	73,300
Gas Prod. Temperature, °C	256	278
Maximum Reaction Temperatures, °C	1013, 1022 1024*	1066
Gas Heating Value, Kj/m^3	6735	6500
Cold Gas Efficiency, %	89.2	87.4

*Temperatures from three different thermal observation wells.

Figures III-3 and III-4 show the comparisons for the gas heating value and the gas production rate respectively. Figure III-5 shows the comparison of experimental and calculated gas compositions for methane and hydrogen. Figure III-6 is a similar comparison for inert gases (nitrogen plus argon) and for carbon monoxide. Figure III-7 shows the comparison for carbon dioxide. In all cases, there is good agreement between experimental and calculated results with maximum deviations on the order of 3 to 4 mole percent except for carbon dioxide.

Gunn, Fischer and Whitman (1978) also carried out a parametric study of the model used. Any realistic model for UCG must contain a number of temperature dependent properties of ash, coal char and coal such as heat capacity, thermal conductivity, density, devolatilization characteristics and reaction rate constants. Much of this data is not available for Hanna coal, and it is necessary to resort to values reported in the literature for coals from other locations. It is important, therefore, to know how much errors in the physical parameters affect the computed data. Fortunately, the parametric study showed the

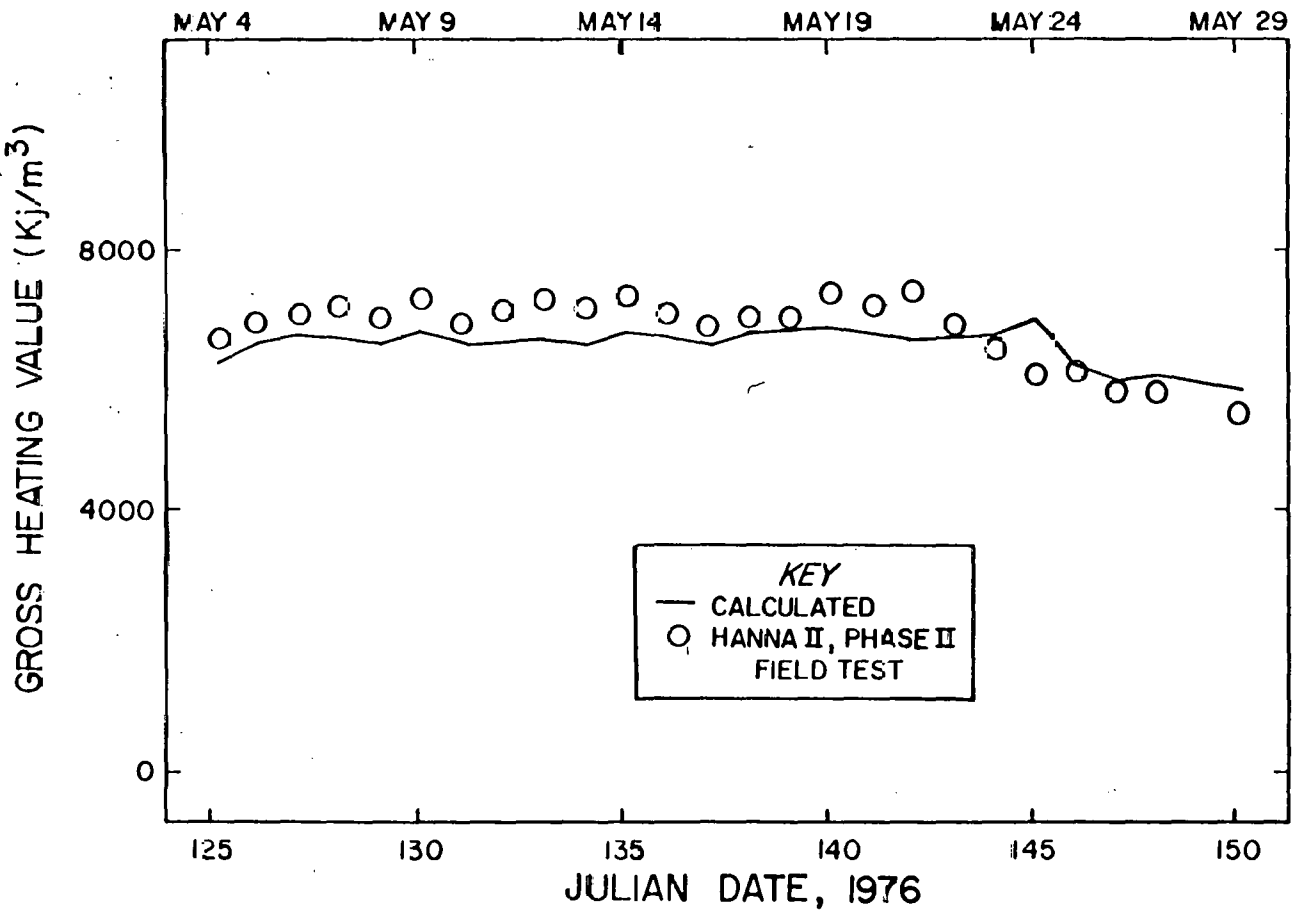

Figure III-3. Experimental and Calculated Gas Heating Values for the Hanna II Phase II Field Test

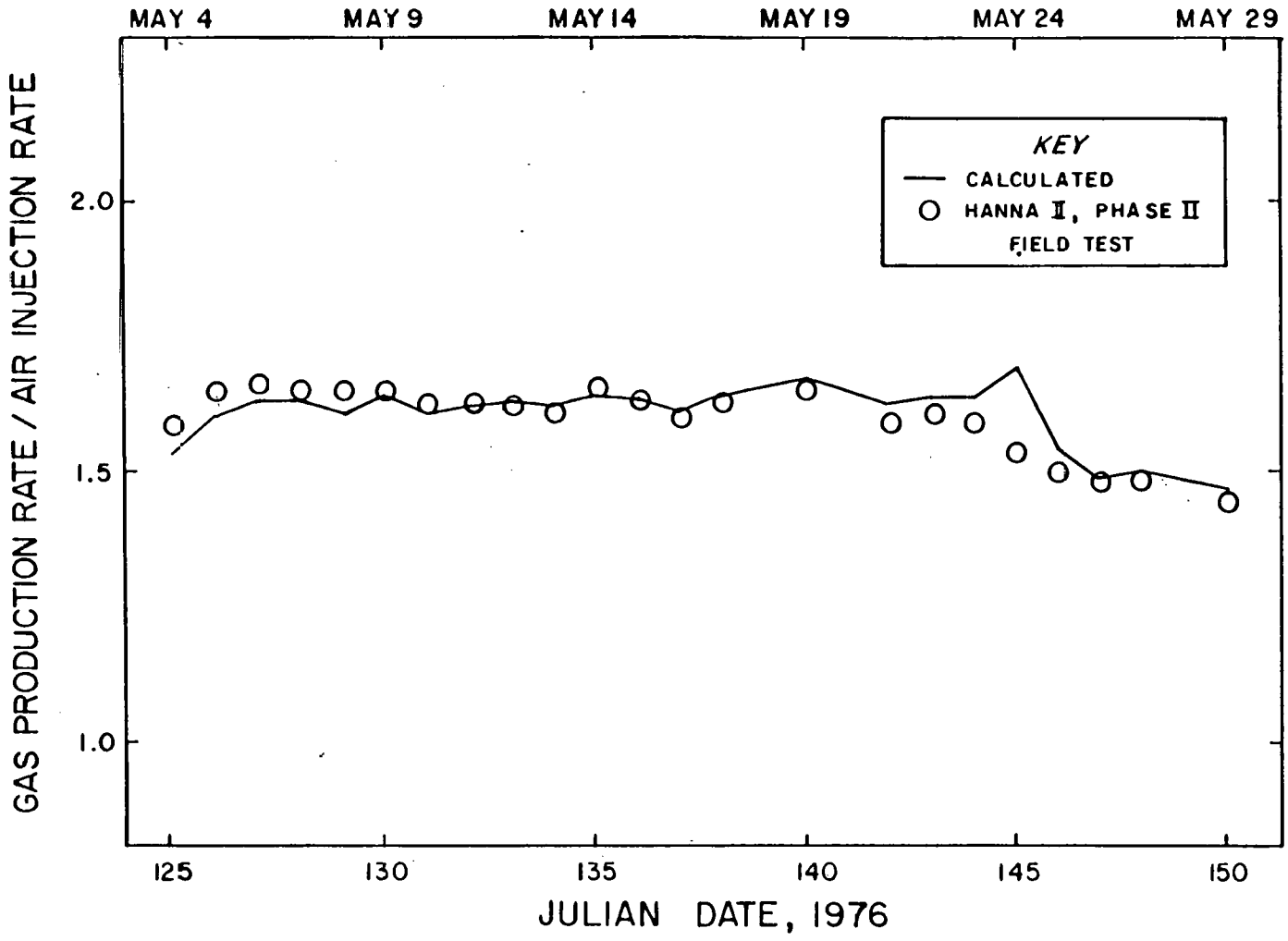

Figure III-4. Experimental and Calculated Gas/Air Ratios for the Hanna II Phase II Field Test

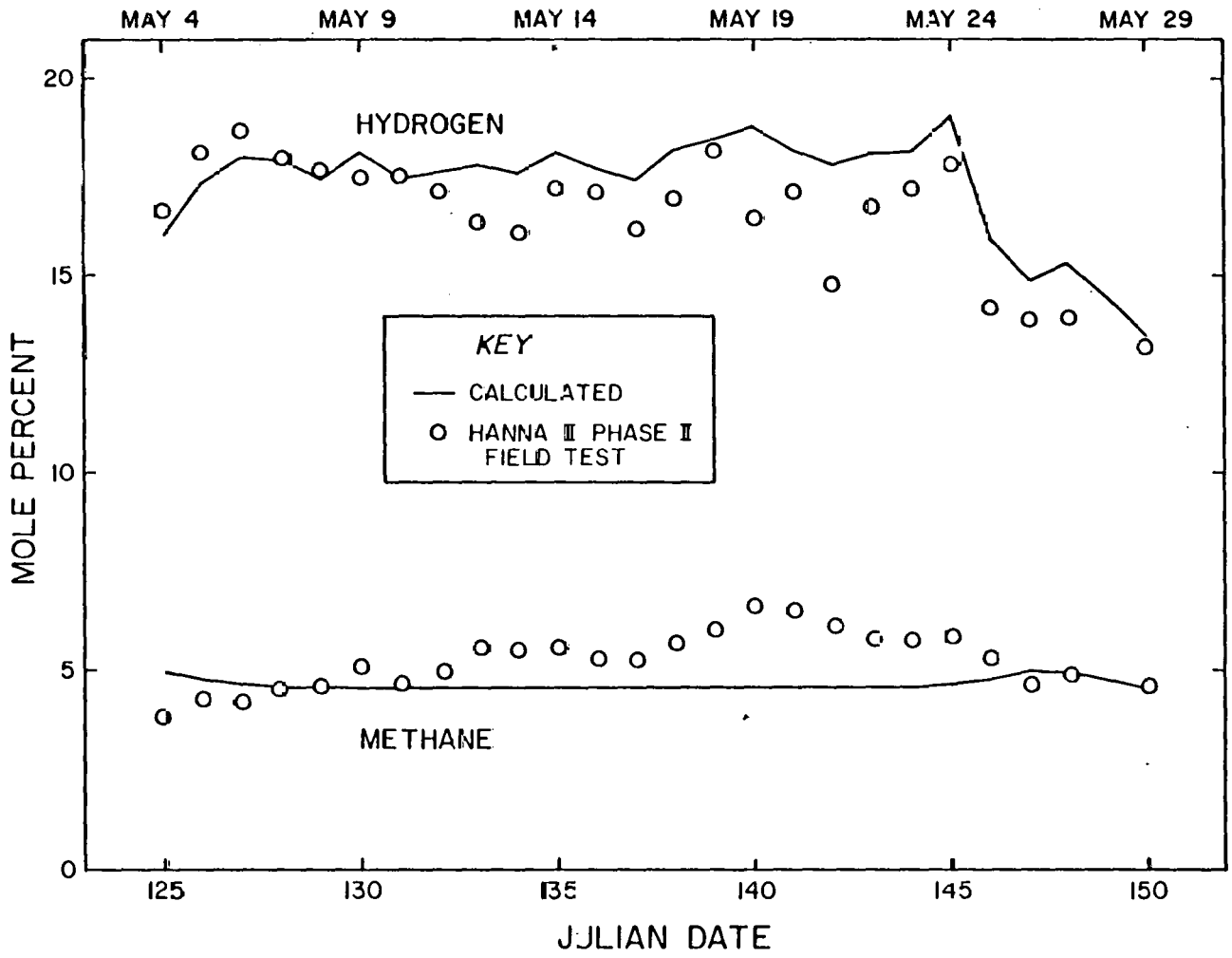

Figure III-5. Hydrogen and Methane Content of Gas Produced During the Hanna II Phase II Field Test

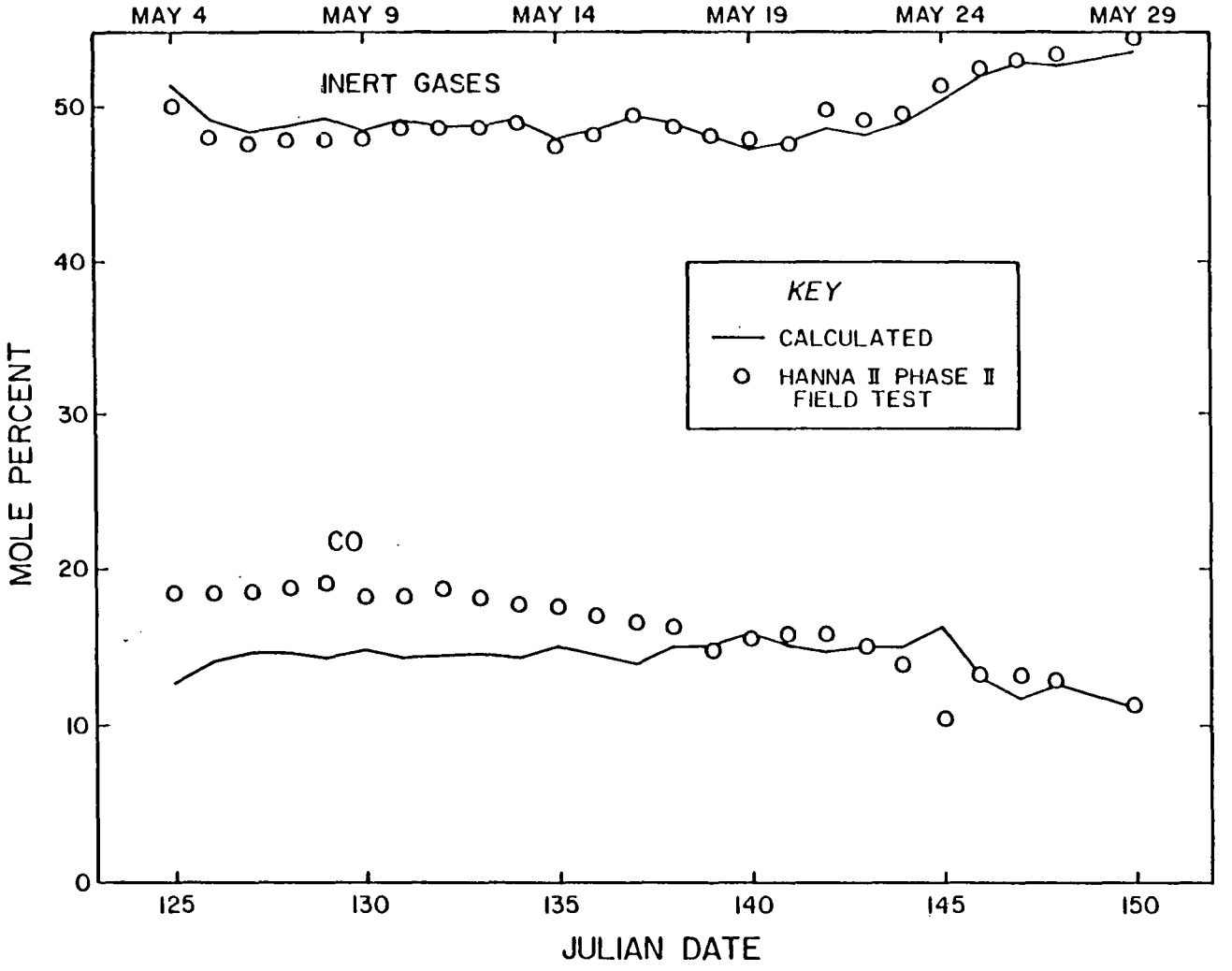

Figure III-6. Inert Gas (Nitrogen and Argon) and Carbon Monoxide Content of Gas Produced During the Hanna II Phase II Field Test

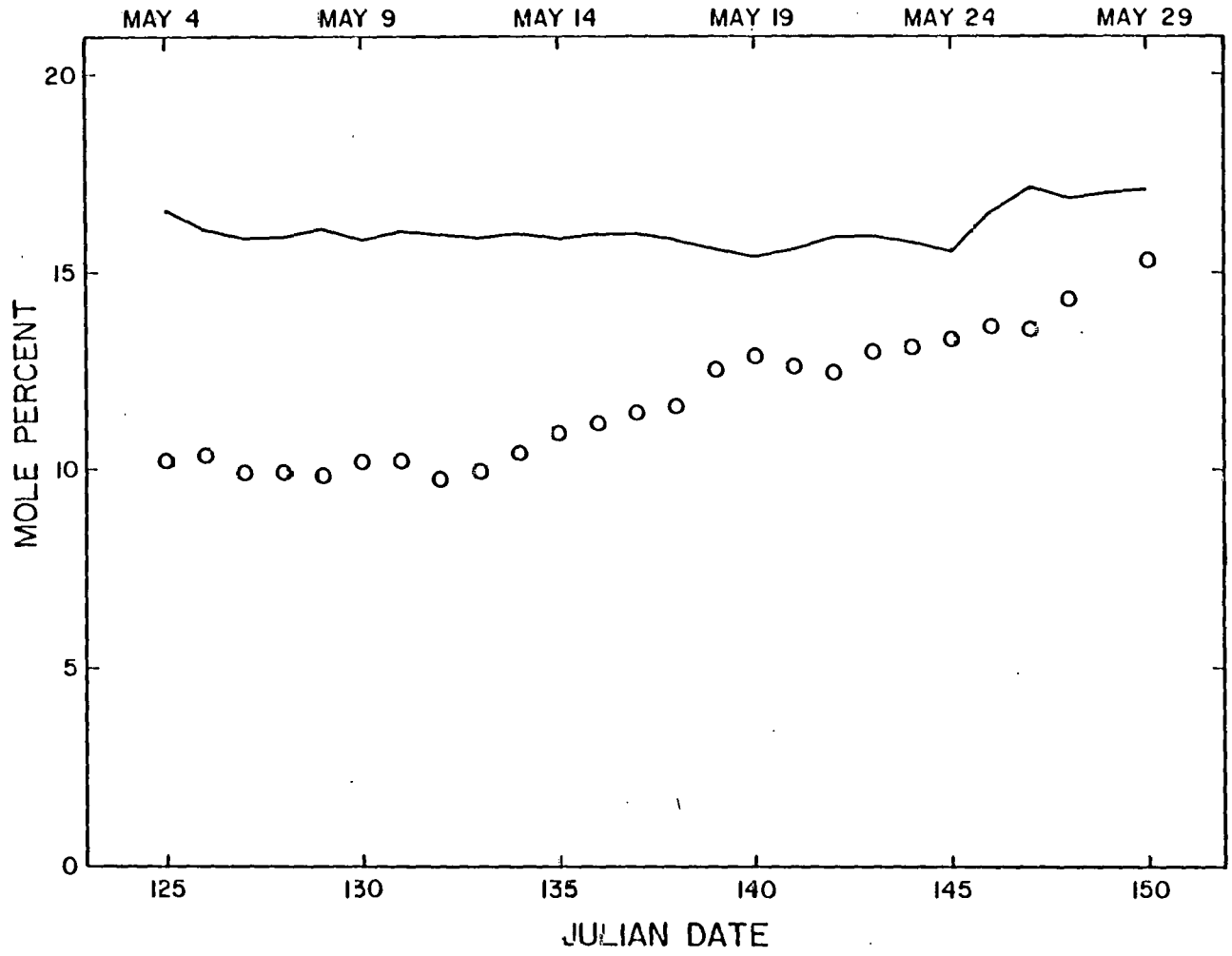

Figure III-7. Carbon Dioxide Content of Gas Produced During the Hanna II Phase II Field Test

model to be insensitive to parameters such as thermal conductivity and heat capacity.

The Lawrence Livermore Laboratory conducted two combustion tube experiments with subbituminous coal from the Powder River Basin in Wyoming using steam and oxygen as the injected fluid. Table III-2 records the comparison between experimental and calculated data. The forward gasification model without modification was used to compute these results, and the good agreement is especially gratifying for this reason. The agreement indicated in Table III-2 suggested a very important implication. It showed that the model could be used to extrapolate to new conditions such as a switch from air to oxygen-steam injection or a switch from field tests to laboratory combustion tube experiments.

Table III-2

Comparison of Combustion Tube Experiments with Model Calculations. Ref. Gunn, Fisher and Whitman (1978).

Property	Data Comparison			
	O_2/H_2O = 0.27*		O_2/H_2O = 0.21*	
	LLL**	Model	LLL**	Model
Gas Composition, mole %				
Hydrogen	34.80	34.81	37.20	31.78
Carbon Monoxide	28.53	28.63	25.43	25.91
Carbon Dioxide	28.53	27.85	30.67	34.04
Methane	8.14	8.71	6.70	8.27
Heating Value Kj/m^3	11,300	11,600	10,700	10,700
Maximum Temp. °C	1,320	1,268	1,140	1,216

* Injection gas composition ratios (moles O_2/moles H_2O)

** Experimental data from the Lawrence Livermore Laboratory (1976)

As discussed in the preceding sections, several factors make it possible to model the behavior of UCG reasonably simply. These predictions, however, are valid only for average or integral behavior such as produced gas compositions. Accurate predictions of temperature profiles is not possible because of the widely varying properties of coal and the

chaotic nature of UCG on a local basis. Certain well formed temperature profiles, however, can be analyzed on the basis of assumed local conditions. A detailed analysis of two such temperature profiles has been reported by Gunn, Fischer and Whitman (1978). While true predictive capability is not present because of the necessity to assume local conditions, the analysis has considerable educational value because specific processes leading to the formation of the profile can be identified. Figure III-8 shows one of the profiles analyzed for a thermocouple located five feet from the bottom of the coal seam. To calculate the profile, it was necessary to assume that local water influx was 2½ times the average for the entire combustion zone on that day. For a thermocouple low in the seam, this would seem to be a reasonable assumption. The calculated data shown in Figure III-8 were obtained with no further assumptions.

Gunn, Fischer and Whitman (1977) reported a comparison of calculated and experimental data for the Hanna II Phase III field test. This field test was especially important because a higher water influx occurred than in any other Hanna test. The analysis of the data is especially interesting because the internal working of the gasification model clearly indicate the specific processes affecting UCG performance when high water influx is present. Table III-3, taken from Gunn, Fischer and Whitman (1977), illustrates this use of the forward gasification model.

In Table III-3, both calculated and experimental data are presented for two different days of the Hanna II Phase III field test, June 30 and July 15 of 1976. On the latter date, water influx was almost 50% higher. This in turn led to a decrease in both the gas heating value and the amount of gas produced relative to the air injection rate. The value of a theoretical analysis now becomes apparent. Not only is the forward gasification model capable of reproducing the field test data with good accuracy but it provides additional information not readily measureable. As shown in Table III-3, when the water influx is not too high, about 50% of the char produced by devolatilization is combusted to provide energy for the endothermic gasification reactions and about 50% of the char is gasified. A fifty percent increase in water influx, however, leads to a fifty percent reduction in the amount of char being gasified; and, surprisingly, a decrease in the amount of water reacted. The energy distribution provides further information. Increased water influx leads to a drastic reduction in the energy available for endothermic gasification reactions and even a reduction in energy used in devolatilization of the coal and cracking of the tars. The energy is diverted to the vaporization of water and to heat losses. The heat losses are primarily energy used to heat the spalled overburden.

An energy distribution such as that reported in Table III-3 cannot be computed from a simple energy balance of the field data. Such data do not determine how much energy is used for gasification or for devolatilization. A simple energy balance will give the heating value of all of the coal consumed, but not the heating value of actual coal char combusted. A model is required to obtain such information.

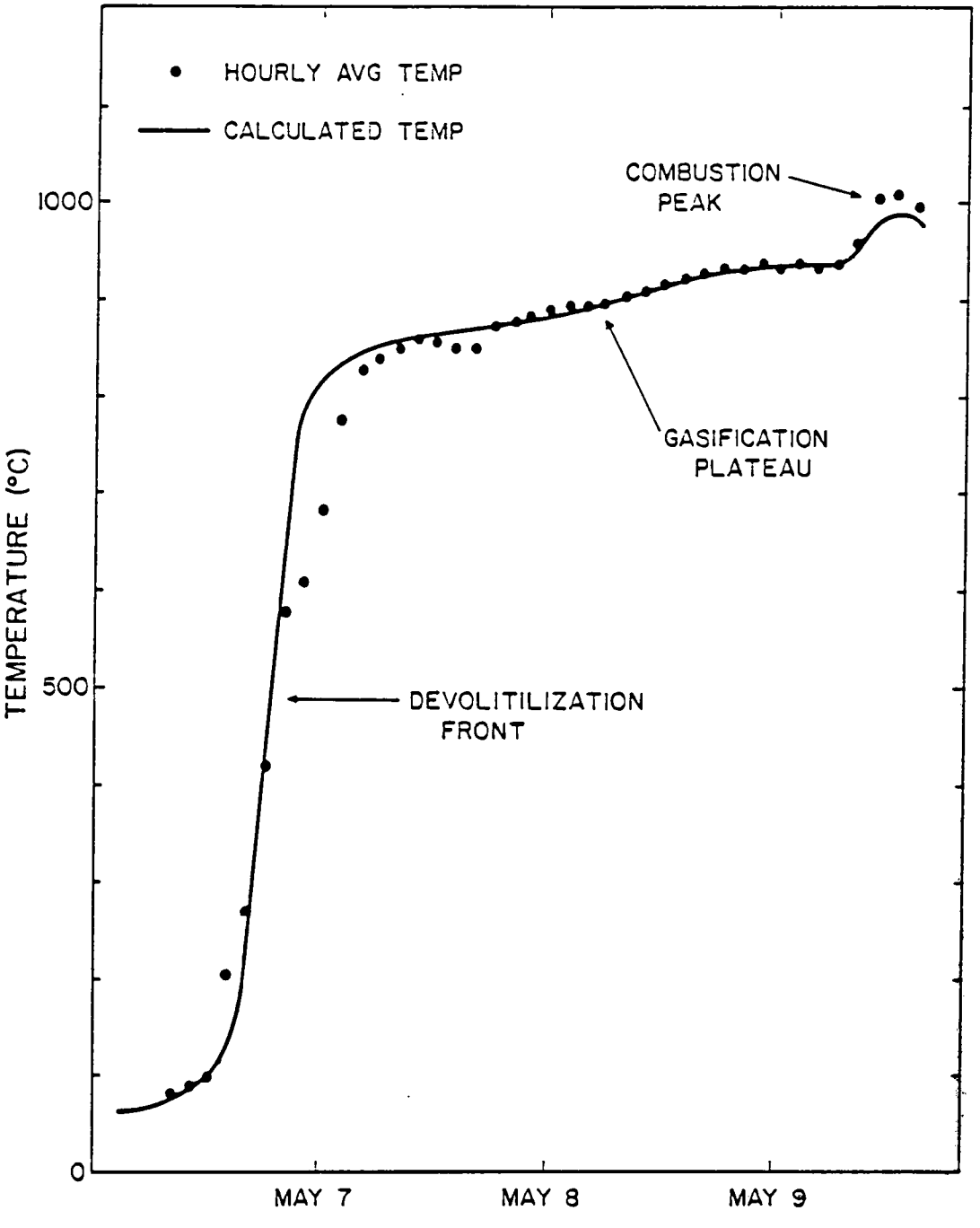

Figure III-8. Temperature Profile from a Thermocouple 1.5 Meters From the Bottom of the Coal Seam at the Hanna II Phase II Field Test Site

Table III-3

Comparison of data for two different days during the Hanna II Phase III field test. Ref. Gunn, Fischer and Whitman (1977).

Operational Data	June 30, 1976	July 15, 1976
Air Injection Rate, m^3/day	122,000	161,000
Water Production Rate kg water produced/ kg coal consumed	0.40	0.58
Gas Heating Value, Kj/m^3	6593 167	4540 115
Gas Production Rate m^3gas produced/ m^3 air injected	1.60	1.40
Calculated Data		
Percent Coal Char Combusted	54	76
Percent Coal Char Gasified	46	24
$\frac{\text{Lb water consumed}}{\text{Lb coal consumed}}$	0.22	0.09
Energy Distribution, percent		
a. Consumed in gasification reactions	30	11
b. Consumed in coal pyrolysis and cracking of coal tar		
c. Consumed in vaporization of water	18	34
d. Heat losses and sensible heat	24	33
Total Energy Consumed	100	100
Energy Generated by Combustion of Char	100	100

Figure III-9 shows a comparison of calculated and experimental hydrogen content of gas from the Hanna II Phase III field test. The interesting point here is that the hydrogen content decreased radically throughout the test due to increasing water influx. This was a direct result of energy being diverted from gasification reactions to the vaporization of water.

Gunn et al. (1980) reported a comparison of calculated and experimental data for the Hanna III field test. This test was especially difficult to interpret for two reasons. First, this test produced the hottest gases of any of the Hanna tests with temperatures at the well head of 650 to 870°K (700 to 1100°F). Second, to reduce the high temperatures, water was injected into surrounding wells. With the experimental data available it is not possible to determine the amount of this injected water which entered the gas stream before the combustion front and how much entered after the combustion zone. Neither is it known what the time lag is between water injection into the coal formation and production of that water at the producing well. These factors do have some effect on gas composition which could be estimated only very crudely because of the lack of information. High well head temperatures also affect gas composition because the low temperature devolatilization of coal is absent. For example, if gas enters the production well bore at a temperature of 700°C, that gas will not contain the enriching products from devolatilization of coal which occurs between 425 and 700°C because in a permeation process the gas cannot be hotter than the coal it contacts. Correct predictions of gas composition were achieved for the Hanna III field test only when the bottom-hole temperature of gas in the production well was included in the mathematical model for forward combustion. In spite of the difficulties just discussed good agreement exists between model calculations and the experimental field test data. Figs. III-10 and III-11 are respectively comparisons for gas heating value and for the ratio of production gas flow rate to the air injection flow rate.

The reason that the Hanna III test produced gases at such a high temperature is unknown. It can be inferred that some channeling may have occurred during the test, and this would cause the gases to be produced at a higher than normal temperatures. Channeling might have occurred if coal permeability at the Hanna III field test site was especially nonisotropic. Complete pressure draw down tests were not carried out so that little is known about the permeability; however, some short duration incomplete tests indicated that the Hanna III test site had very irregular permeability characteristics.

Gunn, Gregg and Whitman (1976) carried out a theoretical analysis of Soviet field test data. The Soviet publications never contain enough information to permit a direct comparison, and it was necessary instead to predict how UCG at the Hanna site would respond to the relevant variables while other variables were held constant. In all cases, however, the behavior calculated was qualitatively the same as that observed in the Soviet field tests. Figure III-12 shows such a comparison for the effect of enriched air on the hydrogen content of the gas. For comparative purposes, a data point for air from the Hanna II Phase I field test is included in Figure III-12. The two calculated lines in

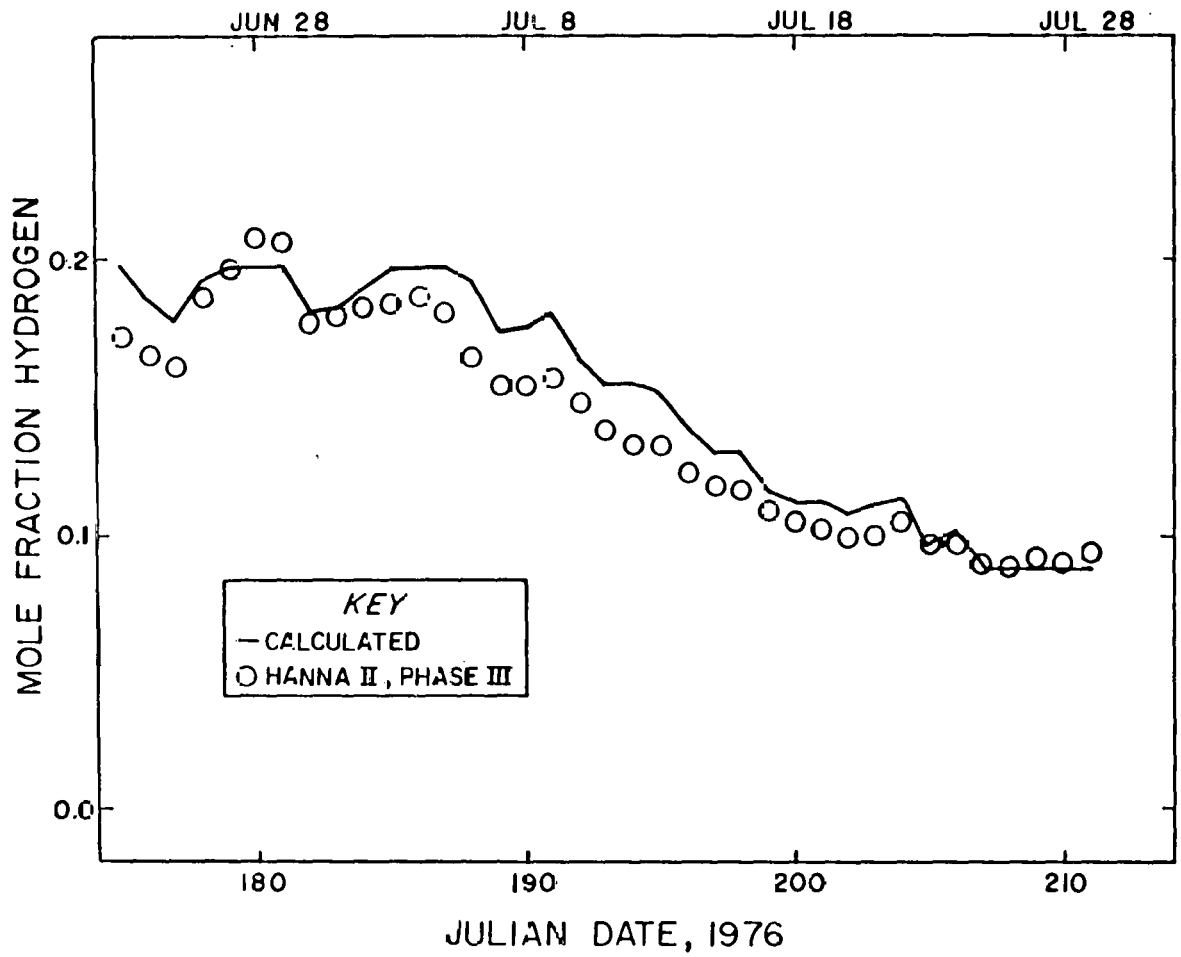

Figure III-9. Hydrogen Content of Gas Produced During the Hanna II Phase III Field Test

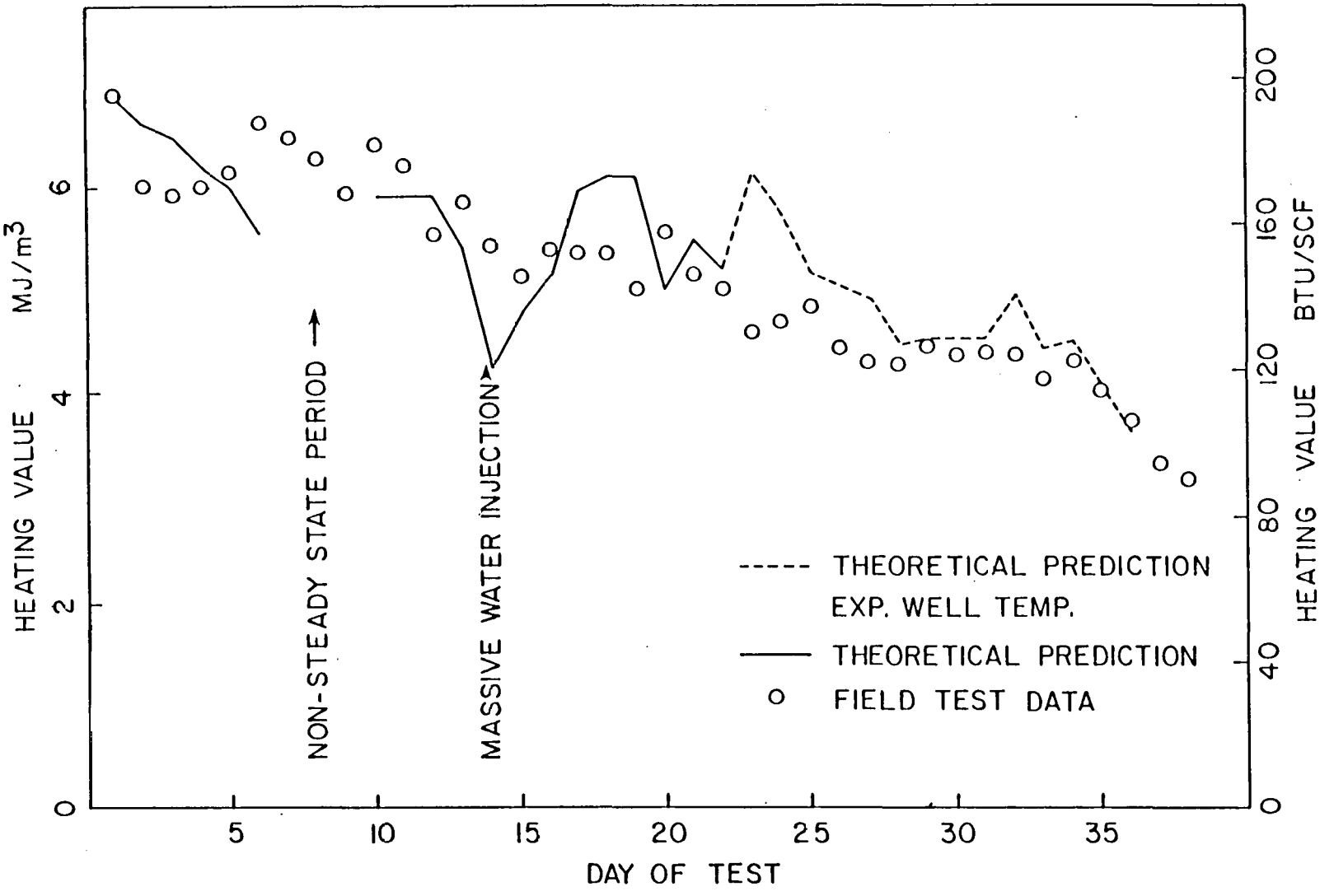

Figure III-10. Experimental and Calculated Gas Heating Values for the Hanna III Field Test

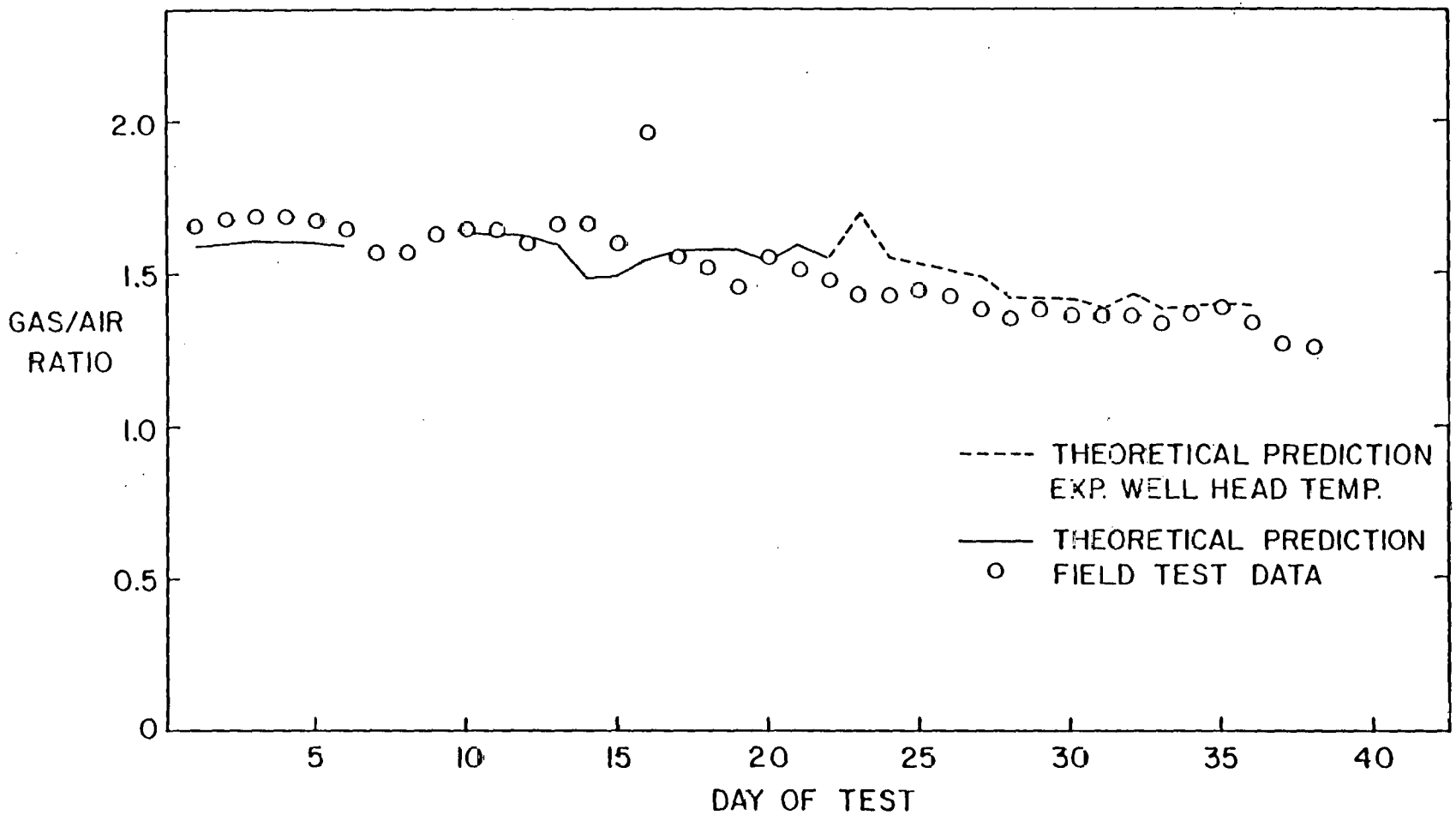

Figure III-11. Experimental and Calculated Gas/Air Ratios for the Hanna III Field Test

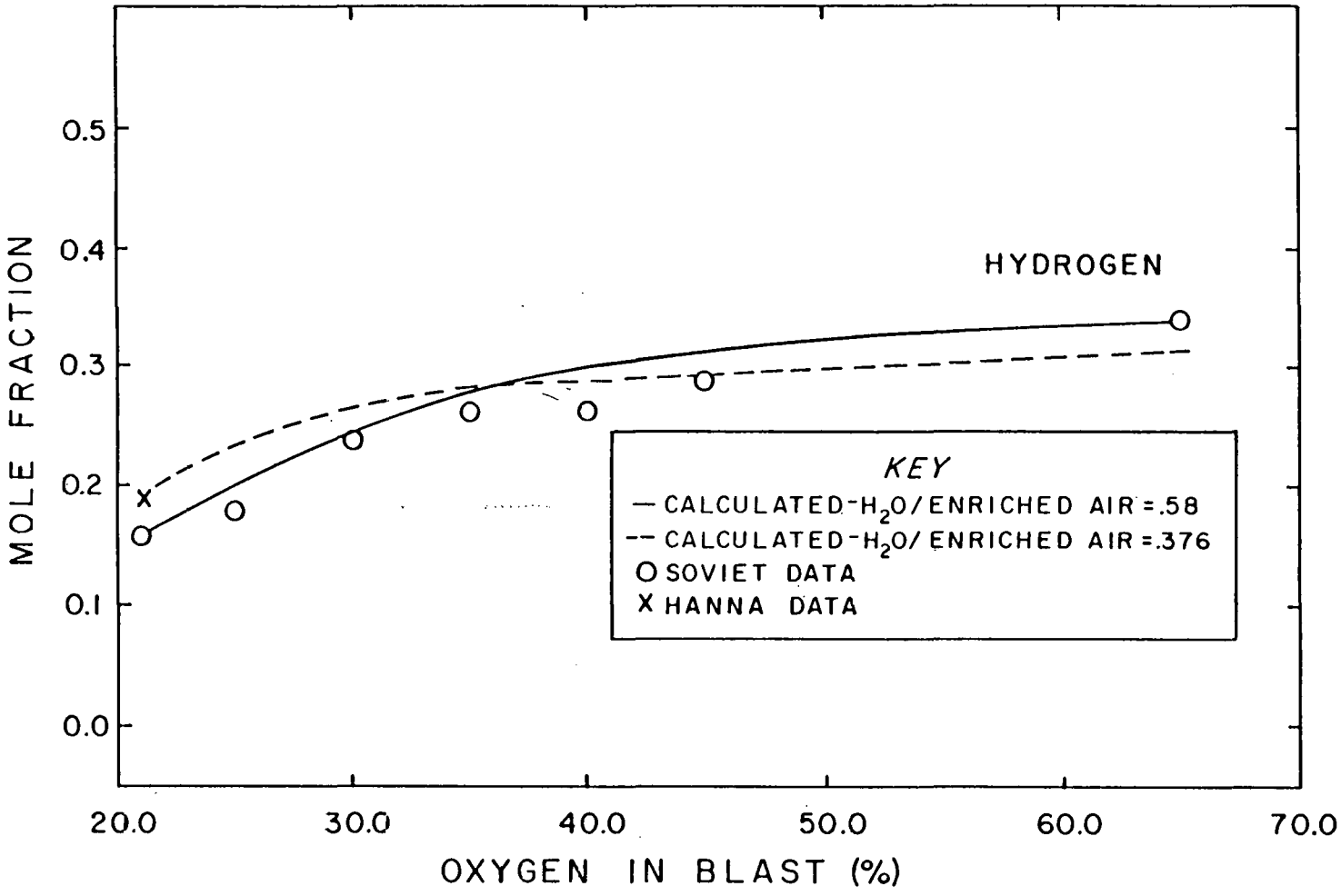

Figure III-12. Effect of Oxygen Enrichment of the Air on the Hydrogen Content of Gas from Underground Coal Gasification

the figure represent data for different ratios of moles of water influx to moles of injected gas.

Other effects investigated were the effects of water influx and oxygen content on gas compositions and heating values; and the effects of seam thickness and ash content on heating value. The Soviet correlations are derived empirically from many different field tests. It is obvious that a few field tests assisted with a modeling effort are greatly superior to many field tests conducted at an enormous expense and correlated empirically. Not only does the theoretical model reproduce the Soviet correlations, but in addition it provides scientific explanations for the behavior observed and shows how three or more variables interact simultaneously. The latter type of information is too complicated to be deduced on a simple empirical basis without a prohibitively large amount of data.

Technology Assessment

This section is concerned with a less common use of mathematical models, that is, the use of theory in assessing the state of technology, identifying potential problem solutions, and identifying and defining the importance of unsolved problems.

Based on the modeling effort and on the analysis of data from the three Hanna II field tests, Gunn (May, 1977) summarized 15 technical problems which were of major concern to the technical community at the time. Of these 15 problems, 5 were considered unsolved and 10 were considered soluble on the basis of a theoretical understanding of the process. Two unsolved problems were considered critical to the successful commercial development - these were water influx and subsidence.

The publication cited (Gunn, 1977) demonstrates that a soundly developed modeling effort can be used successfully for this purpose. A review of this work (Gunn, 1977) shows that it has proved accurate despite nearly 6 years of rapid development in UCG. This remains true in spite of the fact that the source of water influx was unknown at the time of the original publication.

An alternative to using the modeling effort to define research objectives for the field test program has been commercial and feasibility demonstrations. The latter method has been employed repeatedly in a number of different countries for nearly 50 years. The majority of such tests have ended in failure and discouragement. Even when such tests have been successful, they have proved unreproducible through a lack of technical understanding.

Laboratory Experiments

The research just discussed shows that a forward gasification model is an invaluable tool in interpreting field test data. Similarly, a theoretical model can be used to predict expected gasification results for a new type of coal or a new test site. It does not appear desire-

able, however, to design a multimillion dollar commercial project on the basis of model predictions only. Simulation of UCG in the laboratory to determine expected gas compositions and heating values can provide invaluable supporting evidence. Although it has been widely believed that such simulations are not possible, model studies indicate that laboratory simulation of UCG is feasible provided that the appropriate operating parameters are matched. These are coal type, pressure, water/oxygen ratio, injection gas composition and heat loss. Without the aid of a good UCG model, however, it is not apparent that the foregoing parameters are those which must be matched or that they are the most important ones. In fact, it is the lack of theoretical models which has probably prevented successful laboratory simulations in the past.

Bell and Gunn (1980) reported a 3 year successful effort to simulate field results in a laboratory combustion tube. All investigators have found that the operation of a combustion tube is a very difficult task. While the air flow rate does not need to be matched accurately with the field data, the air velocities should be crudely comparable. At the low air velocities characteristic of the Hanna field tests, channeling of the air and of the reaction zone proved to be a major problem in the laboratory tests. Alleviation, but not elimination of these and other problems, was achieved only after a continuous 18 month effort by Greg Bell and three undergraduate student assistants.

Table III-4 summarizes the operating results for four successful combustion tube runs. Table III-5 shows a comparison of one of these runs with data calculated from the forward gasification model and with data from the Hanna II field tests. Table III-5 does show good simulation of field test results, and it is emphasized again that for comparison purposes it is necessary to match the coal type, pressure, water/oxygen ratios, injection gas composition and heat loss as indicated by the forward gasification model.

By the end of the contract period, a more complete analysis of the combustion tube results with additional data was in progress. These results will be reported in a separate publication.

Discussions and Conclusions

The development of the forward gasification model led to a greatly improved understanding of the Hanna field tests and of UCG in general. Major conclusions are:

1. The good agreement between model results and the Hanna field tests shows that UCG under favorable operations in a permeable, nonswelling coal is a permeation process.

2. The conditions at Hanna are favorable for UCG but by no means unique.

3. Careful site selection is imperative for successful gasification.

Table III-4

General Gasification Tube Results

RUN NO.		5B	6B	7B	8B
Air Rate (l/min.)		8.2	8.2	8.2	16.4
Water Rate (cc/min.)		1.0	1.0	1.0	2.0
Bed Density (kg/m^3)		903.	913.	881.	806.
T_{max} Center (°C)		955.	996.	908.	972.
T_{max} Wall (°C)		676.	1140.	825.	801.
Combustion Front Velocity (m/hr.)		0.051	0.080	0.074	0.143
Devolatilization Front Velocity (m/hr.)		0.062	0.081	0.081	0.169
$\frac{\text{Product Gas Rate}}{\text{Injection Air Rate}}$ (mole/mole)		1.20	1.48	1.33	1.51
Gas Heating Value	(KJ/m^3)	3500	6131	4600	5590
	(Btu/ft^3)	88.7	155.3	116.5	141.6
Gas Composition (Mole %)	N_2	65.57	53.19	59.22	54.03
	O_2	0.92	0.74	0.32	0.79
	CO_2	13.34	9.98	12.68	9.49
	CO	9.15	17.53	13.62	18.68
	H_2	7.68	13.30	10.33	12.89
	CH_4	2.83	4.47	3.28	3.45
	C_2H_2	0.34	0.59	0.35	0.41
	H_2S	0.17	0.20	0.20	0.26

Table III-5

Comparison of Laboratory, Numerical Model, and Hanna Test Data

Source of Data		Laboratory Simulation Run 68	Numerical Simulation Run 6B	Hanna II Phase 2 Day 147	Hanna II Phase 3 Day 191
Heat Loss (%)		11.5	11.5	11.5	10.6
$\frac{\text{Water Injection}}{\text{Air Injection}}$	(mole/mole)	.167	.167	.130	.176
T_{max} (°C)		996	1068	NA*	NA*
$\frac{\text{Product Gas Rate}}{\text{Injection Air Rate}}$	(mole/mole)	1.485	1.448	1.477	1.593
Gas Heating Value	(KJ/m^3)	6131	6005	5772	6475
	(Btu/ft^3)	155.3	152.1	146.2	164.0
Gas Composition (Mole %)	N_2 + Ar	53.19	54.77	53.47	49.62
	O_2	0.74	0.00	0.23	0.17
	CO_2	9.98	9.63	13.51	13.91
	CO	17.53	18.29	13.86	14.93
	H_2	13.30	10.97	13.89	15.74
	CH_4	4.47	5.51	4.65	5.10
	C_2H_6	0.59	0.76	0.39	0.53
	H_2S	0.20	0.07	0.00	0.00

*Not Available

4. Heat loss is a major controlling factor in UCG.

5. Water influx is a major heat loss factor.

6. The heating value typically declines throughout a field test because of increasing water influx. A water influx model discussed later explains why water influx increases.

7. The gas heating value is insensitive to variations in the air flow rate.

8. Laboratory combustion tube data can be used to predict field test behavior, but a model capable of calculating both types of data is helpful. The forward gasification model developed in this work shows which parameters must be matched in order for a comparison to be made between laboratory and field test data.

CHAPTER IV - WATER INFLUX

Importance of Water Influx in the UCG Process

Water influx is vital to the UCG process since the principal gasification reaction involves the reaction of water with coal char to form carbon monoxide and hydrogen. Indeed, one advantage of UCG relative to surface gasification processes is that under most conditions, it is not necessary to inject surface water along with the oxidant injection since there is adequate natural water influx in situ. However, this natural water influx is at the same time disadvantageous because it is difficult to control. The Wyoming UCG tests to some extent have been less efficient than possible due to excessive water influx. The vaporization of excessive water influx robs process heat from the endothermic gasification reactions and thus lowers the product-gas heating value. The situation is aggravated further because the water influx appears to increase as gasification proceeds. Hence, the progressive decline in product-gas heating value and quality makes any downstream processing of this gas more difficult.

The role of water in the UCG process depends on whether the water influx is into the hot UCG cavity or downstream into the carbonized link zone. Water influx into the cavity can participate in the principal gasification reaction and also can rob process heat from this reaction. Water influx downstream into the carbonized link can participate directly in the water-gas shift reaction which exchanges carbon monoxide for hydrogen, and indirectly in the methanation reaction; furthermore, it cools the product gas and thus decreases the potential for surface heat exchange to recover the sensible heat of the product gas but, at the same time, reduces high temperature corrosion of the production well and surface piping system.

The apparent mechanisms for water influx include the water naturally present in the coal which is dried and gasified, influx by permeation due to Darcy flow through larger cracks and fissures, and water influx by drying of the coal and rock surrounding the gasification cavity. Simple material-balance calculations indicate that the water naturally present in the coal gasified is grossly insufficient to supply the water indicated by an overall hydrogen balance. Surprisingly, permeation models indicate that for the conditions of the Hanna, Wyoming, UCG field tests, relatively little of the water entered by Darcy flow through the porous media. This is a consequence both of the low permeability of some Wyoming coal seams and of operating pressures close to the prevailing hydrostatic pressure. The possibility exists for substantial water influx by bulk flow through larger cracks and fissures. However, detailed analyses reviewed in this chapter indicate that this was not an important source of water influx in any of the tests analyzed. Simple drying also does not explain the large water influx observed in Wyoming UCG field tests. One-dimensional unsteady-state drying models indicate that only one meter or so of coal or rock can be dried during an entire month of gasification. This follows from the fact that in simple unsteady-state drying, heat must be conducted through the dried material to the advancing steam front. Thus, as the steam front penetrates

further, the drying rate progressively declines to a relatively negligible rate. Hence, none of the four obvious water-influx mechanisms appear to account for the water influx observed in the extensive Wyoming UCG field-test program.

The Wyoming-Colorado UCG research group then focused its efforts on identifying the principal mechanism whereby water invades the UCG process. A further goal of these studies was to develop predictive models for water influx in the UCG process. The ultimate goal of this research was to suggest UCG operating strategies whereby water influx can be controlled and perhaps optimized.

Modeling Studies of Water Influx

The first model which has proven successful in predicting water influx for UCG operations was developed in the thesis of Camp (1980) and has been reported by Krantz et al. (1980). The mathematical details of this model have been described in more detail in Camp et al. (1980). This model is based on the fact that considerable spalling of overburden occurs during the UCG process as these materials dry and eventually collapse into the cavity formed by the burning coal. This overburden material often consists of shale, siltstone, and sandstones. Such materials, even when impermeable, frequently contain 25-40 percent water by volume. Hence, this model is referred to as the "spalling-enhanced-drying model." It incorporates two mechanisms for water influx: permeation by Darcy flow, and spalling-enhanced drying. These mechanisms are interrelated to a gasification-cavity-growth model which is tied to the coal consumption schedule. Each mechanism and the cavity-growth model will be described in some detail here.

Although water influx by permeation was negligible for the UCG field tests conducted in Hanna, Wyoming, it was not insignificant for the field tests carried out at the Hoe Creek site in Wyoming. Water influx by permeation is more significant for coal seams more permeable than the Hanna No. 1 seam. For these reasons, it was decided that a truly general water-influx model must include permeation by Darcy flow through the porous media. The permeation component incorporated into the spalling-enhanced-drying model is intended for coal seams which are water-bearing zones with a permeability considerably higher than the surrounding overburden which consists of siltstones, shalestones, sandstones, and clays. For this reason, the primary flow direction for permeation is assumed to be parallel to the undisturbed bedding planes of the coal; permeation through the relatively impermeable overburden is assumed to be negligible. The two-dimensional Darcy flow model allows for unsteady-state permeation into the cavity or link while incorporating the effects of capillary pressure and a time-varying cavity pressure. The manner in which an analytical solution was obtained for this Darcy flow component of the water-influx model will be outlined here. An overhead or top view and a plan or profile view of the UCG cavity and reverse combustion link are shown in Figure IV-1. Water influx by permeation can occur both into the gasification cavity as well as into the reverse combustion link. Although the reverse combustion link possesses a rather small volume, it has a large surface area through

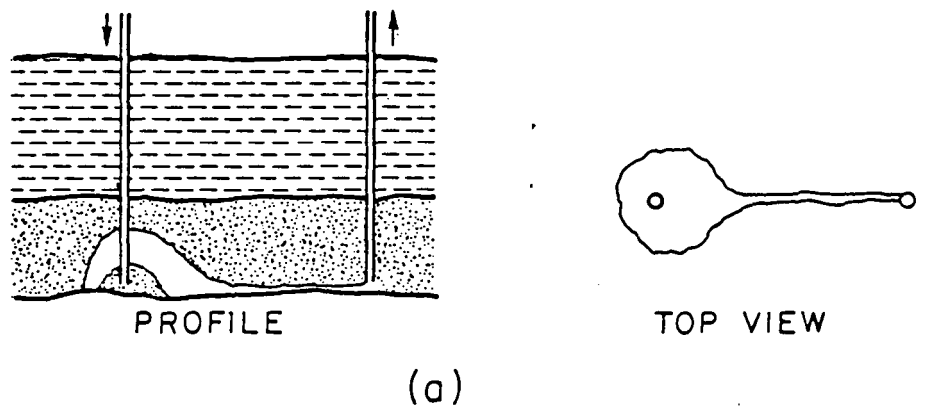

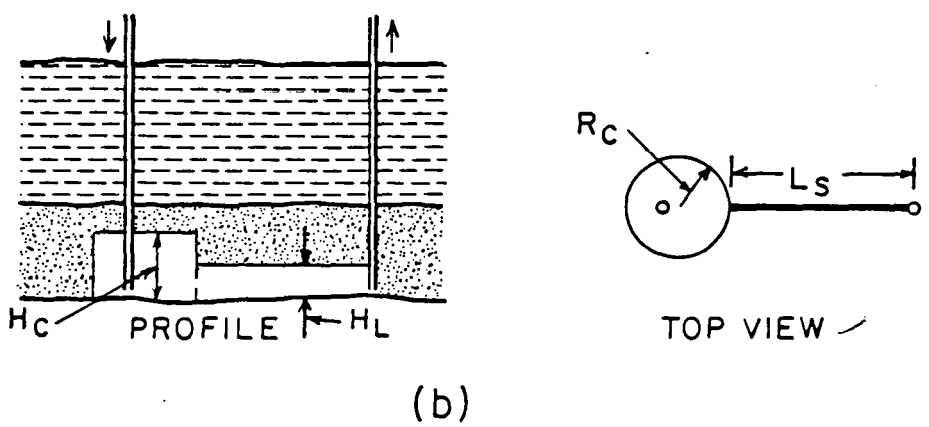

Figure IV-1. Cavity/Link Geometry for Permeation Model

which water can permeate. The water influx into the link relative to that into the cavity can be significant particularly during the early stages of gasification when the link is long. It is important to account for the location of water influx since water entering the link plays a different role in the process chemistry than water entering the cavity. In order to obtain a viable solution, the complex cavity/link geometry shown in the upper two views in Figure IV-1 was idealized as shown in the bottom two views in Figure IV-1. That is, the link was assumed to be negligibly thin with a height determined by the reverse combustion stability model of Gunn and Krantz (1980), and attached normal to the surface of the gasification cavity, which was assumed to be a right-circular cylinder. This cavity/link geometry was transformed via successive conformal mappings into that of an "equivalent" cylindrical cavity; that is, into a cylindrical cavity which would would admit the same total water influx by permeation under the prevailing pressure driving force as would the idealized cavity/link geometry. The radial permeation into this equivalent cylindrical cavity could then be determined analytically. The permeation model allows for the increase in the radius of the equivalent cylindrical cavity due to the expanding gasification cavity. The pressure driving force for permeation was corrected for the effects of capillary forces in the small pores; if the water wets the coal, the capillary effect increases the effective pressure driving force. Two simple models for the pore structure were used to provide estimates of the capillary pressure as functions of the surface tension (water against air), porosity, and the Darcy permeability coefficient. The time-varying cavity pressure was incorporated into the model by invoking the "principle of superposition" for linear differential equations whereby the particular solutions corresponding to infinitesimally short time periods having constant pressure are summed to obtain the general solution. The permeation model allows for both positive and negative water influx by this mechanism depending on whether the sum of the hydrostatic and capillary pressures is greater than or less than the cavity pressure. In the case of negative permeation, the model accounts for the unstable nature of the displacement of water (in the pore structure) by gas (coming from the gasification process); that is, the displacing gas will channel or finger through the water-saturated porous media leaving behind "islands" of water amounting to approximately fifty percent of the water originally in place. Complete details on this permeation model are given in the thesis of Camp (1980).

The spalling-enhanced-drying component of the water-influx model accounts for the accelerated drying which occurs due to spalling or chipping off of small pieces of the overlying coal or overburden rock. Spalling occurs during the drying process because of the thermomechanical stresses which are generated during drying. Spalling results in greatly accelerated drying because the distance through which the heat must be conducted is kept relatively short. For example, whereas only approximately one meter of Hanna overburden rock can be dried by simple drying during a 40 day UCG operation, nearly 30 meters can be dried (and spalled) by the spalling-enhanced-drying mechanism. The spalling-enhanced-drying component allows for the fact that at any instant of time there will be a distribution of ages of the various surface elements comprising the roof of the cavity. That is, there will be a

distribution in the length of time a given surface element has been exposed to the high temperature of the cavity. An idealized sketch of what a section of the cavity roof might look like after several spalls is shown in Figure IV-2. For better visibility, vertical variations in the roof structure are greatly exaggerated in this figure. The water-saturated regions are shown by the dark-shaded areas whereas the dried regions are shown by the light regions. This sketch shows that this section of the roof consists of six elements all of which have been exposed to the high cavity temperature for different exposure times since their last spall. The third element from the left, for example, has experienced four spalls since the overburden surface was first exposed to the high temperature of the gasification cavity. Each area element of the cavity roof shown in Figure IV-2 is drying at a different rate; the fifth element from the left has the largest instantaneous drying rate, whereas the fourth element from the left has the smallest. The instantaneous drying rate of any particular element of the cavity roof can be determined by an appropriate solution to the unsteady-state one-dimensional drying equation for the vapor-saturated region. The average drying rate for a given area of cavity roof composed of a number of surface elements, which have the same area exposed to the hot cavity but are drying at different instantaneous rates, is equal to the sum of the drying rate for each element divided by the total number of elements. This can be stated in precise mathematical terms as follows: the average drying rate for the entire cavity roof is equal to the weighted average of the drying rates for the surface elements, where the weighting function is the surface-age distribution $f(t)$. The latter is defined such that $f(t)dt$ is the fraction of the cavity roof area that has been exposed to the hot gasification cavity temperatures for a duration of time between t and $t + dt$.

The spalling-enhanced-drying model allows for the fact that the initial upward growth of the gasification cavity will involve spalling of the coal since the overburden is not exposed initially. Furthermore, the model recognizes that the overburden is characterized by different strata whose spalling characteristics differ. The spalling properties of the coal or of each stratum of the overburden are completely characterized in this model by specification of the surface-age distribution function or equivalently the average spalling-rate parameter for the particular stratum. If the spalling properties of the entire overburden at a particular UCG site can be characterized by a single value for the spalling-rate parameter, then this parameter can be obtained by curve-fitting the water-influx data from a UCG field test at the site. However, it is doubtful whether a single value for the spalling-rate parameter will characterize complex overburden stratigraphy accurately enough, particularly for longer burns for which the spalling will expose a considerable height of overburden above the gasification cavity. Alternatively, it is possible to determine the average spalling-rate parameter from laboratory core-characterization studies. Camp (1980) determined the average spalling-rate parameter for overburden cores from the Hoe Creek, Wyoming, UCG field-test site by measuring the distance between successive bedding plane cracks shown in photographs of these cores which had been heated to 1270 K in an inert atmosphere. These measurements of the distance between cracks led to determination of the spalling-length distribution $h(L)$; the latter is defined such that

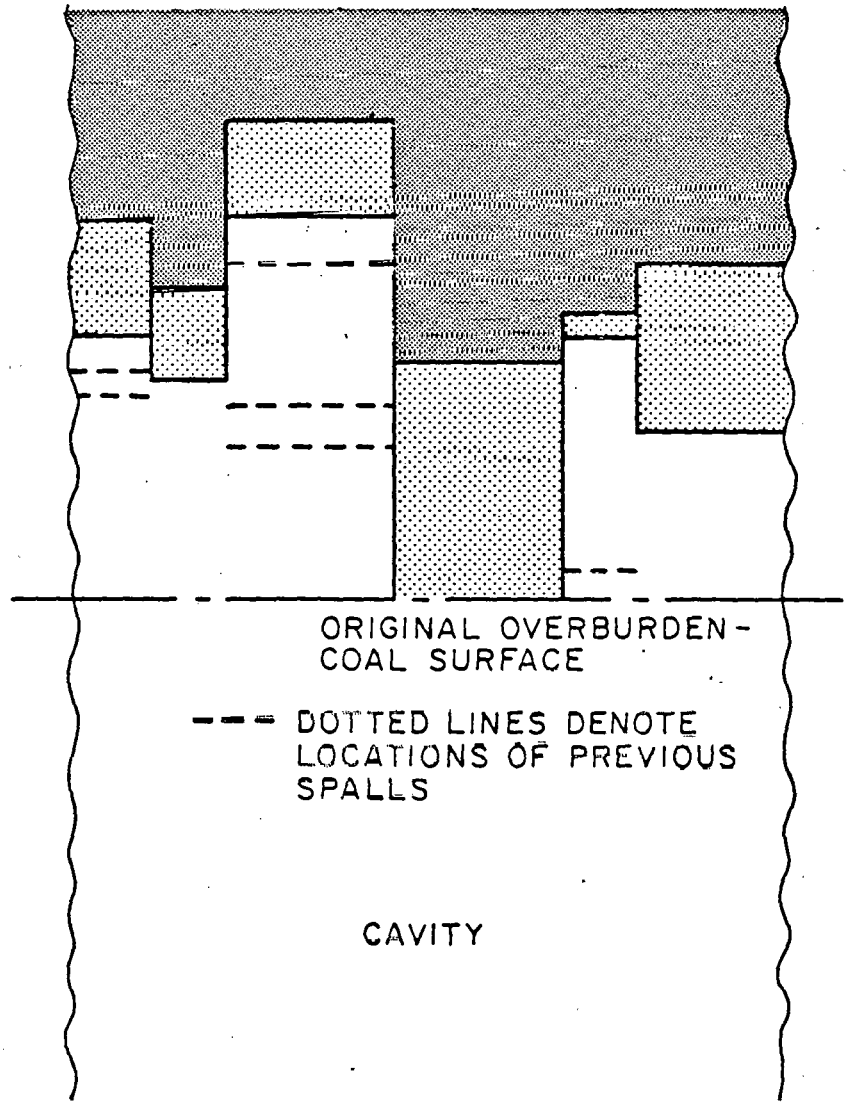

Figure IV-2. Idealized Side View of Cavity Roof After Several Spalls

h(L)dL is the fraction of the exposed surface area that spalls at a dried length between L and L + dL. The surface-age distribution f(t) then was obtained from this spalling-length distribution via an appropriate solution for the unsteady-state, one-dimensional heat conduction problem in the vapor-saturated region. The average spalling-rate parameter for these overburden cores then was obtained directly from the surface-age distribution. Obtaining the average spalling-rate parameter from laboratory core-characterization studies as was done by Camp involves the implicit assumption that spalling in the UCG cavity occurs by the same mechanism that causes cracking of these cores when they are heated to temperatures characteristic of the UCG cavity surface. These core analyses of Camp led to an average spalling-rate parameter of 0.74 m/day (2.4 ft/day) for the Hoe Creek overburden cores corresponding to an average spalled length of 0.027 m (1.1 in).

The permeation and spalling-enhanced-drying components of the water-influx model developed by the Wyoming-Colorado UCG research team are coupled via the lateral cavity growth or sweep model assumed for the UCG process. Whereas the permeation component requires a knowledge of the cavity and link surface area, the spalling-enhanced-drying component depends only on the projected area of the cavity roof. An interesting consequence of this is that if the gasification can be described by a two-dimensional sweep model, then the predicted amount of water influx by spalling-enhanced drying is independent of which two-dimensional sweep model is used. This follows directly from the fact that for a two-dimensional sweep model, the new roof area exposed each day is given by the daily volumetric coal-consumption rate divided by the constant coal-seam thickness. For this reason, the initial version of the spalling-enhanced-drying model for water influx reported in Krantz et al. (1980) and Camp et al. (1980) used the simplest possible two-dimensional sweep model, namely that of a radially expanding right-circular cylinder. In a later version of this water-influx model, Levie et al. (1981) employed the more realistic two-dimensional sweep model of Jennings et al. (1976). This latter refinement in the model had no effect on the water-influx predictions for the reason just given; however, it did change the model predictions for the shape of the cavity which is formed because of spalling. This work will be discussed at length in Chapter V, which treats "Cavity Growth and Subsidence." It should be noted that the permeation component in this water-influx model does depend on the particular sweep model used since it depends on the lateral surface area exposed. However, when permeation accounts for relatively little water influx, the assumption of a cylindrically expanding cavity results in little error in the total water-influx predictions.

Krantz et al. (1980) compared the predictions of their water-influx model with the measured water influx for the Hanna II Phases II and III, Hanna III, and Hoe Creek II UCG field tests. In any comparison between measured and predicted water influx, it is imperative to define unambiguously what is meant by "water influx." "Water influx" here is defined to be water as liquid or vapor that enters the UCG system from the surroundings, minus that portion which is released by drying, pyrolysis, and combustion of the coal, or that is injected into the system. The "UCG system" in this context is defined to consist of the injection

well, the expanding burned-out cavity, and any gas-flow path including the reverse burn link between the cavity and the production well, and the production well itself. As such, solid coal and rock material will be considered as part of the surroundings, and any product gases or steam coming from the coal and/or rock will be treated as input to the UCG system.

Based on the definition given above, the total water influx consists of water influx due to permeation, bulk flow through larger cracks and fissures, spalling-enhanced drying of the coal, and spalling-enhanced drying of the overburden rock. The predictions of Krantz et al. (1980) for the Wyoming UCG field tests incorporate contributions due to permeation and spalling-enhanced drying, but ignore any contribution to the water influx due to bulk flow through large cracks and fissures.

The daily water influx in m^3/day (1 m^3/day = 35.3 ft^3/day) for the Hanna II Phase II UCG field test arising from permeation and spalling-enhanced drying of both the coal and the overburden rock is shown in Figure IV-3. The water influx due to permeation (shown by the short dashed lines) is seen to be insignificant; indeed water influx by permeation was actually negative during a portion of this test since the cavity operating pressure exceeded the hydrostatic pressure. Water influx due to permeation was found to be insignificant for all three Hanna UCG tests analyzed due to both the low permeability of the Hanna coal seam (approximately 0.003 to 0.015 μm^2 or 3 to 15 mD) and to the small pressure driving force available for permeation. The water influx due to spalling-enhanced drying of the coal (shown by the long-short dashed lines) accounts for nearly all the water influx during the early days of the burn during which the UCG cavity is expanding upward due to spalling of the overlying coal. The rate of water influx is higher during these early days of the test because the coal is more friable than the overburden rock and hence tends to spall far more rapidly. Initially the water influx due to spalling of the overburden rock (shown by the long dashed lines) is identically zero since the UCG cavity does not extend upwards to expose the overburden rock until sufficient spalling of the coal has occurred. Note that the increase in water influx due to spalling-enhanced drying of the overburden rock coincides with the decline in water influx due to spalling-enhanced drying of the coal. That is, once the cavity has expanded upwards to expose the overburden rock, water influx due to coal spalling ceases to be the major contribution to the total water influx. Figure IV-4 then compares the predicted total daily water influx (shown by the dashed line) with the measured daily water influx (shown by the solid line) for the Hanna II Phase II field test. The water-influx model of Krantz et al. (1980) appears to be capable of following the general trends in water influx, although it does not follow the short-term fluctuations in water influx. These are probably caused by random fluctuations in the properties of the overlying rock. It is doubtful whether any water-influx model could account for such detailed stratigraphic effects.

In order to make the water influx predictions in Figures IV-3 and IV-4, it was necessary to specify the average spalling-rate parameter for both the coal (denoted by LD in the figures) and the overburden rock (denoted by LR). In the absence of any definitive core-characterization

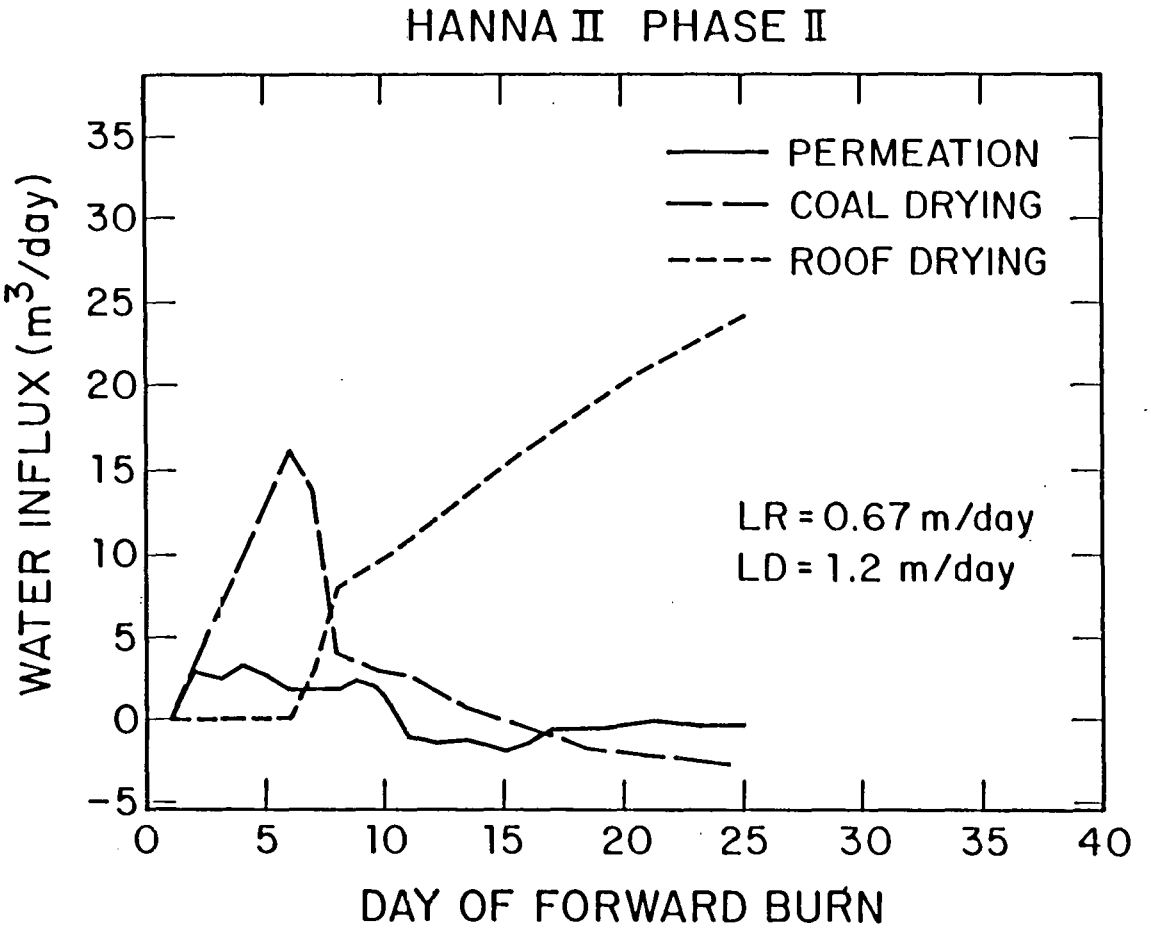

Figure IV-3. Predicted Water Influx Contributions for the Hanna II Phase II UCG Field Test

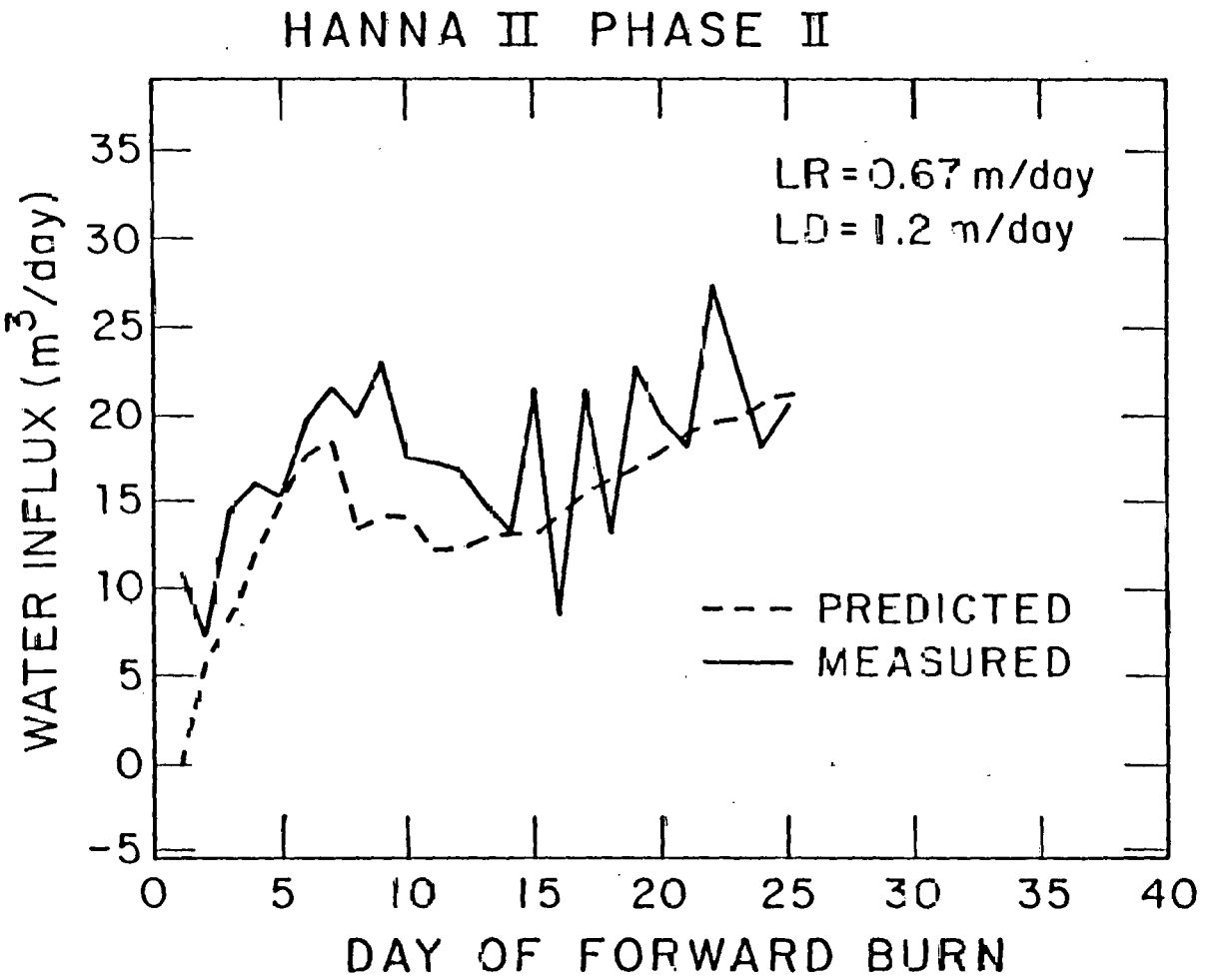

Figure IV-4. Predicted and Measured Water Influx for the Hanna II Phase II UCG Field Test

data from which these parameters could be determined for the Hanna field tests, appropriate values for these two parameters were determined by inspection of the daily water-influx data for these field tests. This determination of the spalling-rate parameters from the field-test data, however, was not an exercise in curve-fitting since the values of these parameters are subject to several constraints. In the absence of any information to the contrary, one must necessarily assume the same pair of values for the spalling-rate parameters for all three Hanna tests. In addition, one would anticipate that the spalling-rate parameter for the coal would be significantly larger than that for the overburden rock since the coal is more friable than the rock. Furthermore, inspection of the measured water-influx data for all three Hanna tests provides a good estimate for the spalling rate of the coal, since the water-influx rate shows a pronounced decrease once the coal has spalled up to the overburden rock which then proceeds to spall more slowly. That is, the early stages of the three Hanna field tests show a marked decrease in the water-influx rate approximately 7.5 days into the burn. A coal spalling rate of 1.2 m/day (4.0 ft/day) would spall upwards through the 9.1 m (30 ft) Hanna No. 1 coal seam in 7.5 days. This value for the coal spalling rate then was used for all three Hanna field tests, whereas a value of 1.1 m/day (3.6 ft/day) was used for the Hoe Creek II field test. The spalling-rate parameter for the overburden rock then was assumed to be 0.67 m/day (2.2 ft/day) for the Hanna field tests and 0.61 m/day (2.0 ft/day) for the Hoe Creek II field test. These empirically determined values for the spalling-rate parameter of the overburden rock do not differ significantly from the value of 0.74 m/day (2.4 ft/day) which Camp (1980) determined from laboratory core-characterization studies of overburden cores from the Hoe Creek site. In fact, Levie et al. (1982) have shown that the water-influx data for the Hanna and Hoe Creek II field tests can be predicted equally well using the 0.74 m/day spalling rate for the overburden rock determined solely from laboratory core-characterization tests.

The predictions of the water-influx model are compared with the measured daily water influx for the Hanna II Phase III, Hanna III, and Hoe Creek II UCG field tests in Figures IV-5, IV-6, and IV-7, respectively. The general agreement between the model predictions and measured daily water influx is comparable for all four tests considered here. A noteworthy observation in the Hanna II Phase III field test is that the daily water influx was approximately twice that of the other two Hanna field tests. The most probable reason for this is that the Hanna II Phase III burn was adjacent to the Phase II burn; the distance between the line of centers between the two sets of injection and production wells was only 18.3 m (60 ft). In addition, a reverse combustion link was established between the two burn areas. Since the Phase III test commenced shortly after the Phase II wells were shut in, it is quite likely that steam generated in the hot Phase II cavity provided an additional water influx into the Phase III cavity through the interconnecting link between the two cavities. In preparing Figure IV-5, this additional water influx due to the adjacent cavity was assumed to be equal to the predicted water influx for the last day of gasification at the Phase II burn. At the time Figures IV-4, IV-5, and IV-6 were prepared, no post-burn coring studies had been conducted at the Hanna site. However, post-burn coring data were available for the Hoe Creek

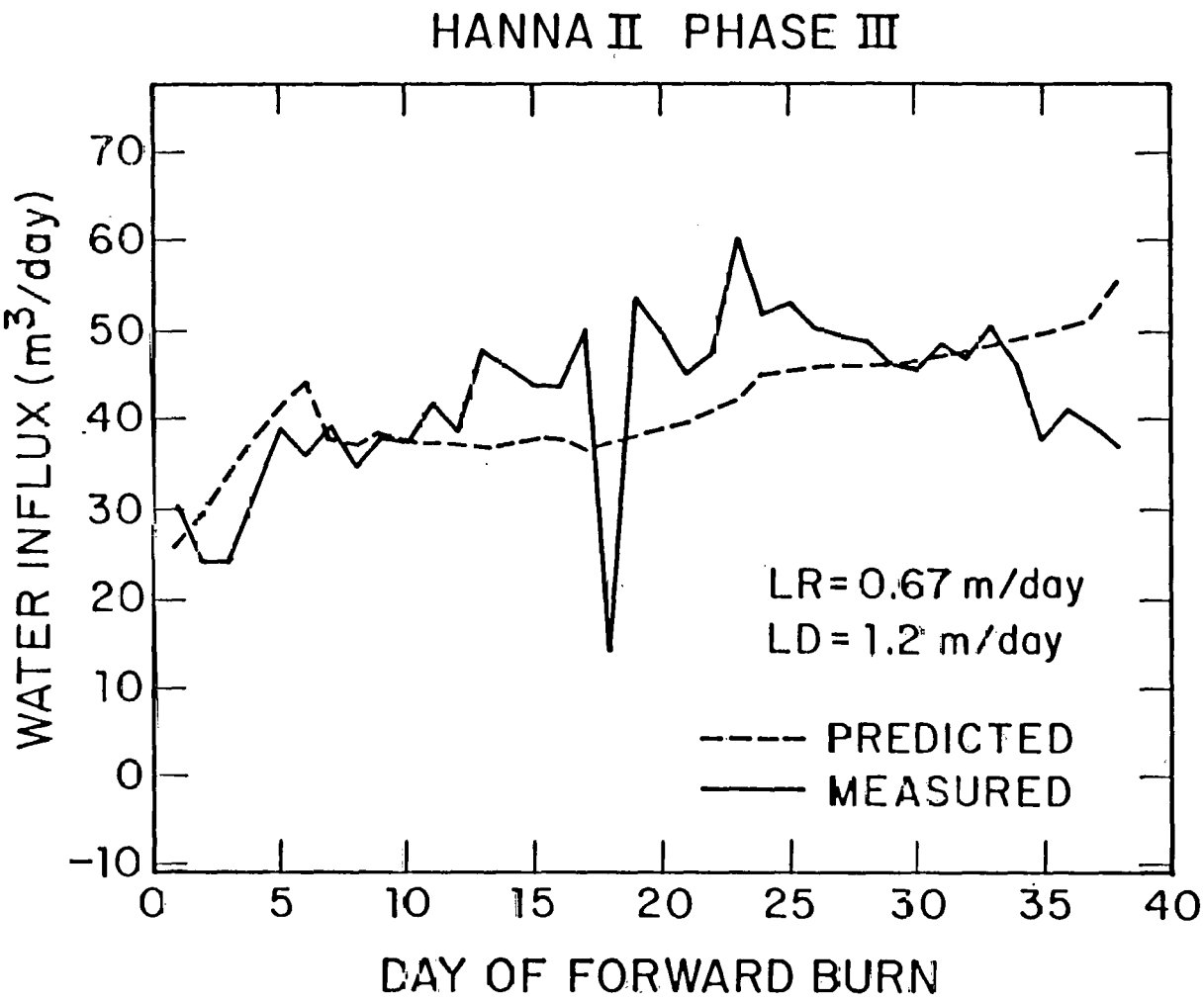

Figure IV-5. Predicted and Measured Water Influx for the Hanna II Phase III UCG Field Test

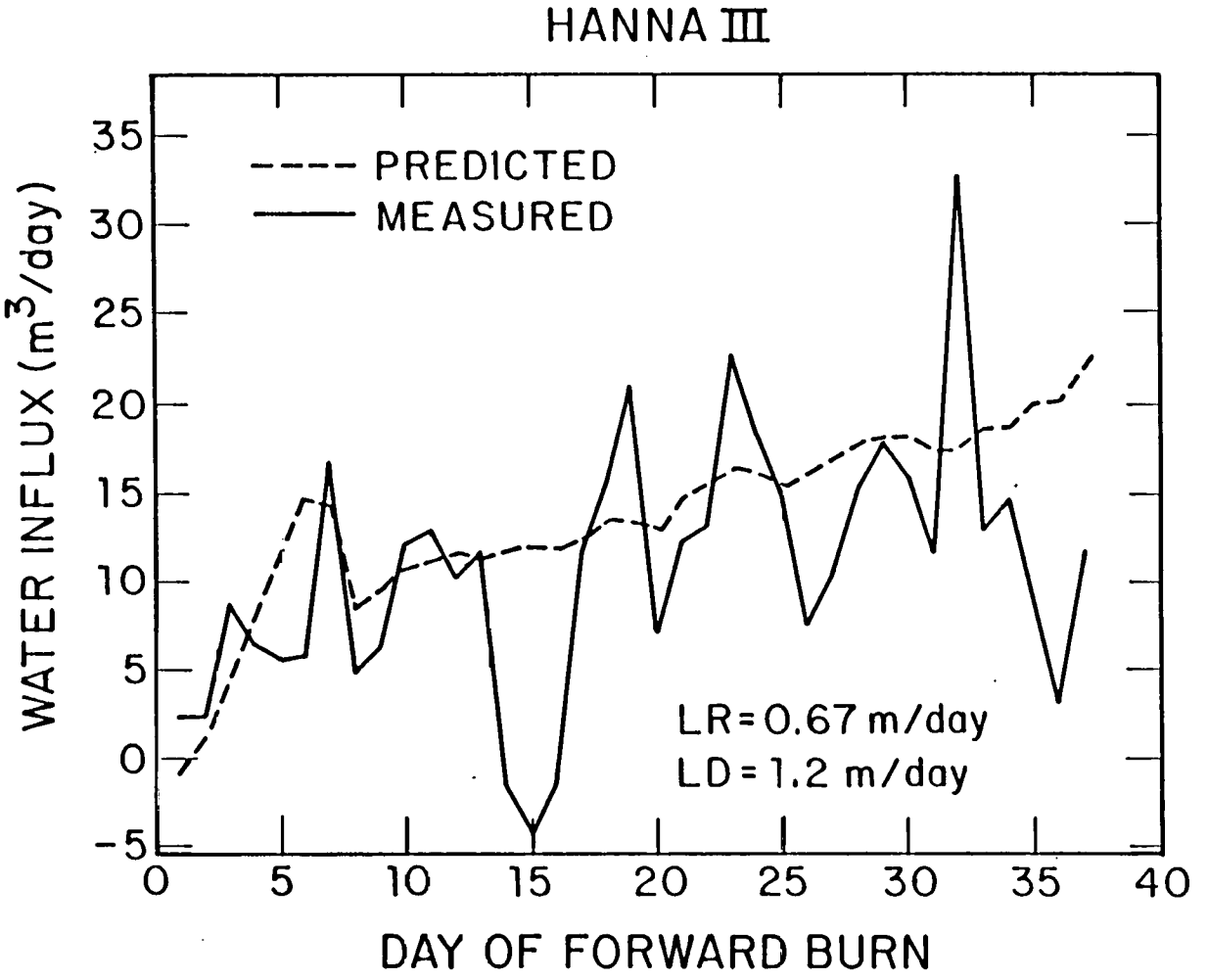

Figure IV-6. Predicted and Measured Water Influx for the Hanna III UCG Field Test

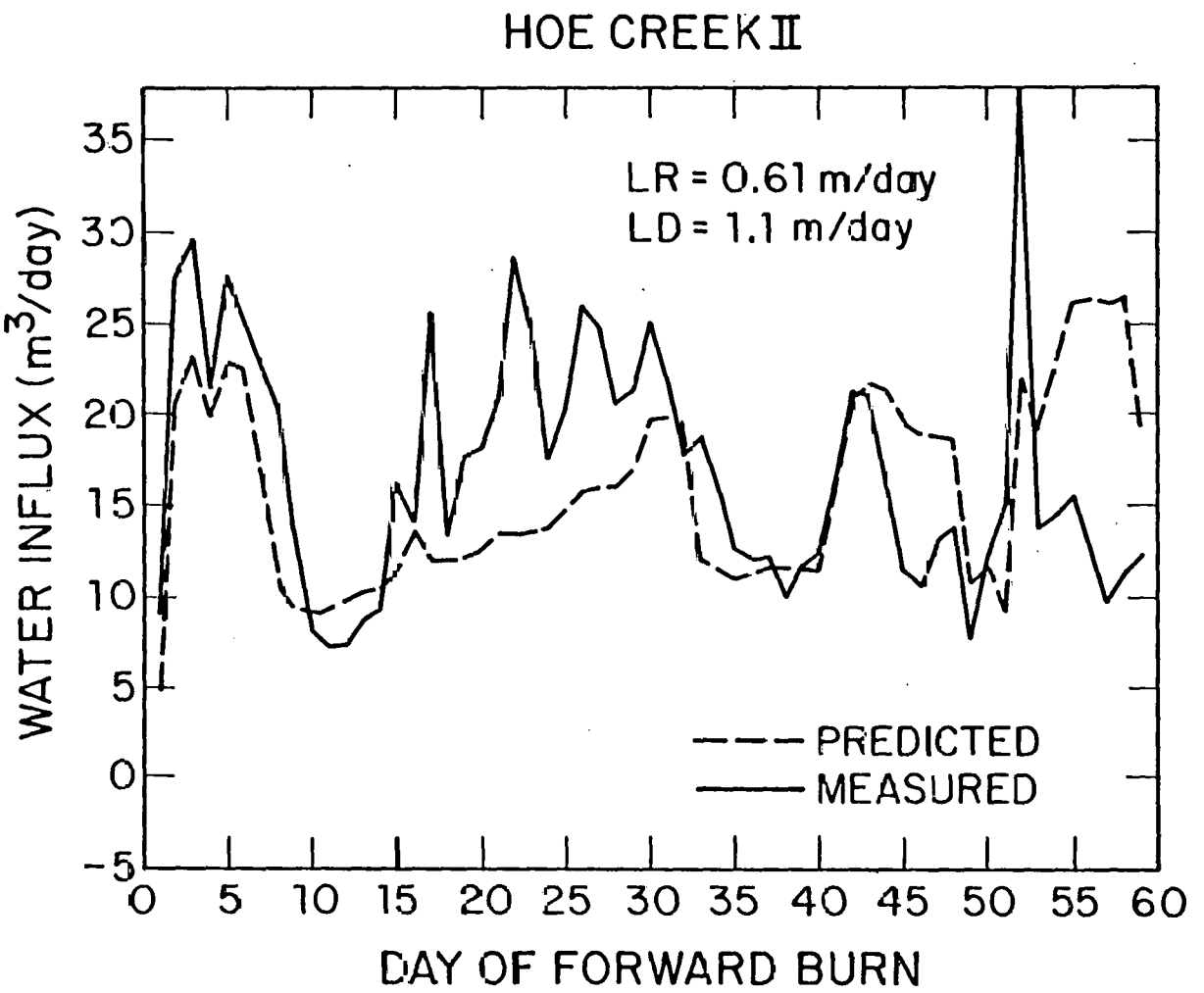

Figure IV-7. Predicted and Measured Water Influx for the Hoe Creek II UCG Field Test

II site. These data indicated that there was an indurated layer of siltstone of high structural integrity approximately 15 m (51 ft) above the Felix No. 2 coal seam. Hence, on the basis of this information, Figure IV-7 was prepared by assuming that the spalling rate of the overburden rock was 0.61 m/day (2.0 ft/day) until this indurated layer was reached; the spalling rate of the harder indurated layer then was assumed to be negligible.

Daily water-influx data such as those shown in Figures IV-4 through IV-7 provide the most demanding test of a water-influx model. The agreement between the predicted and observed daily water influx for these four field tests is quite good on the average and probably is about as good as any model will ever be capable of doing without complete data on local rock properties over closely spaced intervals. A comparison between the predicted and measured water influx in cubic meters for the entire duration of each of these field tests is shown in Table IV-1. This table also indicates the total volume of coal consumed and the contribution to the predicted water influx due to permeation, spalling-enhanced drying of the coal, and spalling-enhanced drying of the overburden rock. For the Hanna II Phase III field test, the predic-

Table IV-1

Measured and Predicted Values of the Water Influx Using the Spalling-Enhanced-Drying Model

Field Test	Hanna II Phase II	Hanna II Phase III	Hanna III	Hoe Creek II
Coal Consumed (m^3)	1,340	2,230	1,730	1,400
Water Influx (m^3):				
Roof Spalling	302	742	538	681
Coal Spalling	56	0	32	0
Permeation	8	-51	-49	278
Bulk Flow	--	931	--	--
Total Predicted	366	1,622	521	959
Total Measured	443	1,650	412	1,030

ted amount of water influx from the adjacent Hanna II Phase II cavity is also shown. The predictions for the cumulative water influx agree with the measured values within an average error of 13.1 percent, which is about the estimated measurement error for these data. The permeation contribution to the cumulative water influx is seen to be negligible for all three Hanna field tests due to the low permeability (3 to 15 mD) of the Hanna No. 1 coal seam. However, permeation contributed approximately 29 percent of the water influx for the Hoe Creek II field test because of the higher permeability (225 to 450 mD) of the Felix No. 2 coal seam. The fact that permeation contributed significantly to the water influx at Hoe Creek but not at Hanna explains why the water influx appeared to be influenced by operating pressure at Hoe Creek but not at Hanna.

The good agreement observed between the predicted and measured water influx for the Hanna and Hoe Creek UCG field tests supports the contention that the water-influx model of Krantz et al. (1980) correctly describes the principal mechanisms for water influx in UCG. In particular, these water influx data show spalling-enhanced drying to be the main contribution to water influx. Additional confirmation of this spalling-enhanced-drying model has been obtained by Levie et al. (1981, 1982) by comparing the predicted post-burn cavity shape resulting from roof spalling with the cavity shape inferred from post-burn coring studies. These cavity-shape predictions will be discussed in detail in Chapter V. Another independent confirmation of the accuracy of the spalling-enhanced-drying model was provided by Gunn and Glaser (1981) who used this model to determine how much process heat was lost in heating the spalled rubble pile in the UCG cavity. Their estimated heat loss of 10 percent for the Hanna III UCG field test agreed well with the heat loss determined from an overall energy balance on this field test. The fact that the same spalling-rate parameters were used to predict water influx, post-burn cavity shape, and the heat lost to the spalled rubble pile shows that the spalling-rate parameter characterizes the physics of the spalling process with reasonable accuracy.

Implications of These Modeling Studies

These modeling studies indicate that water influx in the Wyoming UCG field tests occurred because of permeation of water into the UCG cavity and spalling-enhanced drying of the coal and/or overburden rock overlying the cavity. Capillary pressure effects can be significant in determining the effective hydrostatic pressure which drives the permeation. Calculations indicate that capillary pressure effects increased the effective hydrostatic pressure by 13 percent in the Hanna UCG field tests but only by 3 percent in the Hoe Creek UCG field test. This pronounced difference in the importance of capillary pressure effects between these two field test sites arises because of the smaller characteristic pore size of the Hanna coal (1.4 μm) when compared with that of the coal at Hoe Creek (25 μm). The fact that permeation can occur into both the UCG cavity and the reverse combustion link cannot be ignored when modeling the permeation contribution to the total water influx. Camp (1980) has shown that when the edge of the gasification cavity has progressed halfway towards the production well for an 18.3 m (60 ft)

well spacing, 28 percent of the water influx by permeation is coming in through the link. Water influx into the link cannot rob heat from or participate in the gasification reactions occurring in the cavity. The principal effects of the water influx into the link are to cool the product gas, increase its water content, and perhaps to stimulate conversion of some carbon monoxide to hydrogen gas via the water-gas shift reaction.

The principal mechanism for water influx in the Wyoming UCG field tests was spalling-enhanced drying of the overburden rock. Water influx by permeation was negligible for the Hanna field tests but accounted for 29 percent of the total water influx in the Hoe Creek test. The primary reason for this marked difference in the importance of permeation is the small pore size and associated low permeability of the Hanna No. 1 coal seam relative to the Felix No. 2 seam at Hoe Creek. The dependence of the water influx on the operating pressure and lateral or areal sweep of the gasification process can be markedly different depending on the importance of permeation relative to spalling-enhanced drying as a source of the water influx. The rate of permeation depends on both the cavity pressure as well as the lateral surface area of the instantaneous cavity/link geometry. Spalling-enhanced drying, on the other hand, is independent of the cavity pressure and lateral surface area, but is markedly dependent on the projected cavity roof area. These different characteristics of the permeation and spalling-enhanced-drying water-influx mechanisms explain why the water influx in the Hoe Creek UCG field tests was observed to be somewhat dependent on cavity operating pressure, but was observed to be independent of cavity pressure for the Hanna field tests.

The fact that water influx by the spalling-enhanced-drying mechanism is strongly dependent on the projected cavity roof area implies that the gasification of thin seams is less economic than thick seams. That is, for a fixed rate of coal consumption, more roof area will be exposed for a thin coal seam than for a thick one. If the principal mechanism for water influx is spalling-enhanced drying, this implies that the ratio of heat lost to coal consumed will be larger for a thin seam than for a thick seam. This heat loss constitutes heat lost to heat the spalled overburden rock and to vaporize the water contained in this rock. Greater heat losses per unit mass of coal consumed imply lower thermodynamic efficiencies. Excessively large heat losses can result in a reduced cavity temperature below that at which the endothermic gasification reactions can be promoted at reasonable rates.

The spalling-enhanced drying mechanism also underscores the importance of establishing the reverse combustion link low in the coal seam. Very little, if any, coal can be gasified below the link due to the natural tendency of the hot gases to rise and follow the general direction of the link. Hence, establishing the link low in the seam insures that the full thickness of the coal seam is potentially recoverable. This in turn minimizes the ratio of heat losses per unit mass of coal consumed.

The water-influx model developed here supplies the information needed to make the forward combustion gasification models developed by

Gunn and Whitman (1976) and others fully predictive. That is, all the models developed to date for predicting the UCG product-gas composition, yield, temperature, and heating value, require that the instantaneous water influx be specified as an input parameter. The water-influx model developed here then can be coupled with a gasification model to determine an optimum operating strategy to insure a constant high product-gas heating value. Figure IV-8 shows a plot of product-gas heating value versus day of test for the Hanna III UCG field test. The progressive decline in heating value from a relatively high value (for air injection) of 6 MJ/m^3 (160 Btu/scf) to 3.3 MJ/m^3 (90 Btu/scf) is typical of all the Hanna UCG field tests. Gunn et al. (1980) have shown that this decline in product-gas heating value arises because of progressively increasing heat losses due to spalling-enhanced drying of the overburden. The heat losses increase because the amount of rock heated and dried increases as the amount of roof exposed increases. This suggests that a possible operating strategy to insure a constant high product-gas heating value would be to increase the rate of coal consumption progressively as the UCG burn progresses in order to maintain a constant ratio of heat losses to coal consumed. This could be accomplished by increasing the oxidant injection rate as time elapses. Levie et al. (1981) have shown how such an optimum operating strategy might have affected the Hanna II Phase II UCG field test.

One shortcoming in the water-influx modeling studies discussed here is that accurate predictions require reliable values of the spalling-rate parameters for the coal and distinct layers which constitute the overburden. Whereas only two spalling parameters, one each for the coal and overburden, were necessary to describe the water-influx data for the relatively short duration Wyoming UCG field tests, it is likely that several spalling parameters will be needed to characterize the spalling properties of the greater thickness of overburden affected during longer commercial scale UCG burns. Levie et al. (1982) have discussed the need for a laboratory core-characterization technique for determining the spalling-rate parameters of the overburden and have presented preliminary laboratory study results which suggest that this might be possible. Developing this laboratory core-characterization test for determining the spalling-rate parameters is one of the most pressing needs at this time to enhance our ability to characterize the performance of UCG prior to a field test.

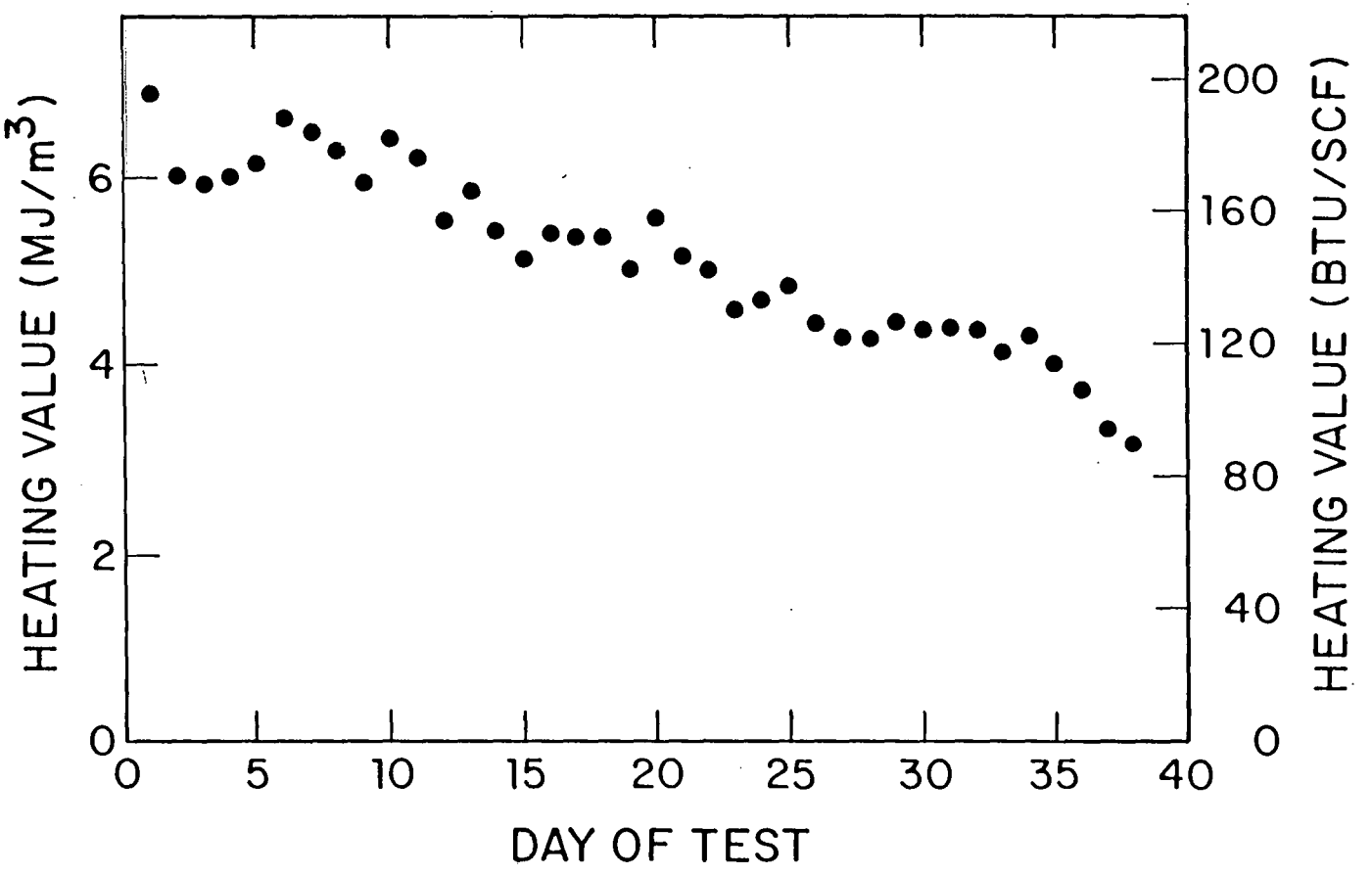

Figure IV-8. Product Gas Heating Values for the Hanna III UCG Field Test

CHAPTER V - CAVITY GROWTH AND SUBSIDENCE

Cavity Growth and Subsidence in UCG

The UCG process necessarily creates a cavity partially filled with rubble, whose lateral extent is determined by the amount of coal gasified and whose vertical profile is determined by spalling of the overburden. That is, the lateral cavity growth due to gasification of the coal, exposes the overburden which can progressively collapse by spalling or flaking off of small pieces of rock. This spalling causes the upward growth of the cavity roof and is responsible for the shape of the cavity roof arch which is ultimately developed.

The shape of the UCG cavity determines the extent of any subsidence which occurs for the particular overburden strata involved at a site. "Subsidence" refers to the adjustment made in the earth in response to the removal of mass from the subsurface. There are four principal types of subsidence: bending, caving, chimneying and plug. Bending subsidence refers to convergence or sagging of the overburden into the underground cavity. Caving subsidence involves the random spalling of pieces of the cavity roof rock into the void. Chimneying subsidence defines the upwards propagation of a relatively small, nearly constant area to the surface due to caving above the cavity. Plug subsidence identifies the sudden failure of the entire mass overlying an underground cavity. Bending, caving and chimneying subsidence have been observed in the large scale Soviet UCG operations as well as in the UCG field tests in the U.S.

Lateral and vertical cavity growth are very important aspects of the UCG process, since they determine both the amount of coal resource that can be recovered for a fixed well bore spacing, and the nature and magnitude of any subsidence effects that might be experienced. Clearly one would like to have a broad lateral sweep or growth of the UCG cavity so that the largest possible amount of coal will be recovered between any particular set of injection and production well bores. The subsidence effects associated with the vertical growth of the UCG cavity have implications with respect to both the environmental impact of UCG as well as the effectiveness of the UCG process itself.

The extent of the environmental consequences of subsidence needs to be understood in order for future UCG operations to meet the requirements of the Surface Mining Control and Reclamation Act of 1977 and to permit the filing of an appropriate Environmental Impact Statement. The potential environmental consequences of subsidence associated with UCG operations include disruption of the ground surface and structures above the UCG site, venting of combustible and toxic gases to the surface, contamination of adjacent aquifers by escaping gases, and gross structural disruption of aquifers.

Subsidence can also affect the performance of the UCG process. Disruption of the overburden can damage supporting equipment and structures on the surface as well as the well bores. The rubble pile created by collapse of the overburden can alter the gas flow paths in the cavity

thereby affecting the burn geometry and resource recovery. The water influx into the UCG process is influenced significantly both by spalling-enhanced drying of the overburden and by direct communication with overlying aquifers due to cracking and faulting of the overburden.

Realizing the importance of cavity growth and subsidence in the UCG process, the Wyoming-Colorado UCG research group focused its efforts on developing predictive models for the areal sweep of the coal gasification and for the cavity dome shape resulting from spalling. Since the spalling process is initiated only after the overburden is exposed due to gasification of the underlying coal, this research group first directed its efforts towards developing an areal sweep or lateral cavity growth model. This sweep model then was integrated into the spalling-enhanced-drying model in order to predict the upward growth of the cavity roof.

A Model for the Areal Sweep

The schematic of the initial stages of the coal gasification process shown in Figure I-1-E shows that the gasification process expands more-or-less radially about the injection well bore until the overburden is reached. The overburden is reached relatively rapidly in a typical UCG process since the upward growth of the UCG cavity is aided by spalling of the overlying coal. For example, the coal spalled at a rate of approximately 1.2 m/day (4.0 ft/day) during the Hanna tests. This rate implies that the overburden rock was exposed in less than 8 days of gasification for the 9.1 m (30 ft) coal seam studied in the Hanna tests. Once the overburden is exposed, the gasification should proceed as a two-dimensional sweep process such that all the coal across the entire exposed vertical faces of the gasification cavity will be gasified. If the link is achieved relatively low in the coal seam, then the entire width of the coal seam will be involved in the gasification process. Under these conditions, a two-dimensional areal sweep model is appropriate to describing the lateral growth of the cavity in the coal seam.

Based on the above considerations, Jennings et al. (1976) developed the first successful sweep model to describe the instantaneous resource recovery for the UCG process. Jennings et al. assumed that the lateral growth of the gasification cavity was a permeation process. That is, the rate of cavity growth at any point along the walls of the cavity was proportional to the air- or oxygen-enriched air-injection flux at that point. The oxygen flux at any point depended on the flow resistance along the flow path to and from the point on the cavity wall extending from the injection well through the rubble-filled cavity to the wall and then through the ungasified coal to the production well. These investigators assumed the UCG system to consist of the low permeability ungasified coal and the very high permeability rubble-filled cavity. The flow through the porous media was assumed to be described by the steady-state, two-dimensional, compressible form of the Darcy flow equation with different permeabilities being assigned to the ungasified coal and the rubble-filled cavity, respectively. The gasification process was assumed to be two-dimensional in that the burn front was assumed to be

perpendicular to the bottom of the coal seam, the entire thickness of which was subject to the burn. In addition, the flow was assumed to be isothermal in order to decouple the solution of the flow problem from that of the energy equation.

The boundary conditions employed in the model involved the specification of the down-hole injection-well pressure and air- or oxygen-enriched air-injection rate. At the cavity walls, both continuity of pressure and mass were demanded. In order to completely specify this flow problem, it was necessary to specify the initial location of the cavity boundary and the manner in which the cavity boundary points moved outwards in response to local gasification of the coal. The initial cavity size was assumed to be negligible. The local velocity of the gasification front, which was assumed to be coincident with the instantaneous cavity boundary, was assumed to be proportional to the local air flux according to the predictions of the gasification model of Gunn and Whitman (1976) which is described elsewhere in this report.

The steady-state, two-dimensional, compressible form of the Darcy flow equation in both regions was then solved using a finite difference technique. A quasi-steady-state solution was obtained by assuming an injection-well pressure and air-injection rate averaged for each successive twelve-hour time period extending from initiation of gasification until breakthrough at the production well. The numerical integration scheme proceeded by determining the pressure gradient at each of several gasification-front tracking points located on the cavity boundary by employing a bilinear interpolation of the pressure gradients at the four grid points in the immediate vicinity of the gasification-front tracking point being considered. The local air flux then was determined from the local pressure gradient using Darcys law. The local flame front velocity then was determined from the local air flux using the relationship determined by Gunn and Whitman (1976). After each twelve-hour time increment, the cavity boundary was advanced appropriate to the local flame front velocity at each of the boundary tracking points. All regions of the numerical grid within the new cavity boundary were then assigned the higher permeability associated with the rubble-filled cavity. The steady-state, two-dimensional, compressible form of the Darcy flow equation in both regions then was solved again numerically for the next twelve-hour time increment to determine the new pressure distribution corresponding to the enlarged cavity boundary. This procedure was repeated until the flame front reached the production well.

As mentioned above, the input data and information required to utilize the areal sweep model of Jennings et al. (1976) are the instantaneous downhole production-well pressure and effective air-injection rate (the rate corrected for the amount of air lost to the formation which is not available for combustion), as well as the (assumed) isotropic permeability of the coal and the relationship between the flame front velocity and air flux determined from the solution of Gunn and Whitman (1976). The Jennings et al. model then determines the instantaneous areal or lateral sweep of the gasification process which is uniquely related to the amount of coal consumed.

Figure V-1 shows the sweep contours predicted by Jennings et al. (1976) for the Hanna II Phase II UCG field test. The legend in this figure indicates the number of days after gasification commenced corresponding to each of the twelve contours. Jennings et al. (1976) also have predicted these contours for the Hanna II Phase I UCG field test. Gunn et al. (1980) report similar calculations for the Hanna III UCG field test. The area of each contour when multiplied by the seam thickness (approximately 9 m for the Hanna No. 1 coal seam gasified in these tests) is proportional to the amount of coal gasified up to the day indicated for any particular contour. The total coal recovery predicted by the Jennings et al. model for the three Hanna tests indicated above is compared with the measured coal recovery in Table V-1 below. In all cases, the predicted coal recovery is slightly greater than the measured recovery. It would appear that the Jennings et al. areal sweep model represents a limiting case, namely the best recovery that can be expected. Channeling during the gasification process, for example, can cause the coal recovery to be much less than predicted, as was the case for the Hanna IV UCG field test.

Table V-1

Comparison of Measured Coal Recovery with that Predicted by the Model of Jennings et al. (1976)

UCG Field Test	Measured Coal Recovery (metric tons)	Predicted Coal Recovery (metric tons)
Hanna II Phase I	1360	1550
Hanna II Phase II	2180	2440
Hanna III	2600	2610

Since a large number of temperature monitoring wells were employed during the Hanna II Phase II UCG field test, it was possible to determine the approximate location of the flame front during this test. These data provide a more definitive test of the Jennings et al. areal sweep model. Table V-2 compares the measured and predicted Julian date for the flame front reaching each of the indicated monitor wells:

The remarkably good agreement between the measured and predicted values shown in Tables V-1 and V-2 may appear surprising in view of the rather tenuous assumptions invoked in developing the Jennings et al. sweep model. However, these assumptions may not be particularly limiting in practice. The isothermal flow assumption appears reasonable when one considers that the reaction zone in coal gasification is less than 0.6 m thick. The pressure drop is determined in large part by the gas

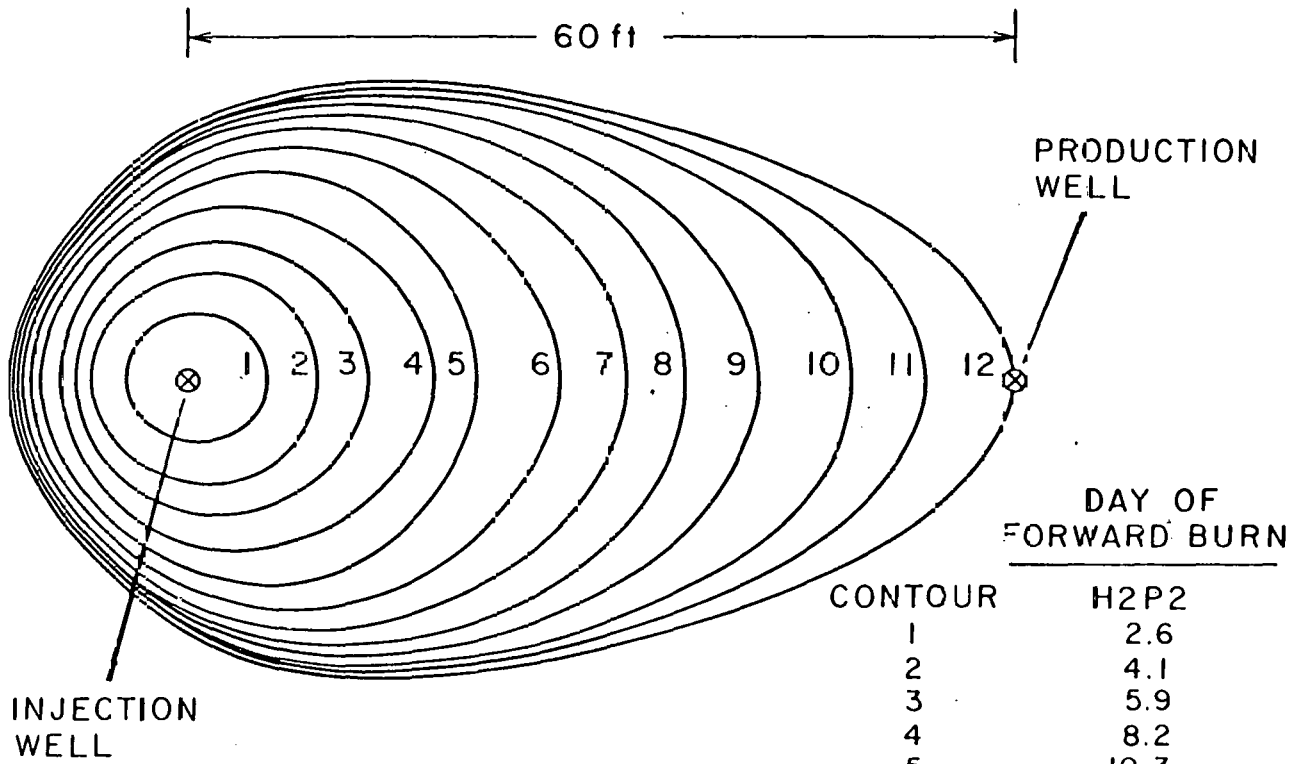

DAY OF FORWARD BURN

CONTOUR	H2P2
1	2.6
2	4.1
3	5.9
4	8.2
5	10.3
6	12.4
7	14.7
8	16.3
9	18.2
10	20.8
11	22.7
12	25

Figure V-1. Areal Sweep Contours for the Hanna No. 1 Coal Seam Based on the Model of Jennings et al. (1976)--Legend Gives Number of Days of Gasification Corresponding to Each Contour for the Hanna II Phase II UCG Field Test

Table V-2

Comparison of the Measured and Predicted Dates for Passage of the Flame Front in the Hanna II Phase II UCG Field Test

Monitor Well	Measured Julian Date	Predicted Julian Data
A	141	140
B	124	124
C	138	138
D	150	148
E	134	135
F	140	140
G	150	151

flow through the coal which is nearly isothermal. Although virgin wet coal typically exhibits a markedly nonisotropic permeability, dry coal is not nearly as nonisotropic. This may explain why the assumption of isotropic permeability does not appear to limit the model severely. The Jennings et al. model totally ignores the presence of any highly permeable link between the injection and production wells. In fact, if one includes any such channel of high permeability in the sweep model, very narrow unrealistic areal sweep patterns are predicted. One reason why the permeable link does not appear to influence the areal sweep significantly is that the region of the link in the vicinity of the gasification cavity may become considerably less permeable due to plugging by tars and collapse of the surrounding coal into the voids in the link. Clearly the reason for the remarkable success of the Jennings et al. sweep model needs to be explored further.

An interesting feature of the Jennings et al. lateral cavity growth model is that the areal sweep contours shown in Figure V-1 apply in general to any two-dimensional gasification process in a coal having the same properties as the Hanna No. 1 seam. That is, the contours shown in Figure V-1 can be scaled to any well spacing, irrespective of the coal seam thickness, and, operating pressure and air-injection schedule for the Hanna No. 1 seam. This is particularly convenient, since this implies that the Jennings et al. numerical procedure need only be carried out once for any particular coal seam with specified properties. The specific coal properties enter the areal sweep determination only through the coal permeability in the Darcy flow equation and the properties required to generate the relationship between the flame front

velocity and the local air flux in Gunn and Whitman's gasification dynamics model. For example, Figure V-1 can be used to predict the areal sweep for any day during an operation in the Hanna No. 1 seam by first scaling contour 12 to the well spacing and total coal gasified up to breakthrough at the production well. The total coal gasified for any of the other contours in Figure V-1 then can be determined by merely scaling the area of the contour under consideration to that of contour 12. The particular number of days of gasification which corresponds to any particular contour will depend on the specific air-injection schedule employed during the UCG burn.

Vertical Cavity Growth

The areal sweep model of Jennings et al. only predicts the lateral cavity growth. The gasification of the coal is assumed to occur such that the entire cross-section of the coal seam advances as a two-dimensional burn front. The gasification of the coal creates a cavity whose growth progressively exposes the overburden material. The unsupported cavity roof is subject to loading due to the weight of the overlying strata as well as due to thermal stresses arising from the high cavity temperatures during gasification. This loading causes failure of the cavity roof by any one of several subsidence modes. In the Hanna UCG field tests, failure of the cavity roof occurred primarily by the spalling or chipping off of small pieces of the roof rock. This spalling then creates the rubble pile which nearly filled the cavity in the Hanna field tests due to a rubble bulking factor of approximately two.

Chapter IV on "Water Influx" discussed a model developed by the Wyoming-Colorado UCG research group for spalling-enhanced drying. "Spalling-enhanced drying" refers to the accelerated drying of the roof rock (also of the overlying coal) which is associated with steepening of the temperature gradients in the cavity roof due to the random spalling of small pieces of the roof rock. This spalling-enhanced-drying model is described in considerable detail in Chapter IV and will not be discussed in depth again here. The spalling-enhanced-drying model, which has been shown to predict the water influx for four Wyoming UCG field tests quite well by Krantz et al. (1980) and Camp et al. (1980), has been used to predict the vertical cavity growth by Levie et al. (1981, 1982).

Recall that the spalling-enhanced-drying model as originally developed by Camp (1980) involved coupling the spalling-enhanced-drying and permeation water-influx mechanisms with a lateral cavity growth or areal sweep model. Whereas the water influx by permeation depends primarily on the surface area of the side walls of the gasification cavity, the water influx by spalling-enhanced drying depends only on the surface area of the cavity roof. The latter is independent of the particular lateral cavity growth or areal sweep model which is chosen as long as the UCG burn is two-dimensional and all the affected overburden strata are reasonably parallel to the coal seam. That is, for a two-dimensional burn, the cavity roof area exposed at any time during the UCG burn is directly proportional to the ratio of the coal consumed up to the time being considered divided by the coal seam thickness. The

latter necessarily must be constant if the UCG burn is to be two-dimensional. Since the water influx in the Hanna tests was primarily due to spalling-enhanced drying (97 percent or more of the total water influx), Camp (1980) chose the simplest possible lateral cavity growth or areal sweep model; he assumed that the cavity within the coal seam was always a right-circular cylinder. Whereas this assumption could cause a serious error in the amount of water influx predicted to occur by permeation, it has no effect whatsoever on the amount of water influx predicted to occur by spalling-enhanced drying, assuming that the UCG burn is indeed two-dimensional.

Although the water influx by spalling-enhanced drying is independent of which two-dimensional sweep model is used, the same cannot be said for the vertical cavity growth profile. That is, roof spalling will occur only after the cavity roof rock has been exposed due to gasification of the underlying coal. The lateral cavity growth or areal sweep model determines where the coal is gasified at any particular time during the UCG burn and hence determines where roof spalling can occur. Clearly a realistic lateral cavity growth model is required if one is to predict the vertical cavity growth accurately.

Levie et al. (1981) used the spalling-enhanced-drying model developed by Camp (1980), to predict the three-dimensional UCG cavity shape by incorporating the areal sweep model of Jennings et al. (1976) in place of the cylindrical sweep model used by Camp. The manner in which the generalized lateral sweep contours such as those shown in Figures V-1 for the Hanna No. 1 coal seam can be used to determine the post-burn three-dimensional cavity shape created by spalling is quite straightforward. First, the actual spacing between the injection- and production-well bores is scaled to the spacing between the injection- and production-well bores shown in Figure V-1. The total amount of coal gasified in the burn is proportional to the area of contour 12 in this figure, with the assumption that the burn is two-dimensional and gasification is carried out to breakthrough. The areas of contours 1 through 11 then can be ratioed to the area of contour 12 and multiplied by the total coal consumption in order to determine the cumulative amount of coal corresponding to each of these contours. The time required to create each contour then can be determined from knowledge of the daily coal gasification rate or air-injection schedule.

The determination of the vertical cavity profiles then proceeds as follows. Consider the data for the Hanna II Phase II UCG field test for which the overburden spalling rate parameter based on the water-influx data shown in Figure IV-5 is LR = 0.67 m/day. It took 25 days to create contour 12. There is no spalling associated with this contour because it is assumed that the burn was terminated at the instant this contour was created. Contour 11 was generated in 22.7 days; hence, spalling can occur for 2.3 days (25 - 22.7 days) above this entire contour. Hence, one generates 1.54 m of spalling (2.3 days x 0.67 m/day) above this contour. Since contour 10 was generated in 20.8 days, spalling can occur for 4.2 days; hence, one generates 2.81 m of spalling above the entire area of contour 10. One proceeds to determine the amount of spalling corresponding to each contour in this manner. However, one must take into consideration that the roof of the coal seam is not

exposed from the inception of the gasification process. That is, it takes several days before the roof of the coal seam is exposed since the cavity must grow upwards through the coal seam both due to gasification as well as rapid spalling of the overlying coal. The water-influx data presented in Figures IV-4, IV-5 and IV-6 suggest that it took approximately 7.5 days to first expose the roof of the coal seam. At this time for the Hanna II Phase 2 field test, the area of roof exposed is somewhere between that shown for contours 3 and 4 in Figure V-1. This area of roof then has 17.5 days to spall (25 - 7.5 days) corresponding to 11.7 m of spalling which should correspond to the maximum height of the cavity above the coal seam. The entire cavity dome shape then is generated by locating the cavity roof created by spalling above each of the contours using the cumulative spalling height determined above.

The procedure for determining the shape of the cavity dome created by spalling as described above, used the same spalling rate parameter for all the overburden material. Longer UCG burns, such as the 38 day Hanna III burn, undoubtedly expose more varied strata which may have markedly different spalling-rate parameters. Indeed, the water-influx data for the Hanna III field test shown in Figure IV-6 suggest that the spalling rate decreases after approximately 25 days into the burn. Although this more complex stratigraphy was not taken into account in generating the water influx predictions shown in Figure IV-6, it needs to be accounted for if reliable cavity shapes are to be predicted.

It is a relatively simple matter to account for the specific spalling rates associated with each stratum above the coal seam. If the stratigraphy of a UCG site is known, one merely has to determine when spalling above a particular contour at the spalling rate associated with the stratum immediately above the coal seam causes one to reach the next stratum. For example, if there is 1.5 m of claystone immediately above the coal seam which spalls at a characteristic rate of 0.82 m/day, which in turn is overlaid by 12 m of siltstone which spalls at 0.18 m/day, one would determine the amount of spalling above contour 4 in Figure V-1 as follows. The rock above this contour has 16.8 days to spall. It took only 1.8 days (1.5 m divided by 0.82 m/day) to spall through the claystone layer thus leaving 15 days for the siltstone to spall, corresponding to 2.7 m of additional spalling. Thus, contour 4 would have a total of 4.2 m of spalling above it. More complex stratigraphy can be accounted for in a similar manner. It is also possible to account for nonparallel strata in the manner described above. Note that in the case of nonparallel spalling strata, the water influx will also depend on which sweep model is chosen.

The Hanna II Phases II and III, and Hanna III UCG field tests permitted a definitive test of the UCG cavity growth model developed by the Wyoming-Colorado UCG research group since the post-burn cavity geometries for these three field tests were determined by coring. Figure V-2 shows the location of the injection, production, coring and drilling holes for the Hanna II Phases II and III field tests. Gasification was carried out in the Hanna II Phase II burn from well 6 to well 5.

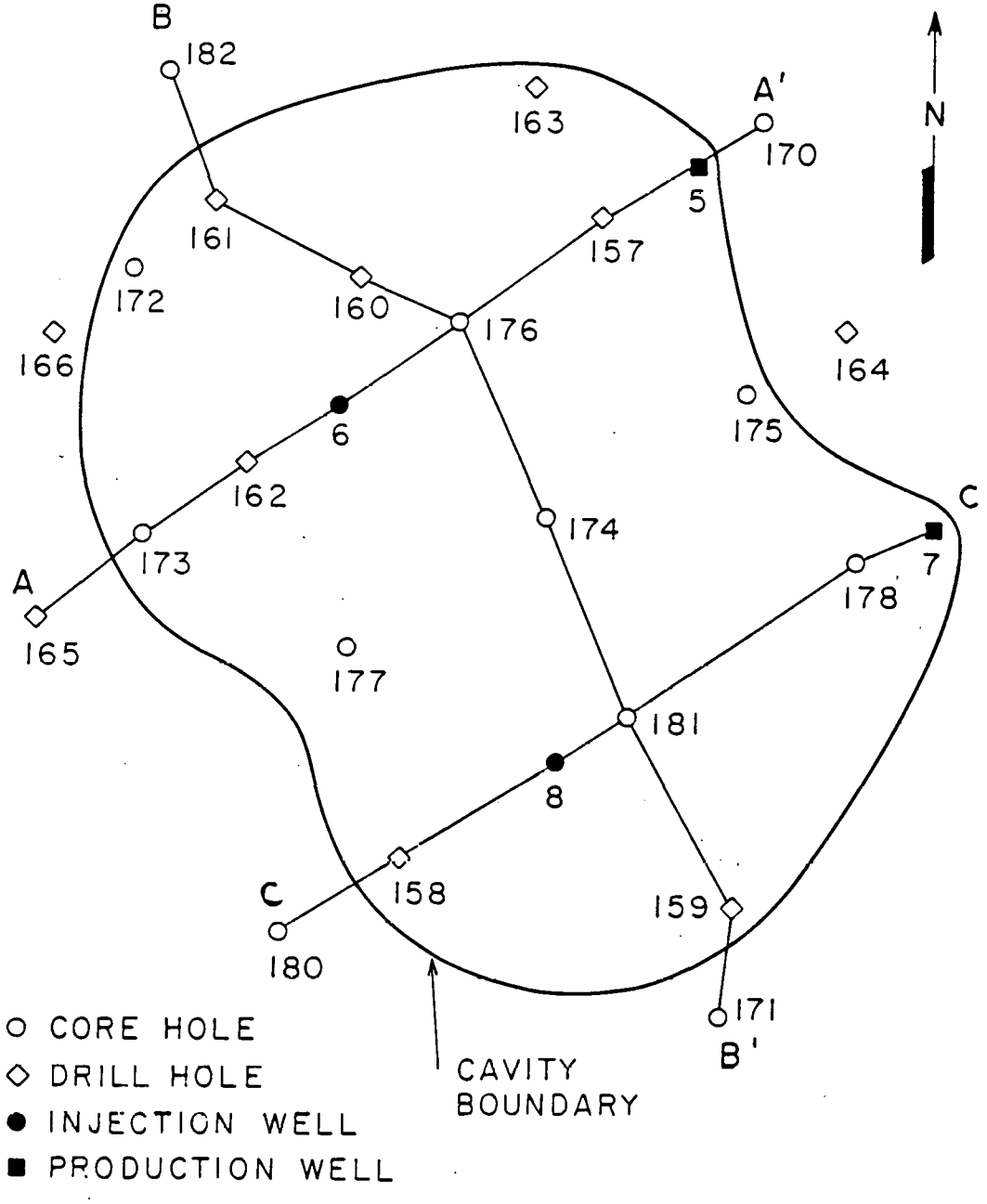

Figure V-2. Location of Injection and Production Wells, and Post-Burn Drill and Core Holes for the Hanna II Phase II and Phase III UCG Field Tests

Figure V-3 shows the predicted post-burn cavity dome profile along the line shown between core holes 173 and 170 in Figure V-2. The rubble pile is not shown in this diagram for convenience in comparing the predicted cavity shape to that determined by post-burn coring. The latter is shown by the nine data points in this figure. The agreement between the predicted and measured cavity profiles is rather remarkable in view of the fact that the same spalling rate parameter for the overburden (LR = 0.67 m/day) was used for these predictions as was used to predict the water influx shown in Figure IV-4. That is, no curve-fitting parameters were used to generate the predictions shown in Figure V-3. In particular, the maximum height of the cavity dome is predicted very well. The coring data indicate backburning behind the injection well which is not accounted for by the model predictions. This may be a result of additional gasification which occurred around the injection well in the Hanna II Phase 3 field test which was carried out shortly after the Phase 2 wells were shut in. The lateral cavity profile along the line connecting core holes 182 and 171 is shown in Figure V-4. Again, the maximum cavity height is predicted well, although somewhat more gasification occurred along the sidewalls then is predicted by the model. Note that this shortcoming in the model appears to arise because of the inaccuracies in the lateral cavity growth or areal sweep model of Jennings et al. (1976), not because of deficiencies in the spalling model.

There are several possible explanations for why the observed cavity shape is both longer (behind the injection well) and wider than predicted by the cavity growth model developed here. The rubble pile could divert the air flow into a wider path than that predicted by the areal cavity growth of the Jennings et al. model which does not account for the effect of the rubble pile on the gasification. Of potential significance to the Hanna II Phase II test, is the fact that the cavities of the Hanna II Phase II and Phase III field tests were linked in an unsuccessful attempt to carry out a line-drive gasification between a four-well pattern. This link provided a channel of communication between the two tests which could have caused a wider sweep pattern particularly behind the injection well in the Phase II field test. Finally, the same spalling mechanism which is responsible for the upward growth of the cavity roof, is also possibly active at least to some extent along the cavity walls. This spalling mechanism could cause more rapid gasification along the cavity walls thus resulting in a wider sweep pattern.

Gasification was carried out in the Hanna II Phase III burn from well 8 to well 7 shown in Figure V-2. Figure V-5 shows the predicted post-burn cavity dome profile along the line shown between core holes 180 and 178 in Figure V-2. The cavity profile as inferred from the post-burn coring studies is shown by the eight data points in this figure. In making the cavity geometry predictions shown in Figure V-5, it was necessary to account for the more complex stratigraphy of the Hanna UCG field test site. Immediately above the 9.1 m Hanna No. 1 coal seam, is a 1 m layer of brown carbonaceous shale. This in turn is overlaid by a 30 m thick layer of sandstone. The upper two-thirds of this sandstone layer is indurated; that is, it contains areas where calcite has replaced the quartz and feldspar grains. This induration

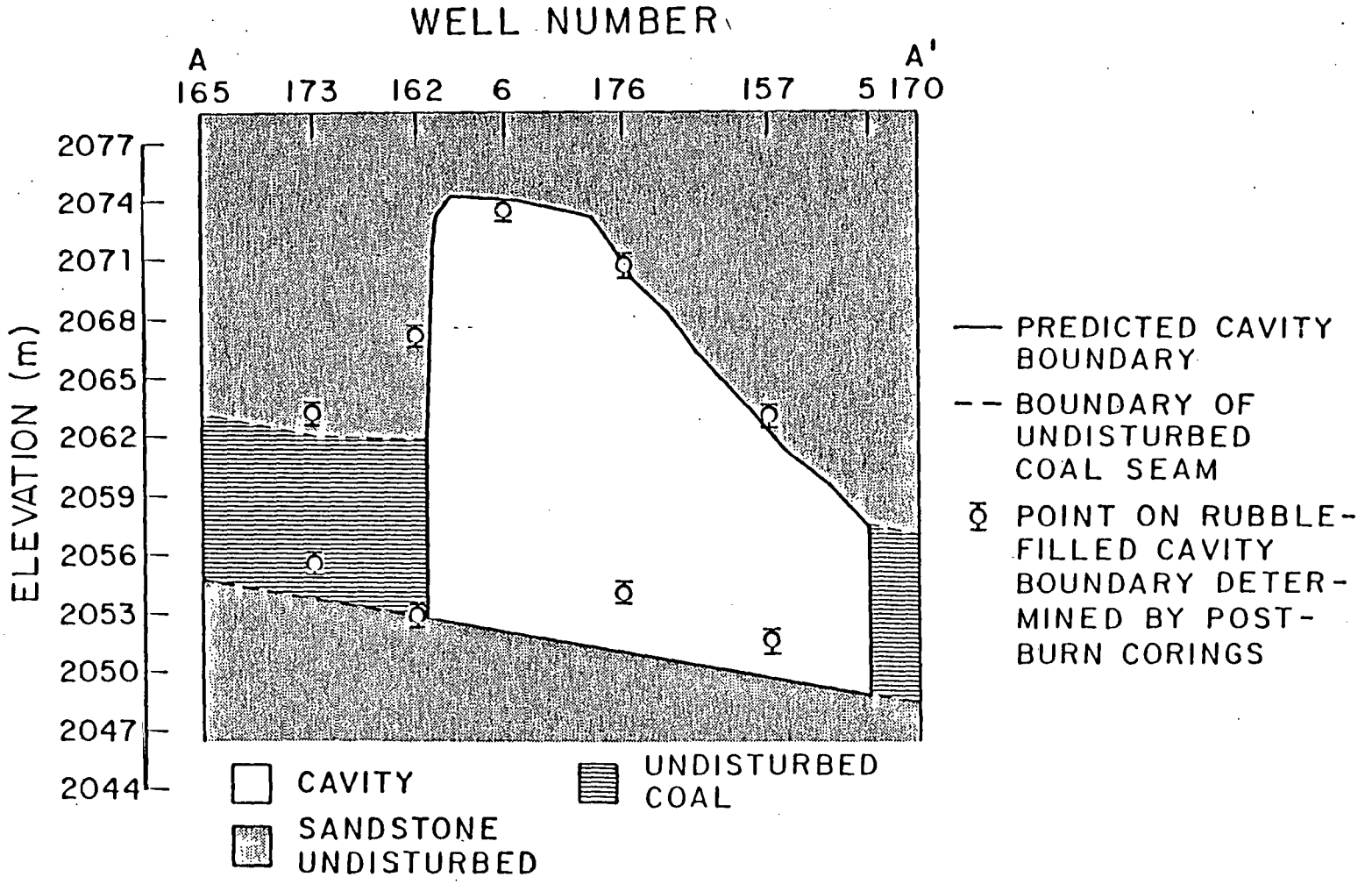

Figure V-3. Post-Burn Cavity Profile Between Core Holes 173 and 170 for the Hanna II Phase II UCG Field Test

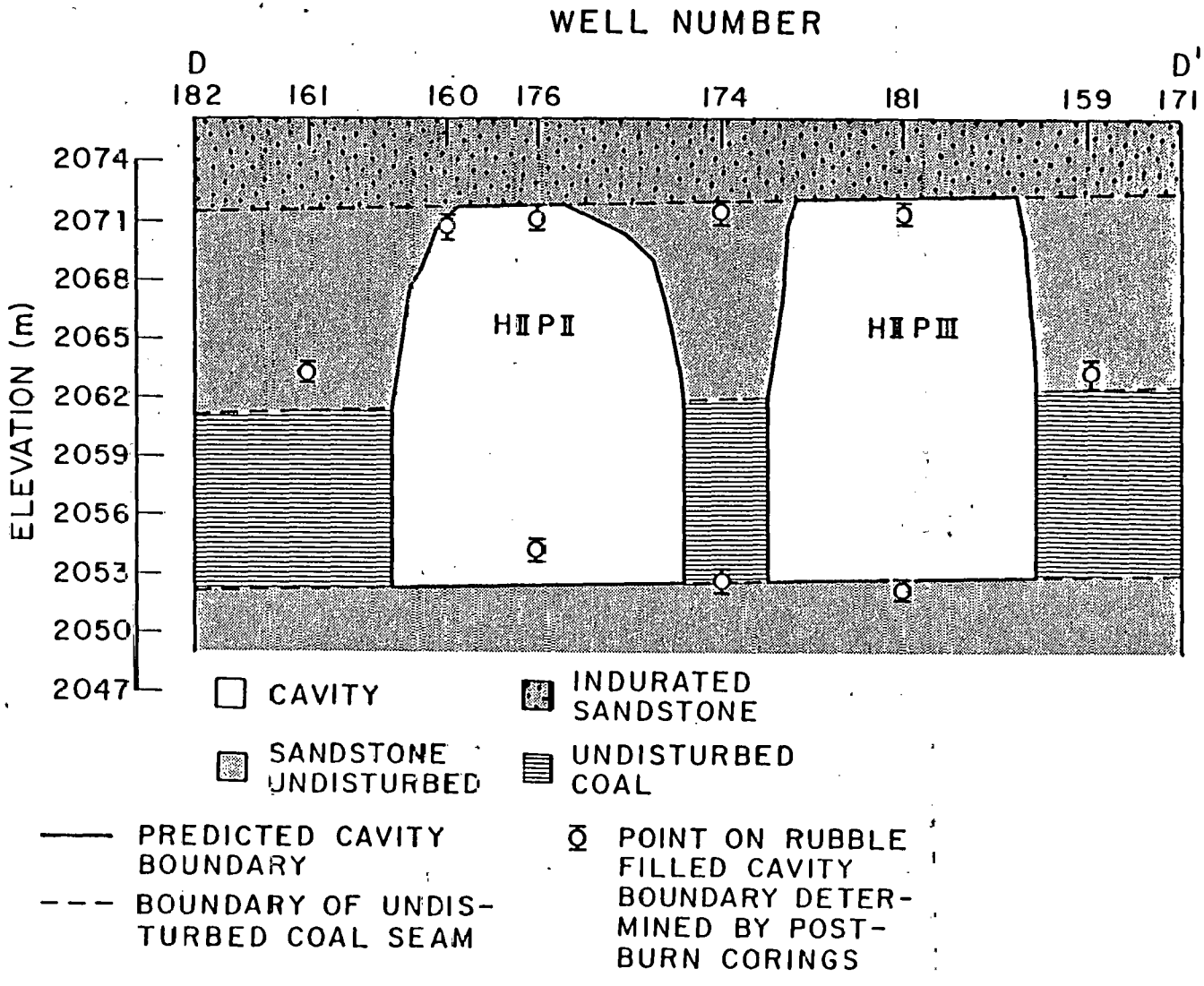

Figure V-4. Post-Burn Cavity Profile Eetween Core Holes 182 and 171 for the Hanna II Phase II and Phase III UCG Field Tests

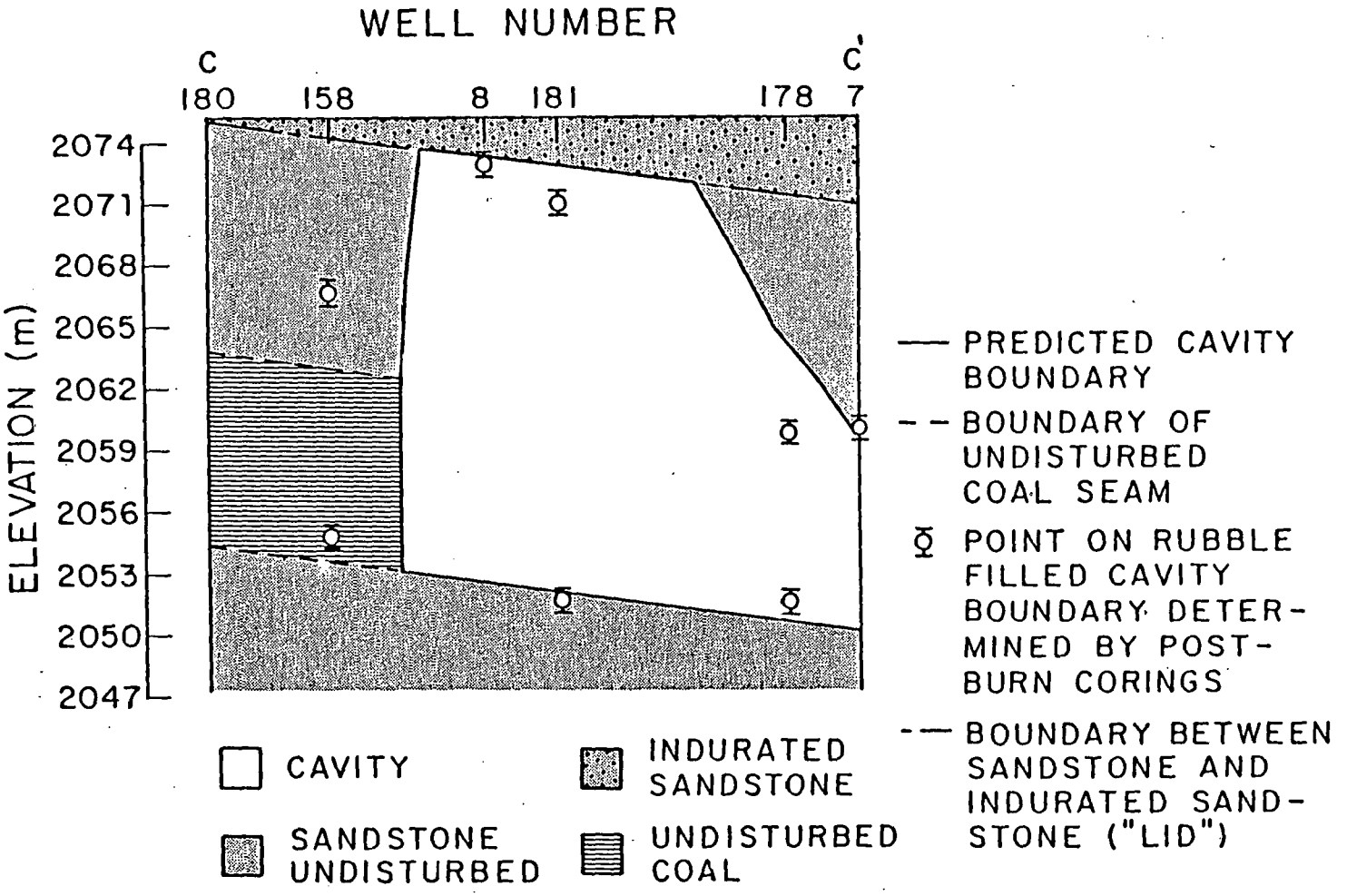

Figure V-5. Post-Burn Cavity Profile Between Core Hole 180 and the Production Well for the Hanna II Phase III UCG Field Test

greatly reduces the porosity of the rock and strengthens it substantially, thus making it considerably more spalling-resistant. This spalling-resistant layer was not reached during the 25 day Hanna II Phase II field test. However, it was reached during the 37 day Hanna II Phase III test. The water-influx data shown in Figure IV-5 show a decrease in the water influx commencing at day 25. This would imply that the spalling-resistant layer was reached approximately 17.5 days after the roof of the coal seam was exposed (25 - 7.5 days to spall through the coal); this means that the spalling-resistant layer began 11.7 m above the coal seam. The predicted upper boundary of the cavity in Figure V-5 then was determined in this manner.

The lateral cavity profile for the Hanna II Phase III field test along the line connecting core holes 182 and 171 is also shown in Figure V-4. Whereas the predictions indicated that the Hanna II Phase II and Phase III cavities were not connected, the post-burn coring data indicate that all the coal between the adjacent cavities shown in Figure V-4 was in fact consumed. Possible reasons for these wider sweep patterns have been discussed above in connection with the Hanna II Phase II field test.

The 38 day Hanna III UCG field test presented the most complex stratigraphy of the three tests considered here. Immediately above the Hanna No. 1 coal seam at this field test site was approximately 1.5 m of claystone. Overlaying this was approximately 2 m of slightly indurated siltstone which was thought to be more spalling-resistant due to cementing by calcite of siderite within its pores. This in turn was overlaid by 5.1 m of sandstone which in turn was overlaid by another thick layer of slightly indurated siltstone. The spalling parameters for these three layers were determined as follows. The sandstone was assumed to spall at the same rate (0.67 m/day) as that of the unindurated sandstone in the Hanna II Phase II and Phase III field tests. The thin layer of claystone was expected to spall more rapidly and was somewhat arbitrarily assigned .hw spalling a spalling rate of 0.82 m/day. The spalling rate of the slightly indurated siltstone then was determined by backcalculating it from the known maximum height of the cavity roof; this led to a spalling rate of 0.18 m/day for the siltstone.

Gasification in the Hanna III UCG field test was carried out from well 1 to well 2 shown in the post-burn drilling and coring diagram in Figure V-6. The predicted post-burn cavity roof profile along the line connecting core holes 204 and the production well is shown in Figure V-7. The cavity profile inferred from the post-burn coring data is shown by the eight data points in this figure. The influence of the more spalling-resistant siltstone layer is quite apparent when this figure is compared with the cavity profiles for the Hanna II field tests shown in Figures V-3 and V-5. The corresponding predicted lateral cavity profile along the line connecting core holes 209 and 207 in Figure V-6 is shown in Figure V-8. Again, the cavity profile inferred from post-burn coring is shown by the nine data points. The agreement between the predicted and measured cavity profiles in both views is quite good. There is no evidence of the broader sweep patterns (relative to that predicted by the areal sweep model of Jennings et al.) that were observed in the Hanna II Phase II and Phase III field tests.

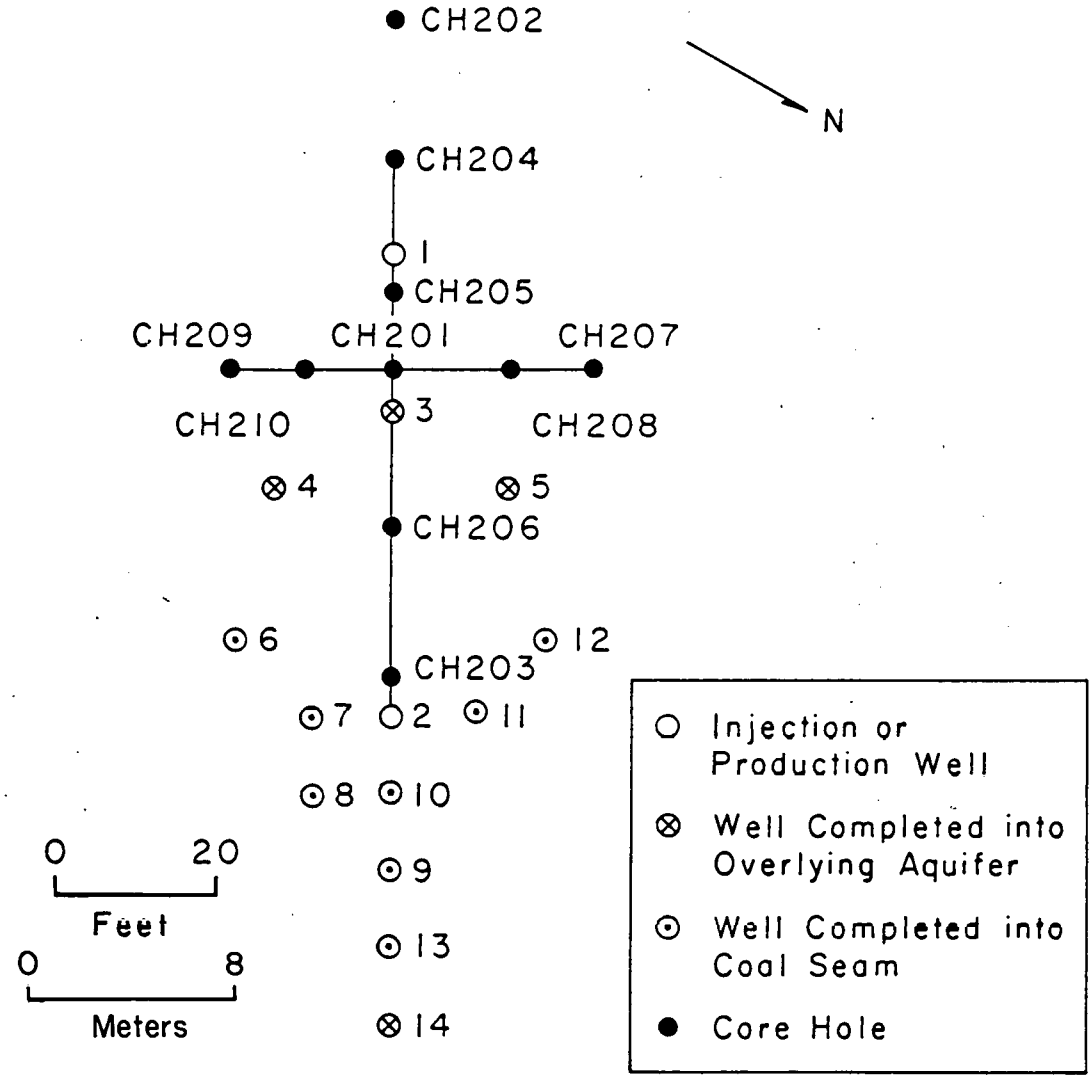

Figure V-6. Location of Injection and Production Wells, and Post-Burn Drill and Core Holes for the Hanna III UCG Field Test

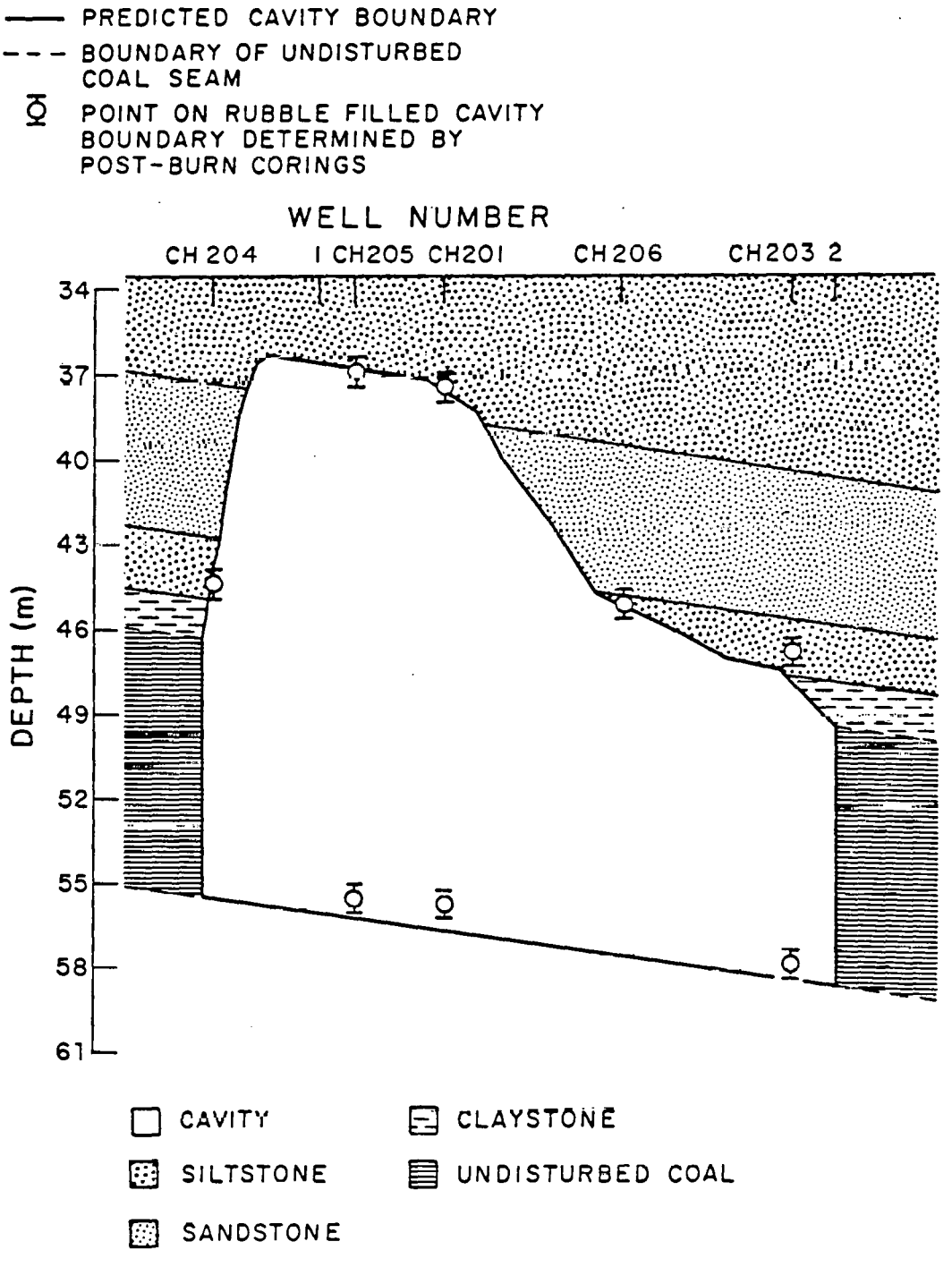

Figure V-7. Post-Burn Cavity Profile Between Core Hole 204 and the Production Well for the Hanna III UCG Field Test

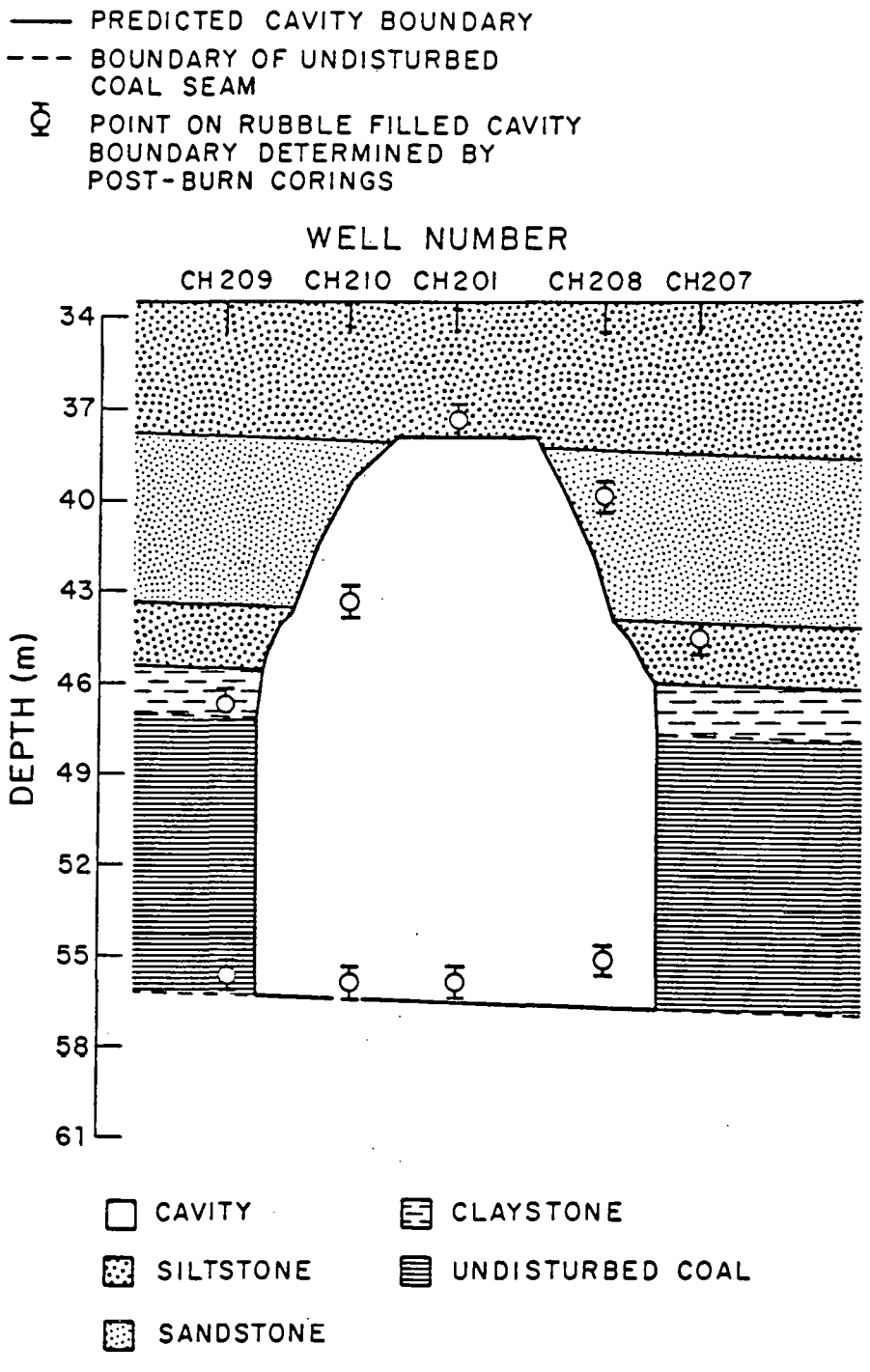

Figure V-8. Post-Burn Cavity Profile Between Core Holes 209 and 207 for the Hanna III UCG Field Test

It should be mentioned here that the somewhat modified spalling-rate parameters used in the cavity growth predictions for the Hanna II Phase III and Hanna III field tests were also used to make revised predictions for the water influx for these two field tests. Accounting for the spalling-resistant "lid" in the Hanna II Phase III field test led to water-influx predictions which followed the trend of the data better than did the original predictions shown in Figure IV-5. In particular, the decrease in the water influx which is seen to commence on approximately day 25, appears to result from the presence of the spalling-resistant lid of indurated sandstone. In the case of the Hanna III UCG field test, the revised spalling-rate parameters account for the decrease in water influx observed for days 10 through 16 and for day 30 and thereafter corresponding to the effect of the two more spalling-resistant slightly indurated siltstone layers.

Implications of These Studies

A significant aspect of the cavity-growth modeling studies presented here is that the model not only describes the post-burn cavity shape, but also allows prediction of the cavity shape prior to any UCG burn. This of course is pivotal to assessing any potential subsidence problems at a UCG site and would be required to prepare a proper Environmental Impact Statement. In order to predict the three-dimensional cavity shape prior to a UCG burn, the following information is required: the two-dimensional areal sweep contours for the particular coal seam as determined from the sweep model of Jennings et al. (1976) and shown in Figure V-1; the projected air- (or oxygen-enriched air-) injection rate schedule so that the daily coal consumption can be estimated; and, the appropriate spalling-rate parameters for the various strata overlying the coal seam which will be encountered during the burn. These spalling-rate parameters can be determined from water-influx data or post-burn cavity-shape data from prior field test studies at the particular UCG site being considered, or from laboratory core-characterization tests of the type proposed by Levie et al. (1982) and described in greater detail in the thesis of Levie (1983). As was stated in Chapter IV, a laboratory core-characterization test for determining the spalling-rate parameters is one of the most pressing needs at this time to enhance our ability to characterize the performance of UCG prior to a burn.

The question arises as to whether these modeling studies suggest any means to control subsidence during a UCG burn. Clearly the cavity dome profile will have a significant influence on any bending or chimneying type of subsidence which may occur at a UCG site. These modeling studies show that the cavity dome profile is determined largely by caving subsidence or spalling of the cavity roof rock, at least in strata such as encountered in the Wyoming UCG field tests. Since the amount of spalling which occurs at any point above the coal seam depends on how long the roof rock has been exposed at that point, the maximum height of the cavity roof is skewed towards the injection well as is readily apparent in Figures V-3, V-5 and V-7. This skewing of the maximum cavity roof height towards the injection well explains why the catastropic chimneying subsidence observed during the Hoe Creek III UCG

field test broke through to the surface where it did. These modeling studies suggest at least two means that are available to minimize the detrimental effects of subsidence during a UCG operation. The first is to design the UCG burn to maintain pillars or walls of unburned coal between adjacent two-well recovery patterns in a multiwell modular recovery scheme. Although the areal sweep model of Jennings et al. was developed for a simple two-well recovery scheme, it can be used to provide an estimate of the affected region of coal in consecutive two-well burns within a multiwell modular recovery scheme. Some caution must be observed in doing this, however, since the application of the Jennings et al. model to the consecutive Hanna II Phase II and Phase III field tests indicated that the model predicts conservative recovery patterns under such circumstances. Developing a reliable areal sweep model for multiwell recovery patterns should be a high priority item in future UCG research efforts. A second means for controlling the effects of subsidence is to limit the amount of spalling which occurs during the UCG burn in order to minimize the maximum cavity dome height. Since the total amount of spalling which occurs depends on the exposure time for the roof element under consideration, one can minimize the amount of spalling during the UCG burn by carrying out the gasification more rapidly by employing high air- or oxygen-injection rates. Although some spalling may occur after the UCG burn is completed, such as was observed after the Hoe Creek III field test, the preponderant amount of spalling usually occurs during the UCG burn due to thermally induced failure associated with the extremely high temperatures encountered during the UCG burn. Whether in fact the effects of subsidence can be minimized by employing these suggested strategies remains yet to be proven by subsequent field tests.

A rather remarkable observation of these modeling efforts is the ability of the relatively simple areal sweep model of Jennings et al. to predict the lateral coal recovery patterns. This is surprising in view of the simplifying assumptions made in developing this model. In particular, this permeation model totally ignores the effect of the reverse combustion link on the air and product gas flow paths. The fact that the model describes the coal recovery patterns reliably for all the Hanna field tests considered here suggests that the reverse combustion link somehow does not present a major flow path directly accessible to the gases emanating from the gasification occurring along the walls in the UCG cavity. Whether this is a consequence of partial plugging of the link in the vicinity of the cavity boundary due to tar deposition, plasticizing of the coal, or spalling of the dried overlying coal into the link, remains to be determined. Certainly more effort needs to be directed towards developing a more comprehensive areal sweep model.

The cavity growth model developed here only accounts for one type of subsidence, namely, the caving or spalling type of subsidence which causes the cavity to grow vertically. As mentioned previously, the resulting cavity dome can significantly influence any subsequent subsidence effects which might be observed on the surface. What is needed at this point is to combine the cavity growth model developed here with a surface bending subsidence model in order to predict both the near and long term subsidence effects of a UCG operation.

CHAPTER VI - MATERIAL AND ENERGY BALANCES

Material and Energy Balances

Macroscopic material and energy balances, unlike other theoretical models, do not possess a truly predictive capacity. Nevertheless, they are probably the most important diagnostic tools available. More sophisticated analyses can in general only be as sound and as accurate as the material balance, for most models either implicity or explicity through boundary conditions must satisfy the macroscopic material and energy balances. For this reason, substantial effort has been expended to provide good material and energy balances for the Hanna field tests. Fischer, et al. (1977) reported material and energy balances for the Hanna II field tests (Phases I, II and III). The material balances are calculated from carbon, hydrogen and nitrogen balances based on the produced gas composition. These three balances permitted the determination of the amount of coal consumed and the water influx. The results of the three tests are summarized below:

	Phase I	Phase II	Phase III
Date	1975	1976	1976
Duration of Test, days forward gasification	38	25	38
Ave. Gas Heating Value (Upper), Kj/m^3	5990	6730	5430
Coal Consumed, metric tons	1140	1890	4180

Results for the energy balance are reported in Table VI-1. In this table, the energy return ratio is the upper heating value of dry gas and liquids divided by the energy consumed in operating the process. Although these values are favorably high, they are lower than would be expected in commercial operation because no attempt has been made in a research investigation to optimize energy usage. In Table VI-1, the process efficiency is the heating value of the dry gas and liquids produced divided by the heating value of the coal utilized plus the energy consumed in operating the process. The cold gas efficiency is simply the upper heating value of dry gas and liquid vapors produced divided by the heating value of the coal consumed. These data show clearly that the thermal efficiency of the UCG process can exceed that obtained from surface gasifiers which typically operate at about 65% efficiency. The forward gasification model shows that this is to be expected because of the excellent insulating properties of the earth which in turn allows the process to operate nearly adiabatically.

For the Hanna I field test, carbon, hydrogen, oxygen and nitrogen balances were used to calculate water influx, coal consumption and char production. As early as 1975, however, the system was abandoned. It had been observed that material balances on a daily basis gave extremely erratic results varying from negative char production (a physical impossibility) to production of char only (no consumption of char). Water influx fluctuated daily from negative amounts to enormous positive production. A simple review of the material balance equations showed them to be algebraically unstable; therefore, the method in use was discontinued in 1975. If the oxygen balance was eliminated from the

Table VI-1

Energy balance data for the Hanna II field tests (energy units in terajoules = 10^{12} joules)

	Phases I	II	III
Heating value of dry product gas	13.3	30.5	43.7
Heating value of liquids produced	1.0	1.9	3.7
Latent and sensible heat of water vapor	0.1	0.4	4.3
Sensible heat of dry product gas	1.0	2.0	3.8
Heat losses	1.9	1.6	6.5
Total energy	17.3	36.4	62.0
Energy in coal consumed	17.3	36.4	62.0
Energy used to operate the process			
Diesel fuel	2.3	7.1	9.4
Electricity	0.2	0.1	0.2
Propane	0.2	0.0	0.9
Energy return ratio	5.3	4.5	4.5
Overall process efficiency (%)	71.5	74.3	65.3
Cold gas efficiency (%)	82.7	89.0	76.0

material balance equations, then the algebraic instability was also removed. Unfortunately, without the oxygen balance, it is not possible to estimate the amount of unburned char left underground.

In 1978, the new method of calculating the material balances was challenged by some. Material balances, including the oxygen balance, were used to show that the Hanna field tests were primarily a carbonization process which accounted for the high gas heating value. According to these calculations about 60 to 70% of the total coal affected was left behind as devolatilized char.

To clarify this problem, Gunn (1979) set forth in detail the reasons for abandoning the oxygen balance which Loison (1952) had also recognized at least as far back as 1952. Gunn (1979) showed that algebraically the oxygen balance leads to division by the difference of large numbers. Hence, the material balance equations are so unstable that an error of one mole percent in the product gas composition can lead to errors as large as 500% in the calculated water influx and to large amounts of negative char production which is a physical impossi-

bility. Unfortunately, experts in chromatography generally recognize errors of one mole percent as the best absolute accuracy that can be achieved with commercial chromatographs under field conditions. In fact, during the Hoe Creek II field test conducted by the Lawrence Livermore Laboratory, the produced gas composition was monitored simultaneously by a mass spectrometer and by a chromatograph. The two methods of measurement consistently deviated from each other by values as high as one mole percent. This deviation was consistently in the same direction so that the error was not averaged out statistically over time.

Gunn showed that even under carefully controlled laboratory conditions material balances which included the oxygen balance often led to large computational errors including negative char production. In these experiments, analysis of the coal prior to the combustion test and of the ash and char after the test eliminated any large uncertainty in the actual amounts of coal consumed and char produced.

Because of these difficulties, the material balance method which includes the oxygen balance is not even qualitatively reliable. Worse yet, the results actually tend to be misleading. Analysis of the post-burn core data from the Hanna II Phase II site indicate that a rather insignificant amount of high temperature (900°C) char was left behind rather than the 60% figure suggested by the oxygen balance method. The clarification of these problems was especially important because the material balance, properly used, remains one of the most powerful and reliable analytical tools in UCG field testing.

Heat Loss During UCG

Field test results in the forward mode of underground coal gasification indicate much larger heat losses than those expected due to simple heat conduction to the surrounding strata. Figure VI-1 is a plot of the daily averaged heat losses for the Hanna III field test. The abcissa gives heat loss as a percent of total energy input into the system, based upon the heating value of the coal consumed. The ordinate is the day of forward gasification in Julian days. The accountable energy is the sensible and latent heat in the product gas. Figure VI-1 is typical of UCG field tests. The magnitude of the heat loss is substantial, and prior to the present work the origin of the heat loss was unknown. An incomplete understanding of major aspects of the process means that future tests run a greatly increased risk of failure. Consequently, work was undertaken to develop a theoretical framework capable of explaining the mechanisms of the large heat loss. Earlier work showed that spalling of the overburden was a major source of water influx. Obviously, in the process of drying, the rubblized overburden represents a substantial heat sink. Glaser and Gunn (1982) reported the results of calculations made to study this phenomena of heating spalled rock as the probable source of the large heat loss during underground coal gasification. In addition to the major objective of a clearer understanding of UCG, the work of Glaser and Gunn (1982) was also intended to determine if the heat loss could be reduced in order to enhance substantially the efficiency of the process. A knowledge of the

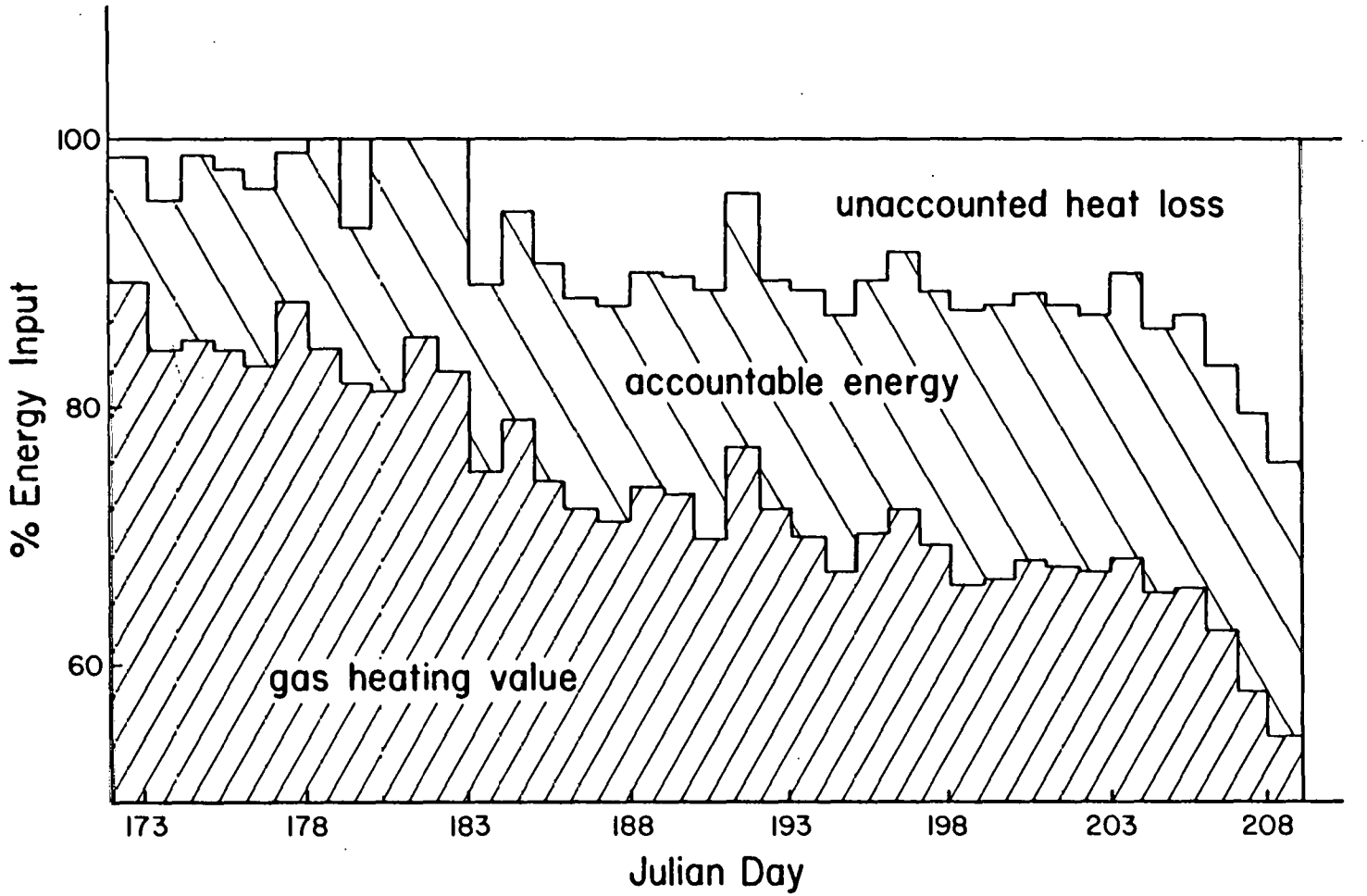

Figure VI-1. Energy Balance for the Hanna III Field Test

mechanism responsible for this heat loss may also suggest a method of reducing or eliminating the decrease in heating value observed in UCG field tests.

A model (Camp, 1980; Camp, Krantz and Gunn, 1980; Krantz, Camp and Gunn, 1980) has been developed to predict water influx during UCG. One component of water influx described by Krantz et al. is from spalling enhanced drying of the overburden. The mechanism responsible for this component of water influx is also the primary mechanism responsible for the heat losses observed in UCG tests. Figure VI-2 is a cross section of the UCG cavity sometime after forward gasification has begun. Thermal radiation from surface 1 (the combustion front) to surface 2 (the cavity roof) dries the overburden and heats the roof. Eventually thermal stress and steam pressure within an element of the cavity roof will cause the element to spall and fall to the rubble pile, where it is heated further.

A mathematical model has been developed to interpret the preceding process. The primary parameters in the model are water influx from spalling enhanced drying, thermo-physical properties of the overburden, cavity geometry and combustion front temperature. A simplified geometry consisting of conical and cylindrical surfaces has been adopted for determining reasonable radiation view factors. The dimensions of the cavity are determined from material balance results and from the amount of water from spalling enhanced drying of the overburden. The amount of water influx from spalling enhanced drying of the overburden enters the model in two places. First, it is used to determine the influx of rock into the cavity. Secondly, it is used directly in the energy balances on the roof elements to determine the latent and sensible heat in the water that evaporates from the cavity roof. Unfortunately, it is not possible to resolve the total water influx into its component parts directly from the material balance with a high degree of accuracy. With this problem in mind, the model predictions are compared with the field test results by employing two different methods for estimating the water influx from spalling. The two methods are the material balance method and the theoretical method.

In the first method, water influx from spalling is calculated directly from the material balance. Since the material balance only determines the total water influx, the water from spalling can be determined only by making assumptions concerning the other components of water influx and estimating the water influx from spalling by difference. Clearly, this approach is not very accurate.

The spalling enhanced drying model of Krantz and co-workers immediately suggests an alternative. The theoretical method employs the spalling enhanced drying model to estimate water influx by spalling. The theoretical model is entirely predictive. In addition to the possibility of providing a better estimate of the water influx from spalling, the theoretical method is a severe test of the water influx model developed by Krantz and co-workers. Figure VI-3 is a plot of the predicted heat loss (line) according to the material balance method compared with the observed heat loss in the Hanna III field test. The observed heat loss is represented by diamonds, with an estimated error

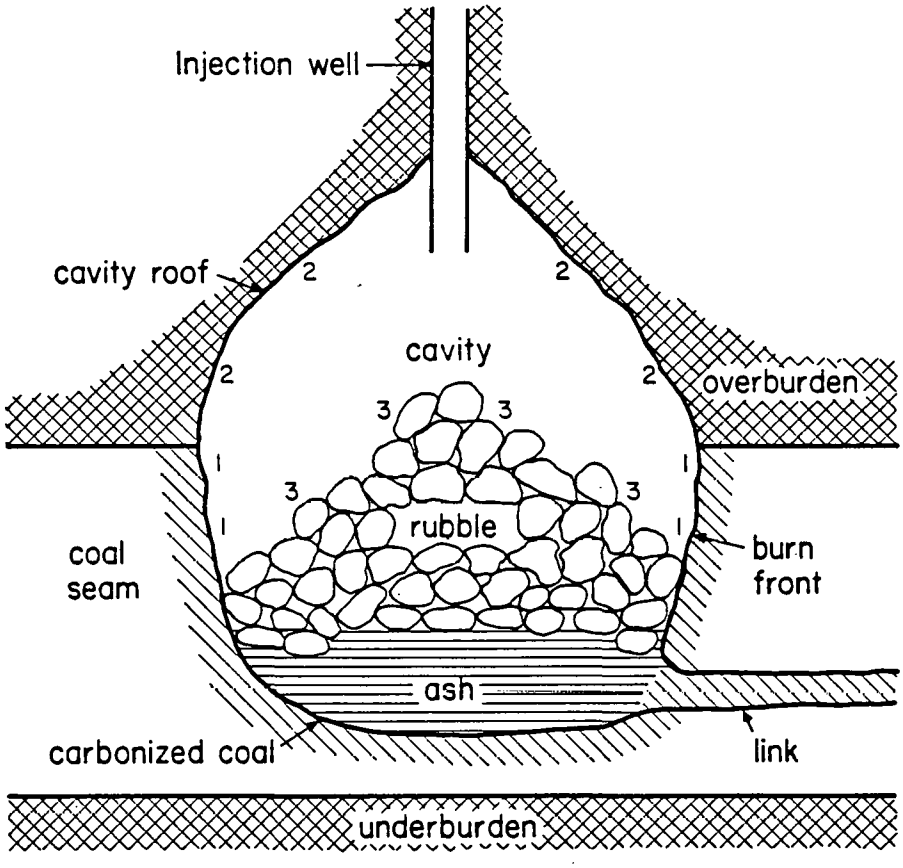

Figure VI-2. Schematic Representation of the Cavity Produced During Underground Coal Gasification.

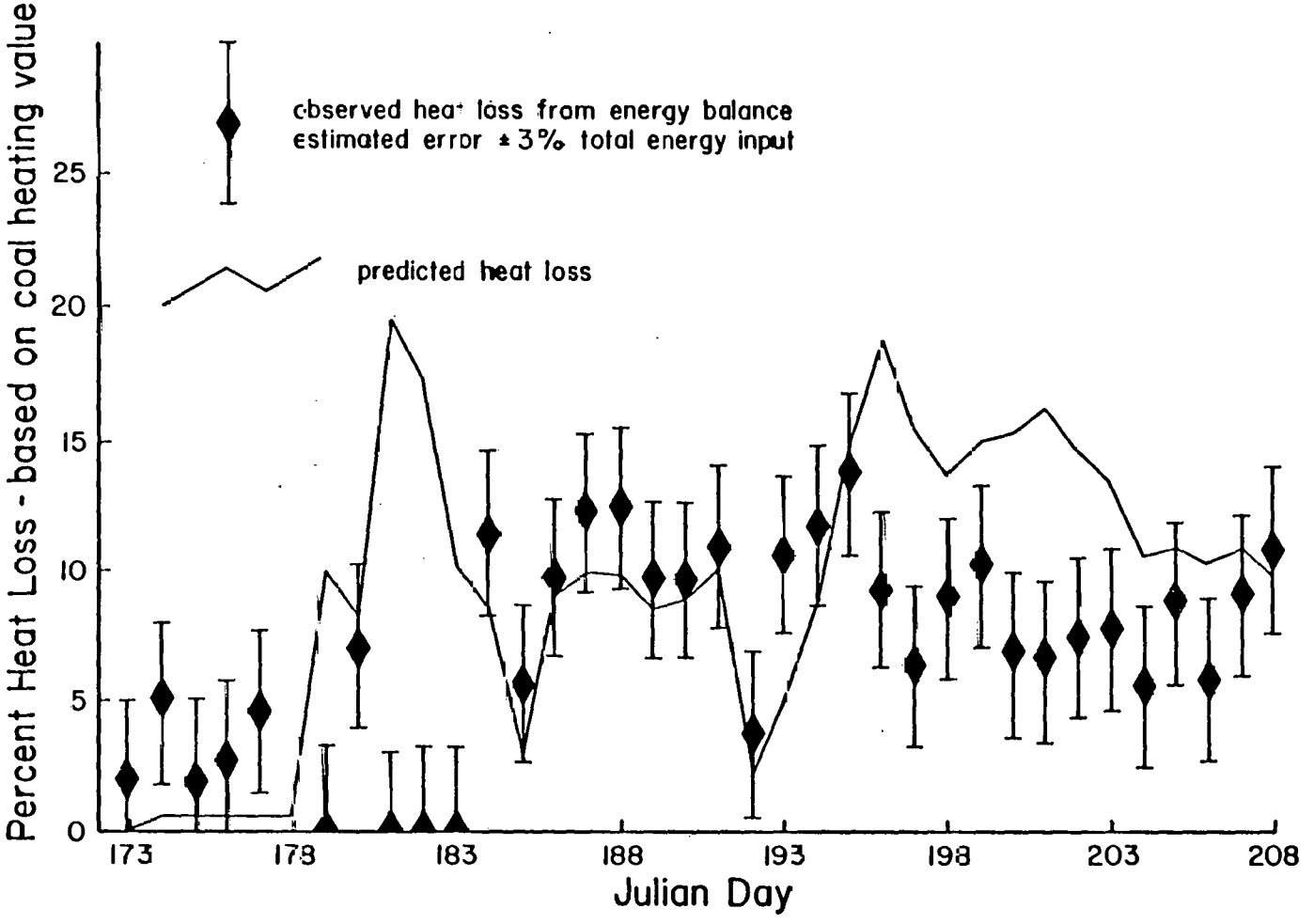

Figure VI-3. Calculated Heat Loss (Material Balance Method) Compared with Experimental Values

of ±3% of the total energy indicated by the bar extensions. Figure VI-4 is a similar plot of the predicted heat loss for Hanna III by the theoretical method. The theoretical method (Figure VI-4) gives a much better fit. This surprising result suggests that the water influx model is more accurate than the material balance estimation of water influx. The poorer fit obtained with the material balance method is partially due to the somewhat arbitrary nature of the assumptions needed to estimate the water influx from spalling. Figure VI-4 demonstrates that the theoretical method provides heat loss predictions well within the accuracy of field test results.

The results of this investigation show that the primary mechanism for heat loss in UCG systems is heating of the overburden, both before and after spalling, through radiant heat transfer. Furthermore, this investigation further confirms the validity of spalling enhanced drying as an important physical phenomena occurring in underground coal gasification systems.

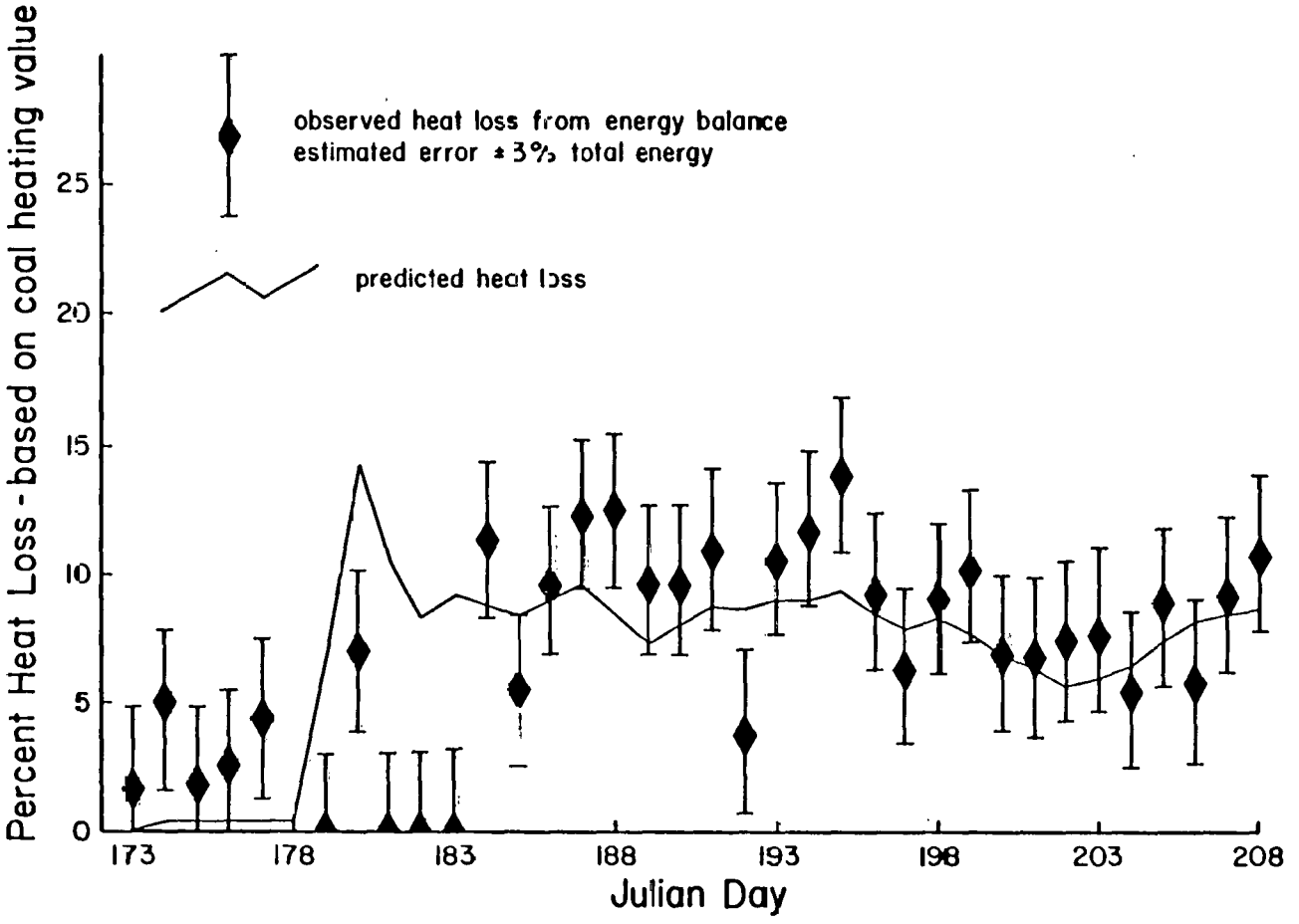

Figure VI-4. Calculated Heat Loss (Water Influx Method) Compared with Experimental Values

VII - EXPERIMENTAL STUDIES

Role of Laboratory Experiments in UCG

Laboratory experiments play a limited but especially important role in UCG. Limitations arise because it is essentially impossible to simulate a process as complicated as UCG on a laboratory scale. Even a single phenomenon such as subsidence is extremely difficult and probably impractical to simulate on a small scale.

Several factors contribute to the extreme importance of laboratory experiments in UCG besides the measurement of relevant chemical and physical parameters. Discussions in Chapter III have already emphasized the necessity of model testing. This testing is best accomplished with field test data; however, because of the size and remoteness of the underground coal deposit, it is nearly impossible to know in sufficient detail all of the relevant spatial variations in coal and overburden. Does the coal exhibit important variations in chemical and physical properties from point to point? Did the depositional environment under which the coal was laid down contribute important variations in properties such as percentage ash, density and water content? Has stream channeling and faulting produced anomalies in seam thickness and permeability? Are there areas especially indurated, permeable, or wet or dry in the overburden? These and many other uncertainties can be removed in laboratory experiments. Thus, in addition to testing with field data, models need to be tested under carefully controlled conditions possible only in the laboratory. When this has been done, then disagreement between a well-tested model and field data often provides the first strong signal that some unexpected and anomalous factor exists in the underground coal seam. An especially graphic example of this principle is discussed relative to the reverse combustion experiments.

Reverse Combustion Experiments

Experimental verification of the reverse combustion model of Kotowski and Gunn (1976) had an especially high priority. One of the predictions of an early prototype of the model was that reverse combustion was a carbonization process and did not burn the coal to completion.[1] Thus, it appeared that the reverse combustion link was not a hole burned through the coal but rather a channel of coal char rendered highly permeable by the partial combustion process. These predictions were widely disputed at the time.

Quantitative predictions with the reverse combustion model were not possible initially because the channel diameter and, therefore, the air flux (rate of flow per unit area) was unknown. Nevertheless, the model indicated remarkable qualitative differences existed between forward and reverse combustion, and some of these differences were observed during

[1] Later versions of the model incorporated this fact as part of the input in order to simplify computations.

reverse combustion linking in the field. For example, the propagation rate of the reverse combustion front was about 2 m/day, a much higher rate than for forward combustion. Gas quality was much lower than during forward gasification which also inferred that the combustion temperatures were low. All of these observations were correctly predicted by theory. However, there were also discrepancies. Theory predicted that the velocity of the reverse combustion front increased with increased air flux. Gas quality and combustion temperatures also increased with higher air fluxes. These predictions were not observed in field experiments. Although the average air injection rate during linking was four fold higher for the Hanna II Phase III field test than for the Hanna III field test, gas composition was essentially unchanged, and the combustion front velocity remained the same. Combustion front velocity was determined by the time required to complete the reverse combustion link for 18 meter well spacing.

This discrepancy suggested that some unknown condition existed in the field. But first, it was necessary to test the model with laboratory experiments under known, controlled conditions.

Lu (1980) reported data for a series of reverse combustion experiments with a combustion tube containing a coal sample 5 inches in diameter and 36 inches in length. A description of the experimental equipment has been given to Lu (1980). Fig. VII-1 shows temperature profiles measured along the central axis of the tube at points 13, 23 and 30 inches from the points of ignition of coal. This figure illustrates two important points. There is good agreement between the experimental and calculated temperature profile. Secondly, the experimental data from thermocouples at three different positions coincide of a single line with only minimal scatter. This shows that the psuedo-steady state assumption used in solving the differential equations in the model is an excellent approximation; otherwise the temperature profiles would change shape as they traveled down the combustion tube. In fact a survey of all the data indicates steady state is nearly achieved within 1 to 4 hours of ignition. The experimental data also show that the combustion zone is very thin, that is, nearly all the temperature change occurs over an interval of about 1.5 cm.

Fig. VII-2 shows a correlation of the peak combustion temperature as a function of air flux. The theoretically calculated correlation agrees with the measured data within experimental error. Fig. VII-3 shows a correlation of the combustion front velocity versus air flux. The theoretically calculated values agree with the measured data to within experimental error. Combustion tube experiments are very difficult to perform, and experimental accuracy tends to be fairly low due to channeling of the combustion front and other difficulties.

The combustion tube experiments confirmed the accuracy of the reverse combustion model of Kotowski and Gunn (1976). Combustion front velocities, temperatures and gas compositions were fairly sensitive functions of the air flux; and this, in turn, confirmed that something was different about field tests because these effects were not present during reverse combustion linking.

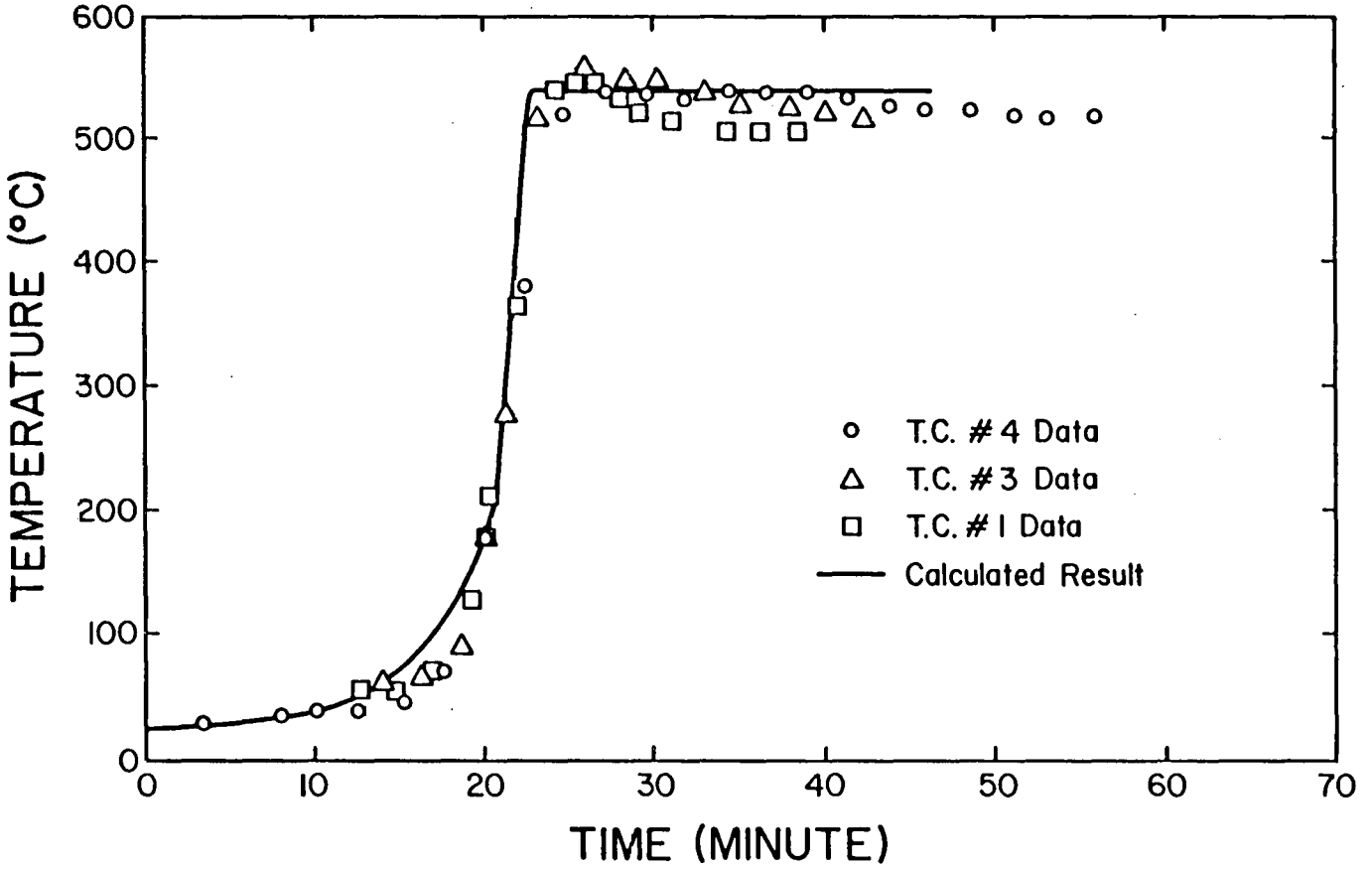

Figure VII-1. Typical Temperature Profile for Reverse Combustion in a Laboratory Combustion Tube Experiment

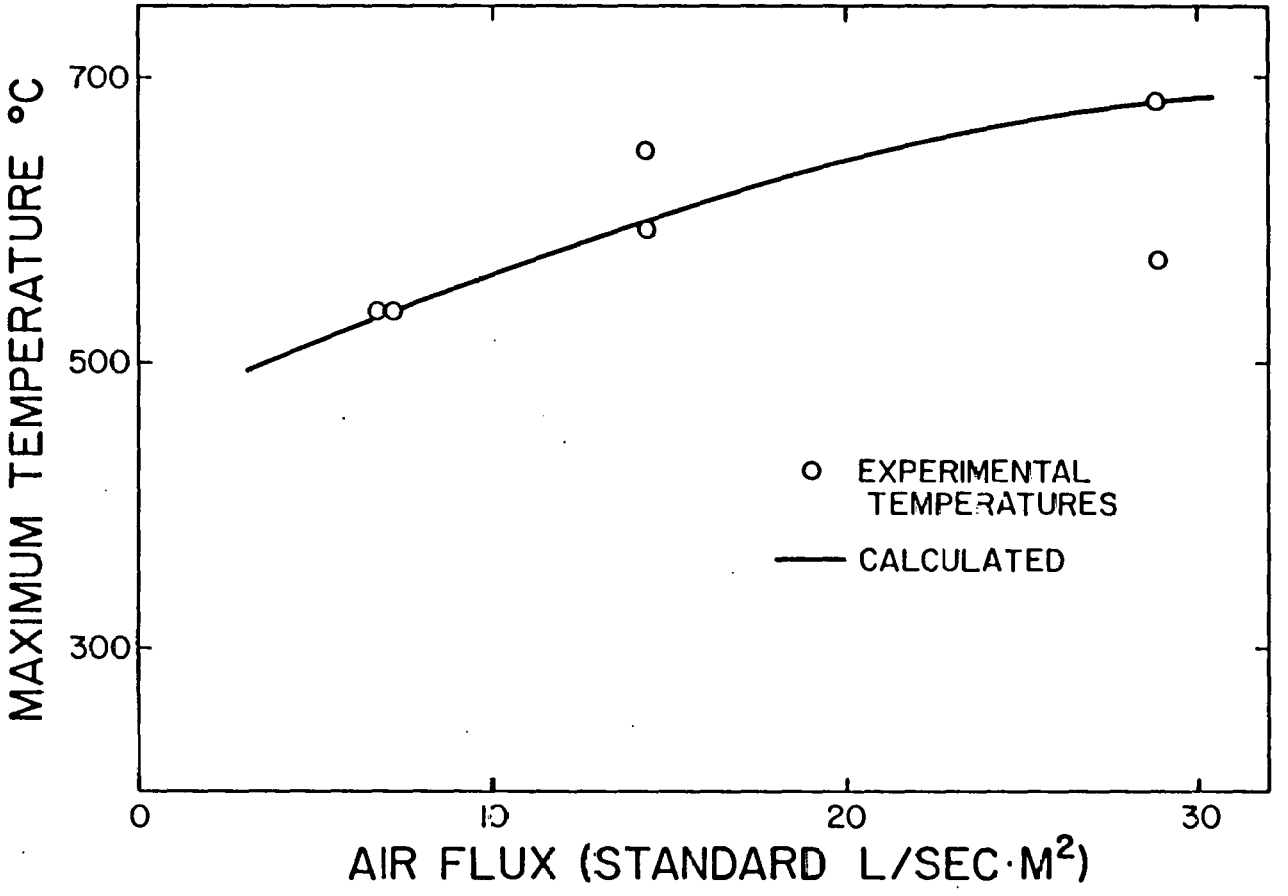

Figure VII-2. Peak Combustion Temperature as a Function of Air Flux for Reverse Combustion in Coal During Laboratory Combustion Tube Experiments

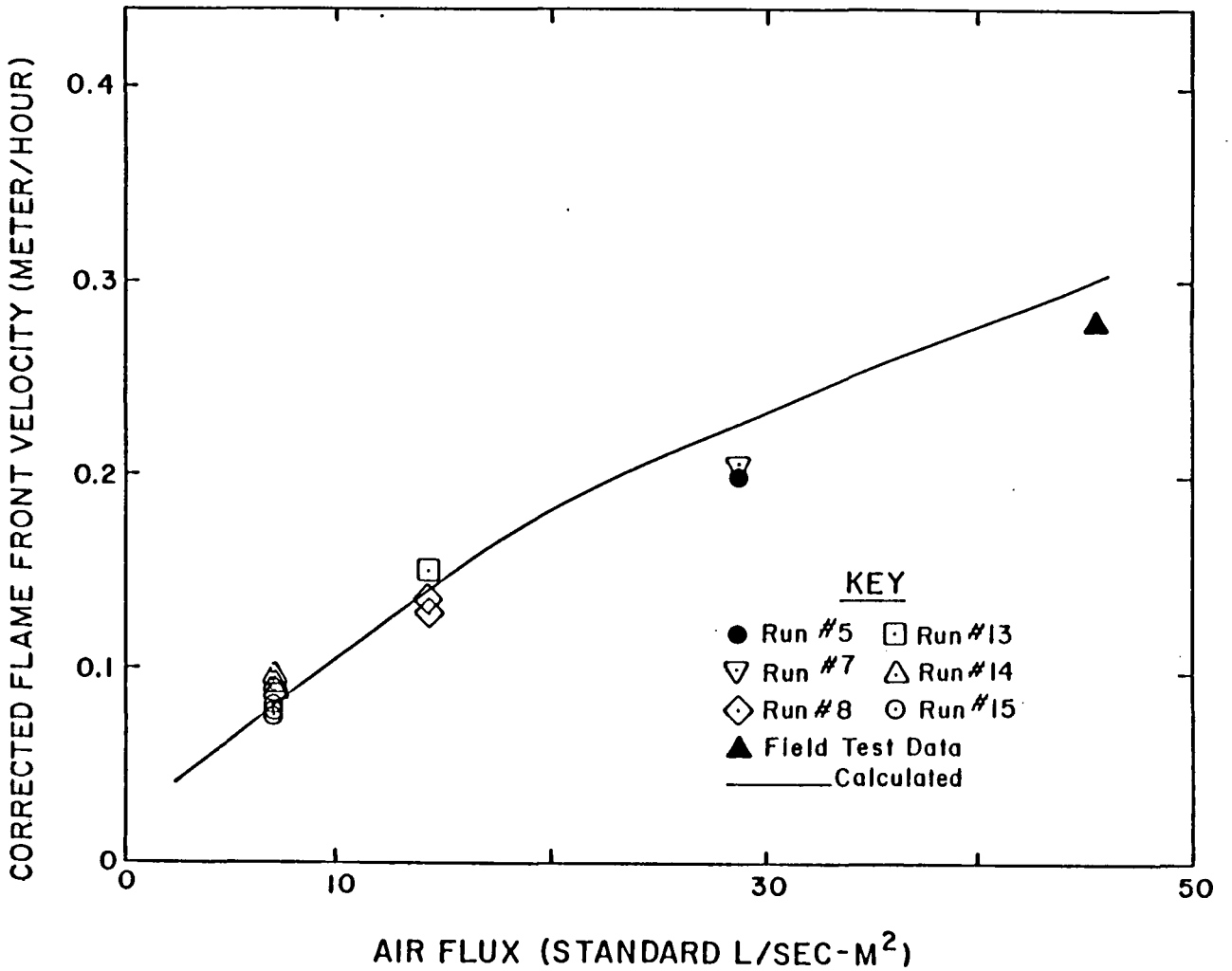

Figure VII-3. Combustion Front Velocity as a Function of Air Flux for Reverse Combustion During Laboratory Combustion Tube Experiments

The stability model of Gunn and Krantz (1980) solved this apparent enigma. This stability analysis showed that, for the operating conditions used, Hanna coal had a completely unexpected characteristic. If the air flow rate at the injection well is increased, then the diameter of the reverse combustion channel expands so that the air flux (flow rate per unit area) remains nearly constant. A decrease in the air injection rate leads to a corresponding shrinkage of the channel always maintaining a nearly constant flux. Because large changes in the air injection rate affect only slightly the air flux at the combustion front, the combustion front velocities and gas compositions were fairly uniform for all of the successful Hanna field tests. The apparent enigma was resolved.

Cavity Growth Experiments

The discussion at the beginning of this chapter has emphasized the importance of laboratory experiments. It is emphasized here that the value of such experiments is usually greatly enhanced if a good theoretical model is available. The model dictates how best to conduct the experiment and what variables should be measured. When experiments involving complicated processes are conducted without prior modeling, important variables are usually not measured; and the experimental data are often nearly meaningless.

A mathematical model is also often necessary in order to place the laboratory data in a field test context. This principle is especially evident for the cavity growth experiments described later in this chapter. The mobility ratio for the Hanna field tests was essentially infinite; however, for the laboratory experiments the mobility ratio was one because the field value could be duplicated only with extreme difficulty and expense. The cavity growth model, however, correctly predicted the laboratory experimental results thus validating the model. The model was then used to predict what changes in the experimental data should occur for a change in the mobility ratio of one to infinity, this latter value being applicable to field tests.

Similarly, the gas composition produced during the laboratory test differed from the gas compositions during the Hanna field tests. Water influx was a major influence affecting gas composition during the field tests. The laboratory apparatus, however, was not designed to permit the introduction of liquid water during a forward gasification simulation. The mathematical model for forward gasification, however, correctly predicted the laboratory results. It further predicted quantitatively the changes in composition that could be expected when water influx was present. In summary, a good mathematical model allows laboratory data to be extrapolated to field conditions even when some field variables cannot be matched or scaled properly in the laboratory experiments.

Whitman (1978) and Whitman, Boysen and Gunn (1978) conducted simulations of underground coal gasification in a 4 x 5 foot simulator filled with a layer of ground coal 7 to 9 inches thick. The objectives of these experiments were to verify mathematical model predictions and

to verify that carefully selected aspects of UCG can be simulated.

Geometrical Effects

A specific objective of these experiments was to verify cavity growth predictions, thus two operating wells 46 cm apart were inserted in the center of the rectangular coal bed in the 1.2 x 1.5 meter simulator. It was not possible, however, to reproduce the same mobility ratio in the laboratory as that in the field; and the mobility ratio has major influence on the size of the combustion pattern. The mobility ratio is defined

$$M = \frac{K_b \, \mu_a}{K_m \, \mu_c}$$

where

M = mobility ratio

K_b = permeability in the burned over area

K_m = permeability of the unburned coal

μ_a = viscosity of the injected air

μ_c = viscosity of the combustion gases

Although the viscosities of air and combustion gases are different, their effect is small. The major effect arises from the permeability differences. In the field tests at Hanna, the combustion cavity consists of void space and large size rubble which spalls from the roof rock. The permeability in this region is very high whereas the permeability of the coal is low, and the mobility ratio is essentially infinite. This spalling of the roof rock is extremely difficult if not impossible to simulate in the laboratory. For the laboratory experiments, the coal was covered with loose soil which subsided into the burned out cavity. Permeability measurements made during the experiments showed that the mobility ratio was about unity.

Table VII-1 shows a comparison of laboratory data, field test data and mathematical model calculations. Because of the difference in the mobility ratio, the field test results and the laboratory data are not comparable. Model calculations, however, are a common link for both; that is, model calculations with the correct mobility ratio predict either type of data correctly. Thus, the first two columns in Table VIII-1 are comparable as well as the last two columns. In Table VII-1, the base area for determining the percent areal sweep is the square of the well separation distance. The third row in Table VII-1, distance behind injection well, refers to the maximum distance that coal is combusted behind the injection well in a direction opposite to the gas production well. In all cases, the data reported in Table VII-1 are believed to be within experimental accuracy.

Table VII-1

Comparison of Experimental and Calculated Gasification Geometry for an Isolated, Two Well Pattern

Parameter	Laboratory Simulator	Mathematical Model		Hanna II, Phase II Field Test
		Unity Mobility Ratio	Infinite Mobility Ratio	
Areal Sweep (% of Base Area)	98	95	59.3	52.4[a]
Maximum Width (% of Well Spacing)	105	98	70.2	67.0[b]
Distance Behind Injection Well (% of Well Spacing)	48	42.5	21.9	ND[c]

[a]Assuming consumption of entire coal seam thickness

[b]Estimate from existing instrumentation wells

[c]No data

All laboratory experiments in the simulator were conducted with pulverized coal because of the cost and extreme difficulty of acquiring and working with unbroken blocks of coal five feet across. Model calculations indicate that gas composition and gas heating value should be affected only slightly by mechanical differences such as particle size. Cavity growth, however, is controlled by the local air flux; flux is controlled by permeability and permeability is very sensitive to particle size. It seems quite probable, therefore, that the mechanical state of the coal may have a substantial influence on cavity growth. For this reason, the data in Table VII-1 are designed primarily to test model predictions for the limiting case of isotropic permeability constant throughout the entire bed. The Hanna field test data also conform to this limiting case for reasons not known at the present time. Permeability in the Hanna coal seam is definitely nonisotropic. The data in Table VII-1, therefore, must be used with considerable caution until further knowledge is developed.

Gas Compositions

The mathematical models described previously show that the total gas heating value can be simulated in the laboratory. In addition, gas compositions can be simulated provided both heat loss and water influx are the same for both the laboratory test and the field experiment. The 4 x 5 foot simulator had no provision for injecting water; and, therefore, gas compositions could not be matched. Model calculations, however, should predict both results, that is, a mathematical model can be used to extrapolate laboratory data to field conditions when water influx cannot be matched.

Figure VII-4 depicts the gas composition as a function of time for a representative test. After a short unsteady-state period, the concentrations of carbon monoxide, methane and hydrogen begin to decrease roughly linearly with time, and the carbon dioxide concentration increases with time. Model calculations indicate these trends are caused by the increasing heat loss as the combustion zone expands and more and more heat is lost by conduction and radiation to the nonreactive confining layers of earth and by increasing sensible heat in the production gas. The total heat loss for the test depicted in Figure VII-4 increased from 13% early in test to 40% in the later stages. Because the simulated coal seam or bed of coal contains only its natural moisture content, about 9%, the decline in gas quality shown in Figure VII-4 is not related to excessive water influx which often occurs in field tests. A rapid drop in CO, H_2 and CH_4 content occurs near the end of the experiment because of breakthrough of the leading edge of the reaction zone to the production well.

Figure VII-4 shows that the carbon monoxide content is as much as 26 mole %, which is much higher than the carbon monoxide content of gases produced during the Hanna field tests. An excess of water influx existed during the Hanna field tests; therefore, water vapor was always present to produce carbon dioxide from carbon monoxide via the well-known shift reaction. When water vapor is lacking as occurred in these laboratory tests, the char reacts with carbon dioxide via the Boudouard

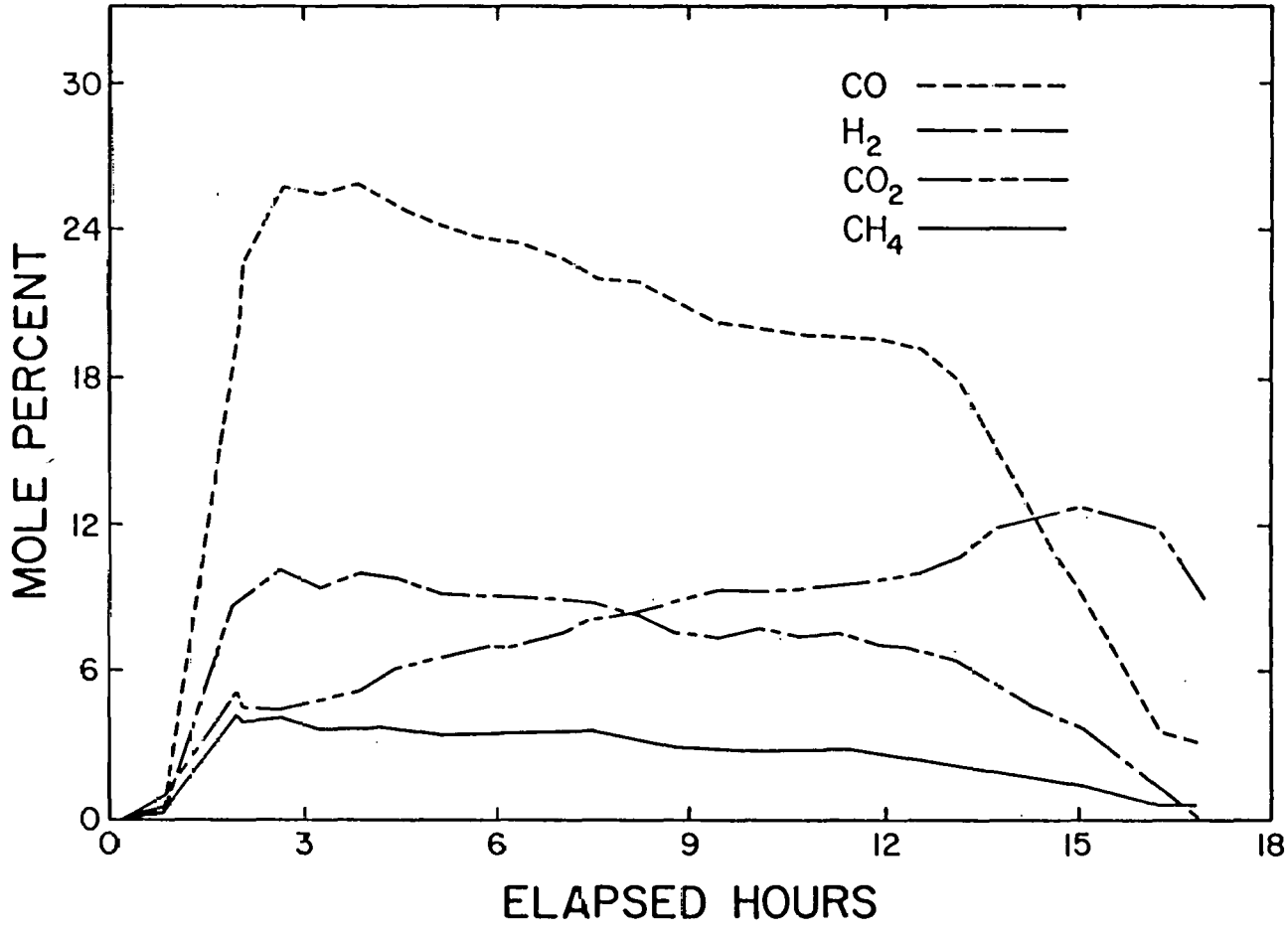

Figure VII-4. Gas Composition During Forward Combustion Laboratory Experiments in a Two-Dimensional Simulator

reaction to form only carbon monoxide. Because the presence of water vapor promotes different reactions and different gaseous products, laboratory simulations of field tests must match the water influx. If this is not done, the laboratory simulation will produce gas with a different composition. Even so, a good mathematical model can predict the composition difference to be expected. Figures VII-5, VII-6 and VII-7 illustrates this concept and shows respectively the hydrogen, the carbon monoxide and the carbon dioxide content for the gases produced in both the laboratory simulation and the Hanna II Phase III field test. The laboratory simulation lasted for 17 hours, the field test for 38 days; and the two sets of data cannot be compared directly. To provide a common basis of comparison, Figures VII-5, VII-6 and VII-7 show dimensionless time, that is, experimental time divided by the total duration of the experiment. This is a rigorous basis for comparison provided that heat loss increases linearly with time. This was approximately true for both the field test and the laboratory simulation.

Figures VII-5, VII-6 and VII-7 show that there is a definite difference in gas compositions from the field test as compared with the laboratory simulation because of the shortage of water vapor in the simulation. The mathematical model, however, accounts correctly for this difference with a common set of physical parameters. The mathematical model also shows that the gas heating value is not sensitive to differences in the availability of water vapor. Figure VII-8 shows that heating values of gas for the laboratory tests and the Hanna II Phase III field test, respectively, coincide reasonably well and are in agreement with the calculated values as well. The maximum scatter is about 15%.

CONCLUSIONS

1. A mathematical model for cavity growth has been developed, but is limited to the special case of uniform, isotropic permeability in the coal bed.
2. The combustion pattern geometry predicted by the model has been verified in a 4 x 5 foot laboratory UCG simulator.
3. The model also correctly predicts the Hanna field test results: however, the reasons for this are not understood because the permeability in the Hanna seam is strongly nonisotropic. For this reason, caution is recommended in applying the existing model to field test predictions because almost all coal seams have nonisotropic permeability.
4. Model calculations agree well with the gas composition data from these test.

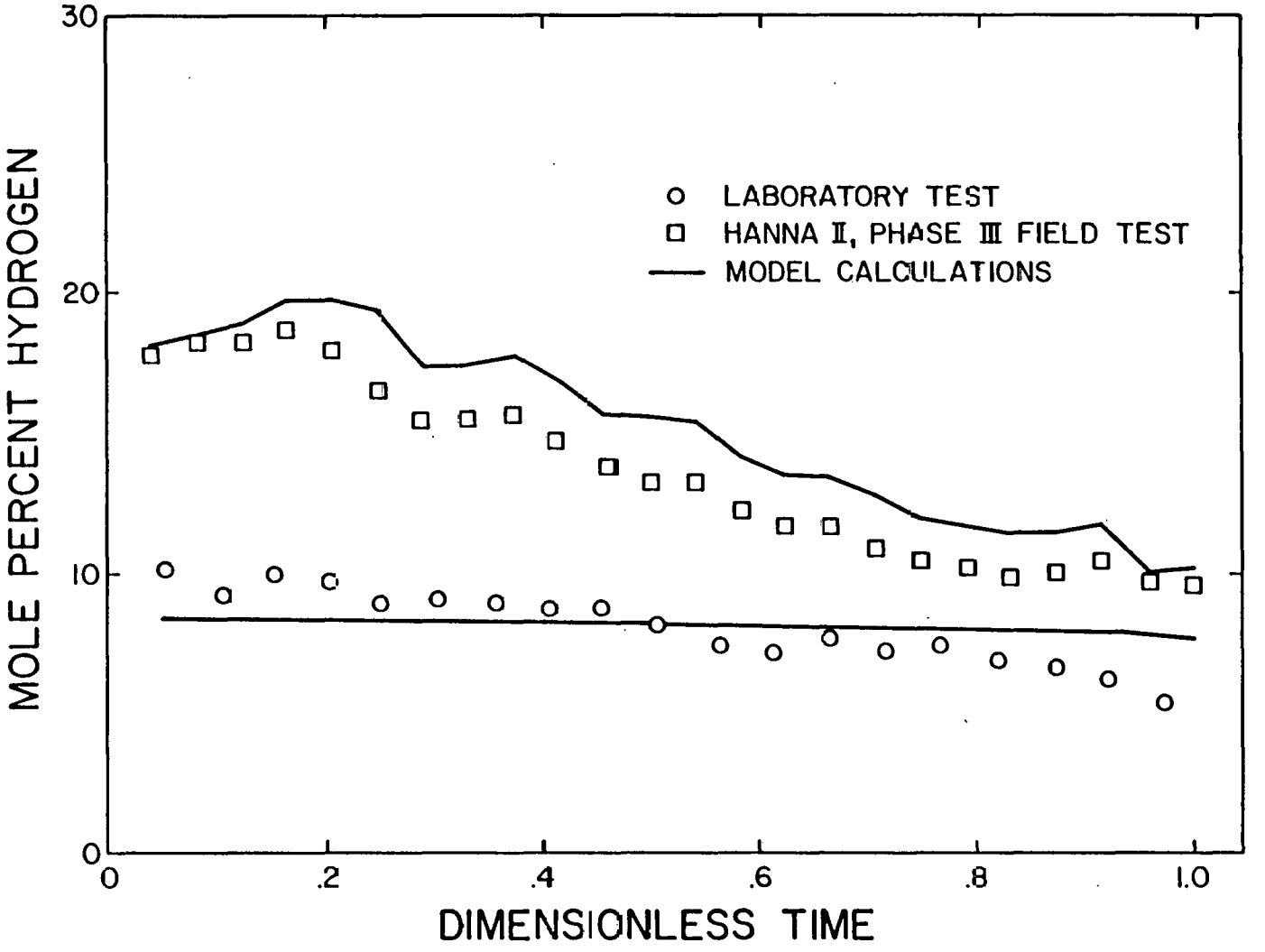

Figure VII-5. Hydrogen Content of Product Gas from the Two-Dimensional Simulator

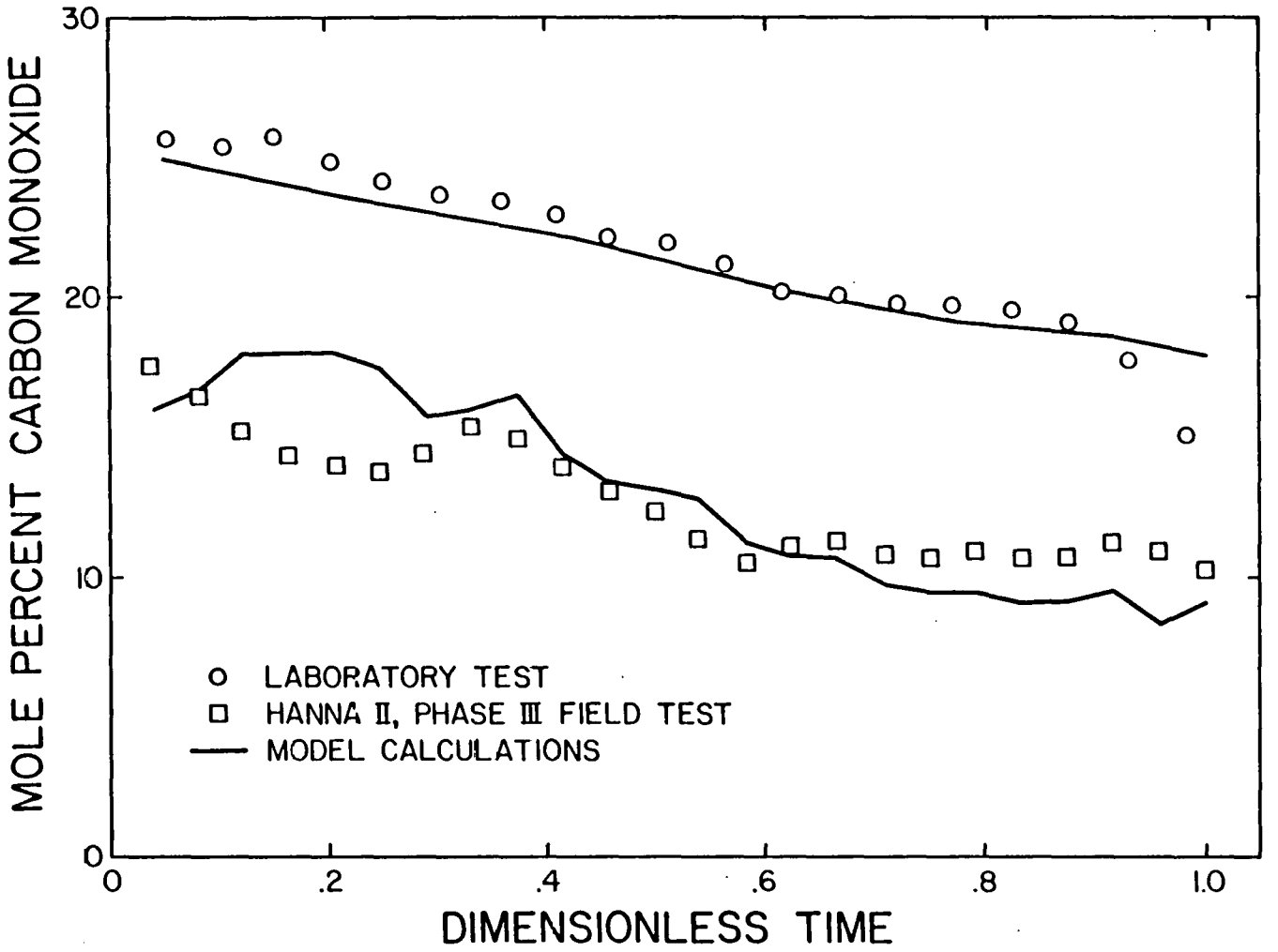

Figure VII-6. Carbon Monoxide Content of Product Gas from the Two-Dimensional Simulator

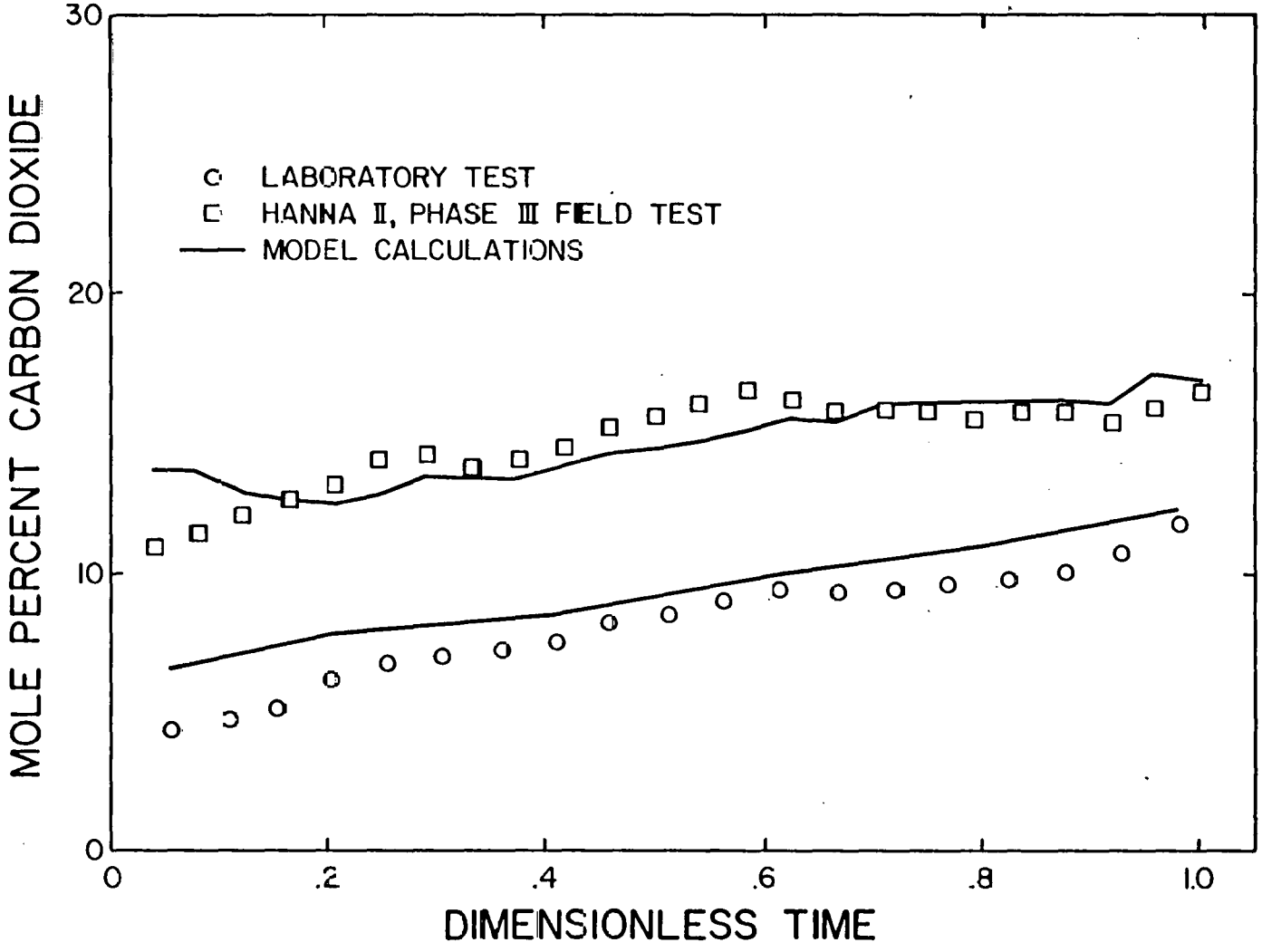

Figure VII-7. Carbon Dioxide Content of Product Gas from the Two-Dimensional Simulator

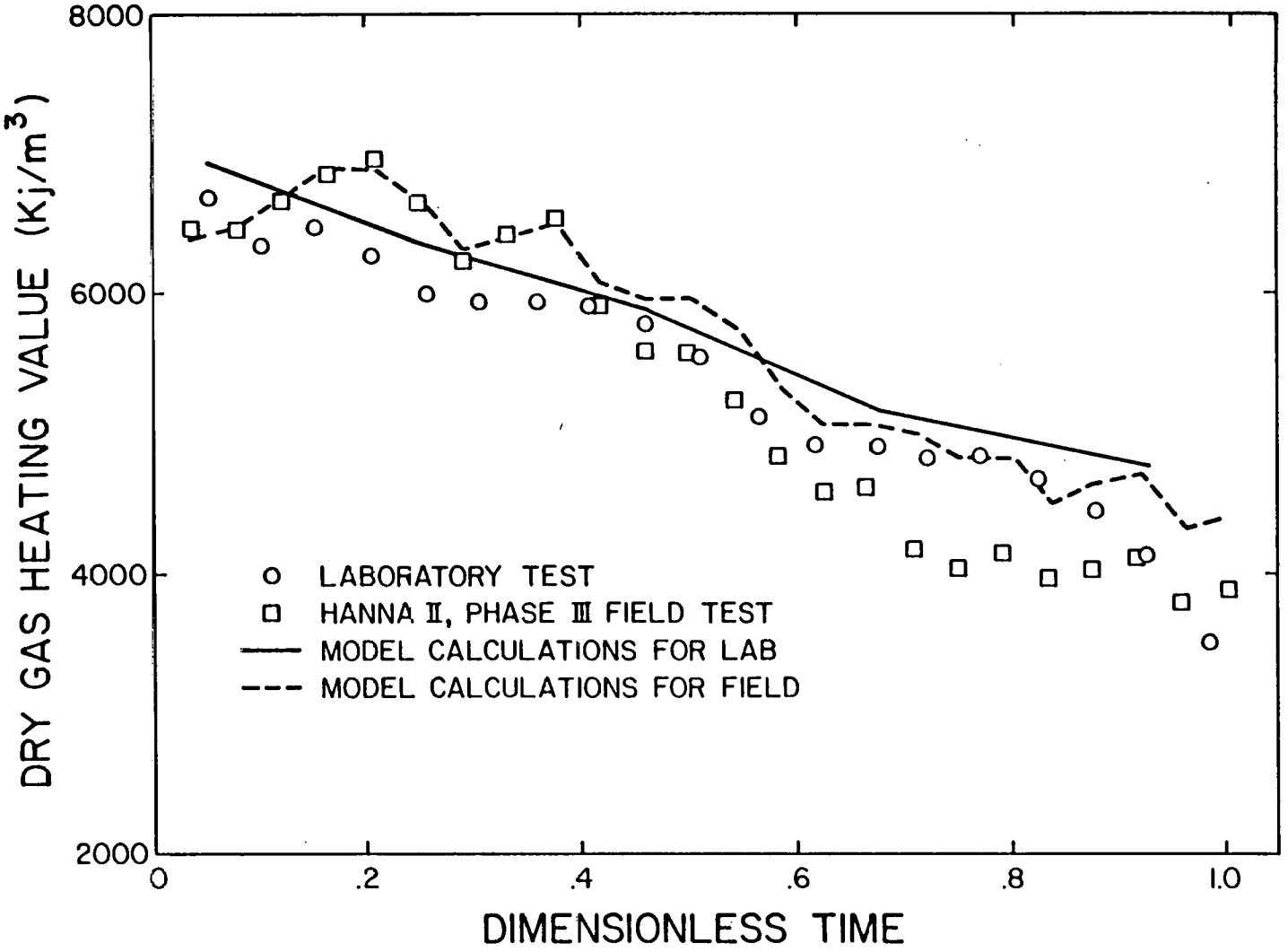

Figure VII-8. Comparison of Product Gas Heating Values

CHAPTER VIII - ECONOMICS

Economics

Economic analysis plays a very important and very difficult role in research. On the one hand, sound research decisions require a knowledge of economic parameters such as potential production costs or pay out time. Such parameters help to determine potential economic benefits from specific research projects and to assist in the selection of the most favorable technologies for major support. On the other hand, economic studies of developing technologies can be completely misleading unless they reflect accurately the future development of the technology. Almost by definition, in research no one can be certain of future development; however, the research scientists, who best understand the technology, will probably make the soundest assumptions for the economic study. For these reasons, engineers rather than economists usually make the initial economic studies for a new developmental project. A lack of complete economic sophistication by the engineer is small compared to large technical errors made by those unfamiliar with the technology or engineering principles. Similarly, the research scientists or engineers will probably make the best economic analyses of a new technology in an active research mode.

With these factors in mind, one of the authors of this report undertook an economic analysis of UCG in 1977. At that time, a number of economic studies for UCG were already available. All of these studies, however, had some shortcomings and important questions remained unanswered. The more important shortcomings are listed below:

1. Unnecessary and sometimes contradictory assumptions.

2. Predicted gas selling price varied by more than a factor of four leading some to believe that enormous uncertainties existed in the process.

3. Failure to reduce the process design to the minimum number of independent variables.

4. Failure to utilize the economic study to define future research needs, that is, what uncertainties in the process affect the economics most seriously.

The economic study initiated by the University of Wyoming and the Laramie Energy Technology Center was completed in 1978, and the results have been reported in several publications (Gunn and Boysen, 1978; Boysen, Gunn and Whitman, 1978; Boysen and Gunn, 1979). This work demonstrated clearly that previous economic studies fell into two distinctly different classifications: those which depended entirely on field test experimental data and those which failed to use experimental data in one or more important categories.

Garon (1976) presented an economic analysis of the latter type. Although this analysis is generally very thorough and well done, the

study was based on a much too high pressure drop across the coal seam during the forward gasification phase. It has been shown experimentally that, with reverse combustion linking in subbituminous coal, the pressure drop between the air injection and gas production wells is rather small. Theoretical considerations confirm this result as well. A too high assumed pressure drop for the economic analysis led to unrealistically high gas product costs compared with other economic studies. For example, the cost of gas produced with a heating value of 126 Btu/scf was reported as being infinite (see publication cited, Table 6, Western location, steam injection, LHV gas). The reason for this result is that, in the technical calculations, air compression used more energy than the process produced. The actual Hanna I field test, with an average gas heating value of 126 Btu/scf, had a favorable energy balance and a low pressure drop within the coal seam.

The other classification of economic analyses made use of experimental data at all critical points. The only disadvantage of these studies is that, in the absence of theoretical correlations, the economic analyses could not be extrapolated to conditions for which there was no data.

The economic analyses of Boysen and Gunn (1979) showed that the process design portion involved a minimum of six independent variables. Two of these variables, seam depth and seam thickness, are fixed immediately on selection of a gasification site. Thus, only four of the variables depend on uncertainties within the gasification process itself. A total of 1296 different cases were studied in order to determine the effect of variations in all six variables. These variables are listed below along with the different values used in the economic analyses.

1. Seam thickness - 3.05, 6.10, 9.15 m
2. Seam depth - 91.5, 183, 305, 600 m
3. Well spacing - 18.3, 30.5, 45.7, 61.0 m
4. Dry gas heating value - 3950, 4935, 5922, 6909 Kj/m^3 (100, 125, 150, 175 Btu/scf)
5. Volumetric combustion sweep efficiency - 50, 65, 80%
6. Gas leakage - 0, 10, 20%

A complete matrix of all possible combinations of the parameter values listed above comprises the 1296 economic analyses reported. Process variables, other than those listed have often been employed along with arbitrarily assumed values for them. Such parameters usually are not independent of the variables listed above, for example, the cold gas efficiency or the thermodynamic efficiency of the process can be shown theoretically not to be independent of the gas heating value. This means that the gas heating value also defines the efficiency of the process.

The flexibility of the computer program developed for the economic analyses enables comparisons to be made with economic studies by other groups. Such studies by different investigators differ in the projected cost of producing gas by more than a factor of four. Many investigators have cited these differences as examples of the enormous uncertainties

in the design of the UCG process. Our own comparison, however, shows that these differences stem primarily from differences related to site selection, that is, seam thickness and seam depth. The table below shows a comparison of two gas production costs, the first cost comes from the original report but scaled to 1978 dollars and the second cost is calculated by Boysen and Gunn (1978) at comparable conditions.

Table VIII-1

Comparison of Gas Cost According to Original Report with Gas Cost Estimated by Boysen and Gunn (1978)

Investigator	Gas Cost (Original Study) $/mm Btu	Gas Cost Boysen and Gunn (1978) $/mm Btu
Buder and Terichow (1977)	$0.76	$0.96
Garon and Schwartz (1977)	$1.30	$1.16
Moll et al. (1977)	$1.40	$1.40

A comparison of the right and left hand columns in Table 1 shows that when four different studies are compared on a comparable basis there is a maximum difference of $0.20 per million Btu's. This is indeed a remarkable degree of agreement when it is considered that each of the four groups worked entirely independently of each other using different design procedures, cost data and experimental data. The differences of a factor of two in the first column arise from the use of different seam thicknesses and depths and the inclusion or exclusion of extensive gas clean up facilities.

There definitely exist uncertainties concerning the commercialization of UCG. If these do not lie in the design of the process, they must lie with the process itself. The economic study of Boysen and Gunn (1978) focuses on what some of these uncertainties are and which ones are the most important. After a gasification site has been selected, four variables remain undetermined - well spacing, gas leakage, sweep efficiency and gas heating value. Boysen and Gunn (1978) showed that gas leakage up to 20% of the total gas produced and that sweep efficiencies varying from 50 to 80% had relatively little impact on the project economics except for thin, marginally-economic coal beds. The important economic factors are gas heating value and well spacing. For the very thick coal beds of Wyoming, even well spacing becomes relatively unimportant because well drilling and completion costs are a relatively small fraction of the air compression costs. The economic factor of overriding importance, therefore, is gas heating value. For example, a decrease in gas heating value from 175 Btu/scf to 100 Btu/scf (other

variables constant) typically doubles the energy production cost. Obviously, all factors affecting the gas heating value are of primary importance for the commercialization of UCG and an understanding of these factors is a major research goal. Major factors affecting gas heating value are the permeability of the overburden, linking success, water influx and subsidence. At the present time, subsidence appears to be a factor in gas heating value through the interdependence of water influx and subsidence. Large scale field tests are similarly needed to define the effect of large burn patterns on subsidence and water influx.

While the economic study of Boysen and Gunn (1978) provided economic data over a much wider range of conditions than any other published study, at conditions established by experimental field tests the analysis provided no new information. As shown in Table VIII-1 there is close agreement between this work and work by large industrial groups.

Conclusions:

1. Factors affecting gas heating value have major economic significance. Experimental investigations and a theoretical understanding of these factors are research goals of critical importance.

2. To be meaningful, an economic analysis must make use of either a complete and consistent set of experimental data or must make use of valid theoretical correlations.

3. There is wide, consistent agreement by different groups concerning gas production costs once a consistent set of process parameters has been determined.

BIBLIOGRAPHY

Bell, G.V. and R.D. Gunn, "Adiabatic Coal Gasification Tube Experiments - Forward Combustion", IV 31, Proc. 6th Underground Coal Conversion Symp., Shangri-La near Afton, OK, July 13-17, 1980.

Boysen, J.E., R.D. Gunn and D.L. Whitman, "An Economic Sensitivity Study of UCG Based on Field Performance, Theory, and Operational Experience", p. 125, Proc. 4th Underground Coal Conversion Symp., Steamboat Springs, CO, July 17-20, 1978.

Boysen, J.E. and R.D. Gunn, "An Economic Sensitivity Study of UCG Based on Field Performance, Theory and Operation Experience", DOE/LETC Bulletin 79/1, Laramie Energy Technology Center, Nov., 1979.

Britten, J.A., W.B. Krantz and R.D. Gunn, "Modeling Studies of Reverse Combustion Linking at High Pressure", p. 515, Proc. 8th Underground Coal Conversion Symp., Keystone, CO, Aug. 15-19, 1982.

Buder, M.K. and O.N. Terichow, "An Economic Comparison of In Situ Gasification of Horizontal and Steeply Dipping Coal Beds", p. 376, Proc. 3rd Ann. Underground Coal Conversion Symp., Fallen Leaf Lake, CA, June 6-9, 1977.

Bumb, A., "The Effects of Cylindrical and Spherical Geometry on the Stability of Reverse Combustion in Underground Coal Gasification", M.S. Thesis, Univ. of Wyoming, Laramie, WY, 1981.

Camp, D.W., A Model of Water Influx for Underground Coal Gasification, M.S. Thesis, Univ. of Colorado, Boulder, CO, 1980.

Camp, D.W., W.B. Krantz and R.D. Gunn, "A Water-Influx Model for UCG with Spalling-Enhanced Drying", 15th Intersociety Energy Engineering Conf., Seattle, WA, Aug. 18-22, 1980.

EPRI, Underground Coal Gasification Simulation, EPRI AP-3496, Electric Power Research Institute, 1984.

Fischer, D.D., J.E. Boysen and R.D. Gunn, "An Energy Balance for the Second Underground Coal Gasification Experiment, Hanna, Wyoming", Trans. Soc. Mining Eng. of AIME, 262 (4), 341 (1977).

Garon, A.M. and G.B. Schwartz, "UCG Cost Predictions Based on Field Performance", p. 367, Proc. 3rd Ann. Underground Coal Conversion Symp., Fallen Leaf Lake, CA, June 6-9, 1977.

Glaser, R.R. and R.D. Gunn, Informal Report to the Laramie Energy Technology Center, 1982.

Gunn, R.D., D.W. Gregg and D.L. Whitman, "A Theoretical Analysis of Soviet In-Situ Coal Gasification Field Tests", p. 274, Proc. 2nd Ann. Underground Coal Gasification Symp., Morgantown, WV, Aug. 10-12, 1976.

Gunn, R.D. and D.L. Whitman, An In-Situ Coal Gasification Model (Forward Mode) for Feasibility Studies and Design, LERC/RIG 76/2, Laramie Energy Technology Center, 1976.

Gunn, R.D., "Problems Solved and Problems Not Solved in UCG", Symp. In-Situ Processing of Coal, Am. Chem. Soc., Div. Fuel Chem., Montreal, Canada, May 29-June 2, 1977.

Gunn, R.D., D.D. Fischer and D.L. Whitman, "The Significance of Natural Aquifers in Underground Coal Gasification", p. 318, Proc. ANS Topical Mtg., Energy and Mineral Resource Recovery, Golden, CO, Apr. 12-14, 1977.

Gunn, R.D. and J.E. Boysen, "The Role of Field and Laboratory Data and Mathematical Models in Reducing the Uncertainty of Economic Studies", p. 221, Proc. 4th Underground Coal Conversion Symp., Steamboat Springs, CO, July 17-20, 1978.

Gunn, R.D., D.L. Whitman and D.D. Fischer, "A Permeation Theory for In-Situ Coal Gasification", Soc. Pet. Eng. Journal, 18, 300, (1978).

Gunn, R.D., Material Balance: Its Applications and Misapplications in Underground Coal Gasification, LETC/RI-79/05, Laramie Energy Technology Center, July, 1979.

Gunn, R.D., G.J. Bell, T.C. Bartke, D.W. Camp and W.B. Krantz, "A Technical Analysis of the Hanna III Field Test Data", p. VIII-6, Proc. 6th Underground Coal Conversion Symp., Shangri-La near Afton, OK, July 13-17, 1980.

Gunn, R.D. and W.B. Krantz, "Reverse Combustion Instabilities in Tar Sands and Coal", Soc. Pet. Eng. Journal, 20, 267, (1980).

Jennings, J.W., R.D. Gunn, C.F. Brandenburg and D.L. Whitman, "The Areal Sweep Efficiency of the In-Situ Recovery of Subbituminous Coal", Reprint No. SPE 6181, 51st Ann. Fall Mtg., Soc. Pet. Eng., New Orleans, LA, Oct. 3-6, 1976.

Kotowski, M.D. and R.D. Gunn, "Theoretical Aspects of Reverse Combustion in the Underground Gasification of Coal", LERC/RI-76/4, Laramie Energy Technology Center, March, 1976.

Krantz, W.B. and R.D. Gunn, "The Linear Stability of Reverse Combustion for In-Situ Coal Gasification", p. 146, Proc. 3rd Ann. Underground Coal Conversion Symp., Fallen Leaf Lake, CA, June 6-10, 1977.

Krantz, W.B., D.W. Camp and R.D. Gunn, "A Water Influx Model for UCG", p. III-21, Proc. 6th Ann. Symp. Underground Coal Conversion, Shangri-La near Afton, OK, July 13-17, 1980.

Krantz, W.B. and R.D. Gunn, "An Overview of Underground Coal Gasification - A Comparison of Modeling Studies with Field Test Data", Proc. Coal Symp., CIC, Halifax, Nova Scotia, June 1-3, 1981.

Krantz, W.B. and R.D. Gunn, "Use of Stability Theory in Interpreting UCG Field Test Data", In Situ, 5(3), 199, (1981).

Levie, B.E., W.B. Krantz, D.W. Camp, R.D. Gunn and A.D. Youngberg, "Application of the Spalling-Enhanced Drying Model in Predicting Cavity Geometry and Operating Strategy for the Hanna 2 Phase 2 UCG Field Test", p. 236, Proc. 7th Underground Coal Conversion Symp., Fallen Leaf Lake, CA, Sept. 8-11, 1981.

Levie, B.E., W.B. Krantz and R.D. Gunn, "A Model for Roof Spalling and Its Applications to Predicting Cavity Shape for the Hanna III UCG Field Test", p. 321, Proc. 8th Underground Coal Conversion Symp., Keystone, CO, Aug. 15-19, 1982.

Loison, R., Etude de la Gazeification Souterraine aux USA, Centre d' Etudes et Recherches des Charbonnages de France, Dec. 30, 1952.

Lovell, R.W., Wet Reverse Combustion during Underground Coal Gasification, M.S. Thesis, Univ. of Wyoming, Laramie, WY, 1982.

Lu, H.S., Laboratory Simulation of Reverse Combustion in UCG, M.S. Thesis, Univ. of Wyoming, Laramie, WY, 1980.

Moll, A.J., J.A. Alich and R.L. Dickenson, "Low BTU Gas Produced by UCG in Western U.S. - Economics and Prospects", p. 361, Proc. 3rd Ann. Underground Coal Conversion Symp., Fallen Leaf Lake, CA, June 6-9, 1977.

Puri, R., Theoretical Modeling of Reverse Combustion Instabilities in Coal and Tar Sand, M.S. Thesis, Univ. of Colorado, Boulder, CO, 1979.

Schlichting, H., Boundary Layer Theory, transl. J. Kestin, McGraw-Hill, New York, NY, 1960.

Whitman, D.L., The Permeation Theory of Underground Coal Gasification, Ph.D. Dissertation, Univ. of Wyoming, Laramie, WY, 1978.

Whitman, D.L., J.E. Boysen and R.D. Gunn, "Two Dimensional Laboratory Simulation of an Underground Coal Gasification Field Test", p. 461, Proc. 4th Underground Coal Gasification Symp., Steamboat Springs, CO, July 17-20, 1978.

☆U.S. GOVERNMENT PRINTING OFFICE:1980-540-122/60026